University of Szeged

Faculty of Pharmacy

Institute of Pharmaceutical Technology and Regulatory Affairs

Head: Dr. Habil. Ildikó Csóka Ph.D.

Formulation of microcomposites and pastilles using spray-drying and melt technology

Ph.D. Thesis

By

Dr. Gábor Katona

Pharmacist

Supervisor:

Prof. Dr. Habil. Piroska Szabó-Révész D.Sc.

Szeged

2017

CONTENT

Publications related to the thesis

1. **Katona G.**, Jójártné Laczkovich O., Szabóné Révész P.: A trehalóz, mint amorfizálódásra hajlamos segédanyag, rekrisztallizációjának vizsgálata, *Acta Pharm. Hung.* (2014), 84, 7-14.

2. **Katona, G.**, Sipos, P., Frohberg, P., Ulrich, J., Szabó-Révész, P., Jójárt-Laczkovich, O.: Study of paracetamol-containing pastilles produced by melt technology, *J. Therm. Anal. Calorim.* (2016), 123, 2549-2559. **(IF: 2.042, Citation: 2)**

3. Jójárt-Laczkovich, O., **Katona, G.**, Aigner, Z., Szabó-Révész, P.: Investigation of recrystallization of amorphous trehalose through hot-humidity stage X-ray powder diffraction, Eur. J. Pharm. Sci. (2016), 95, 145-151. **(IF: 3.773, Citation: -)**

4. **Katona, G.**, Szalontai, B., Budai-Szűcs, M., Csányi, E., Szabó-Révész, P., Jójárt-Laczkovich, O.: Formulation of paracetamol-containing pastilles with in situ coating technology, Eur. J. Pharm. Sci. (2016), 95, 54-61. **(IF: 3.773, Citation: -)**

Other publications

1. **Katona G.**, Jójártné Laczkovich O., Szabóné Révész P.: Fagyasztva szárítás az innovatív gyógyszerkészítmények előállításában, *Gyógyszerészet* (2014), 58, 546-553.

2. Bartos, Cs., Szabó-Révész, P., Bartos, Cs, **Katona, G.**, Jójárt-Laczkovich, O., Ambrus, R.: The effect of an optimized wet milling technology on the crystallinity, morphology and dissolution properties of micro- and nanonized meloxicam, Molecules (2016), 21, 507. **(IF: 2.465, Idézettség: -)**

Presentations related to the thesis

1. **Katona Gábor**, Jójártné Laczkovich Orsolya, Szabóné Révész Piroska: Porlasztva- és fagyasztva szárított trehalóz visszakristályosodásának vizsgálata. Congressus Pharmaceuticus Hungaricus XV., Budapest, Magyarország, 2014. április 10-12. (poster presentation)

2. Jójártné Laczkovich Orsolya, Mártha Csaba, **Katona Gábor**, Szabóné Révész Piroska: Gyógyszertechnológiai formulálások során alkalmazott cukrok, cukoralkoholok amorfizálódási tulajdonságai. MKE Kristályosítási és Gyógyszerformulálási Szakosztály 7. Kerekasztal Konferenciája, Szeged, Magyarország, 2014. május 16-17. (verbal presentation)

3. Jójártné Laczkovich Orsolya, **Katona Gábor**, Szabóné Révész Piroska: Trehalóz rekrisztallizációs kinetikájának termoanalitikai vizsgálata. Termoanalitikai Szeminárium. Szeged, Magyarország, 2014. november 21. (verbal presentation)

4. Orsolya Jójárt-Laczkovich, **Gábor Katona**, Zoltán Aigner, Piroska Szabó-Révész: Investigation of amorphous trehalose using hot-humidity stage X-ray powder diffraction. 6th BBBB - Conference on Pharmaceutical Sciences: Strategies to Improve the Quality and Performance of Modern Drug Delivery Systems, Helsinki, Finland, 2015. szeptember 10-12. (poster presentation)

5. **Gábor Katona**, Péter Sipos, Patrick Frohberg, Joachim Ulrich, Piroska Szabó-Révész, Orsolya Jójárt-Laczkovich: Formulation of paracetamol-containing pastilles with in situ coating technology. 6th BBBB - Conference on Pharmaceutical Sciences: Strategies to Improve the Quality and Performance of Modern Drug Delivery Systems, Helsinki, Finland, 2015. szeptember 10-12. (oral poster presentation)

6. **Katona Gábor**, Sipos Péter, Frohberg Patrick, Ulrich Joachim, Szabó-Révész Piroska, Jójárt-Laczkovich Orsolya: Paracetamol tartalmú pasztillák előállítása "in situ coating" technológiával. Gyógyszertechnológiai és Ipari Gyógyszerészeti Konferencia 2015. Siófok, Magyarország, 2015. október 15-17. (verbal presentation)

7. Jójártné Laczkovich Orsolya, **Katona Gábor**, Bónis Erzsébet, Szabóné Révész Piroska: Kíméletes technológiák, amelyek alkalmasak fehérje természetű anyagok formulálására. Gyógyszerkémiai és Gyógyszertechnológiai Szimpózium '16, Herceghalom, Magyarország, 2016. szeptember 15-16. (verbal presentation)

8. **Katona Gábor**: Paracetamol tartalmú pasztillák formulálása "in situ coating" technológiával. XII. Clauder Ottó emlékverseny, Budapest, Magyarország, 2016.10.20-21. (verbal presentation)

ABBREVIATIONS

Anhydrous TRE	anhydrous trehalose
API	active pharmaceutical ingredient
CCDC	Cambridge Crystallographic Data Centre
DDS	drug delivery system
DSC	differential scanning calorimetry
DXR	dispersive Raman spectroscopy
HH-XRPD	hot-humidity X-ray powder diffraction
HPβCD	hydroxypropyl-β-cyclodextrin
HPMC	hydroxypropyl methylcellulose
MAN	mannitol
MLR	multiple linear regression
PCT	paracetamol
PEG	polyethylene glycol
PSD	particle size distribution
PVAc	polyvinyl acetate
PVP	polyvinylpyrrolidone
Raman	Raman spectroscopy
RH	relative humidity
SEM	scanning electron microscopy
SORB	sorbitol
T_g	glass transition temperature
TGA	thermogravimetric analysis
TRE dehydrate	trehalose-dihydrate
TRS	transmission Raman spectroscopy
XRPD	X-ray powder diffraction
XYL	xylitol

1. INTRODUCTION

Nowadays pharmaceutical industry uses many technological operations and the number of excipients applied during production is growing. The diversity of the operation parameters can influence the quality of the product. With the innovation of production protocols, raw materials or waste elimination could be utilized efficiently, the use of toxic and/or hazardous reagents and solvents can be avoided in the manufacture and application of products. Through the minimization of the number of applied excipients, pharmaceuticals would be more "natural". It is an important aspect for patients to reduce the contamination with different chemicals, thereby to decrease the incidence of allergy.

Conventionally used techniques as spray-drying or melt technology can offer innovation in the preparation of novel forms. These technologies can be applied in an organic solvent free manner, which adapts well to the increasing effort in the industry to introduce "green" pharmaceutical practice. Through the optimization of operation parameters, energy, production time and costs can be saved. With the reduction of e.g. temperature, the API can be protected from decomposition, moreover, the intermedier (microcomposites) or product (pastille) can be produced in one single operation step. In the preformulation a DDS can be developed using a factorial design, taking special requests (e.g. paediatric preparations) into account.

In paediatrics, low amounts of APIs are incorporated in DDSs, so the formulation of DDSs plays a key role in the production process. Children are special patients, their compliance can be increased by choosing a liked administration route (e.g. per os) instead of injections or suppositories. It is known that "value added" preparations are especially important in paediatric therapy, which belongs to the category of "unmet medical need". So with the application of conventional technologies as spray-drying (Thi et al., 2012, Aguiar et al., 2016, Kaushik et al., 2015) or melt technology (Phaemachud et al., 2010) there is an opportunity to develop innovative paediatric preparations (e.g. dose sipping form and lozenge)

2. AIMS

The aim of our research work was to apply conventional technologies such as spray-drying and melt technologies with new approaches to research and develop innovative PCT containing solid DDSs for paediatric administration. The spray-drying process was applied to prepare microcomposites for dose sipping form and the melt process was suitable to formulate pastilles with "*in situ* coating" technology as lozenge. For both technologies our research work consisted of two parts (i) development of a DDS in preformulation and (ii) incorporation of API in the DDS as carrier system. The technologies and investigations are presented in Figure 1.

Spray-drying

Preformulation of microcomposites prepared with spray-drying
- Study of recrystallization kinetics (HH-XRPD, XRPD, DSC)

Incorporation of PCT in the microcomposites
- Structural investigations (DSC, XRPD, SEM)
- *In vitro* dissolution studies

Melt technology

Preformulation of pastilles produced with melt technology
- Determination of phase-diagrams (DSC)
- Optimization of eutectic formula (DSC, Box-Behnken experimental design)
- Viscosity and contact angle measurements

Incorporation of PCT in the pastilles
- Distribution of API (Raman)
- Determination of polymorphic forms (XRPD, Raman)
- Geometric parameter and hardness determination
- *In vitro* dissolution studies

Fig. 1: Applied technologies and investigations in the research work

The main aspects of the research work are the following:

I. to survey the literature background of the preparation of innovative forms used in paediatric therapy with conventional methods, spray-drying and melt technology,

II. to use these technologies innovatively, as organic solvent free methods, for producing dosage forms which do not contain any colouring agents or preservatives,

III. to investigate the excipients used in preformulation studies of carrier systems with different screening methods,

IV. to incorporate a low amount of PCT as model drug in the carriers, thereby designing a composition in paediatric therapy,

V. to suggest a formulation for industrial utilization.

3. THEORETICAL BACKGROUND

3.1. Formulation of innovative products in the pharmaceutical industry

Conventional pharmaceutical manufacturing is generally accomplished using batch processing with laboratory testing conducted on collected samples to evaluate quality. This conventional approach has been successful in providing quality pharmaceuticals to the public. However, today significant opportunities exist for improving pharmaceutical development, manufacturing and quality assurance through innovation in product and process development, analysis and control (Web reference 1). Novel trends like nanotechnology or biotechnology are in the spotlight of innovation, but the conventionally used technological processes can have new approaches, which result in innovative products. Variously applied operations such as spray-drying or melt technology can be used well for innovative formulation. Using these methods we can minimalize the number of excipients and reduce some process steps by being more efficient, saving energy and assuring better quality of products, moreover, compositions which satisfy specific needs, e.g. paediatric expectations, can be formulated.

The other aspect of the above-mentioned technologies is the "green" pharmaceutical practice, which is a future trend in the pharmaceutical industry. It began in recent years when residues of pharmaceuticals were discovered in water, thanks to the development of new analytical technologies, which can measure increasingly lower concentrations (Kümmerer et al., 2007). There have been many suggestions for designing environmentally-benign products and processes to address the environmental issues of both products and processes in the research and development of new medicines. The basic aspects of green technological techniques are the organic solvent reduction, the use of water-based methods in pharmaceutical manufacturing, and ongoing programs for reducing emissions, effluents and wastes. Organic solvent reduction can be achieved by using amphiphilic materials (e.g. cyclodextrins: Reti-Nagy et al. 2015, Róka et al., 2015) increasing the water solubility of lipophilic agents or by using novel techniques (e.g. microwave processing (Szepes et al., 2005, Szepes et al., 2007)) for the structure modification of the API. The above mentioned technologies (spray-drying or melt technology) can be also used for the production of "green" pharmaceuticals if the basic aspects of "green" technology (e.g., raw materials, solvents, waste management) are complied with.

So the conventionally applied technologies are suitable to meet new demands and in this context to formulate innovative products. In general, these products contain very specific carrier(s) because they comply with several criteria (Alpar et al., 2005, Van Arnum et al., 2010). The carriers are generally amorphous or semicrystalline polymers which are water-soluble, and by using spray-drying the API can be incorporated in them for the purpose of controlled or modified

release (Pomázi et al., 2013, Al-Zoubi et al., 2016). Crystalline materials as carriers can be processed by melt technologies (Szűts et al., 2011), especially using extrusion (Krause et al., 2009).

3.2. Viewpoints of development of paediatrics

The Paediatric Committee (PDCO) is the European Medicines Agency's (EMA) scientific committee responsible for activities on medicines for children and to support the development of such medicines in the European Union by providing scientific expertise and defining paediatric needs (Web reference 2). Because of the immature metabolism of children, the most important aim in the development of paediatric formulations is the minimization of APIs and auxiliary agents (de Zwart et al., 2004). Children are special patients, who have to be convinced to accept medication. Their compliance can be largely increased when the taste, colour and smell are in harmony in the formulation (Nataha et al., 1999). Instead of artificial sweetening and colouring agents and fragrances, natural excipients are preferred to avoid allergic reactions or malformations (Farkas et al, 1971). The application of lactose has to be reduced to avoid intolerance (Heyman et al, 2006). The classical source of sweetener is sucrose (derived from cane or beet in the form of liquid or dry state), dextrose, fructose, glucose, liquid glucose and maltose. The sweetness of fructose is perceived rapidly in the mouth as compared to sucrose and dextrose. Fructose is sweeter than sorbitol and mannitol and thus used widely as a sweetener. Polyhydric alcohols such as sorbitol, mannitol, isomalt and maltitol can be used in combination as they additionally provide good mouth-feel and cooling sensation (Mäkinen et al., 2011). Polyhydric alcohols are also less carcinogenic and do not have a bitter after taste, which is a vital aspect in formulating oral preparations. The sweetness property of most of the polyols is less than half of that of sucrose except for xylitol and maltitol, the sweetness of which is similar to that of sucrose (scale of 0.8–1.0) (Dixit et al., 2009). However, it should be noted that the use of natural sugars in such preparations needs to be restricted in people who are on diet or in the case of diabetic patients (Mennella et al., 2008, Hutteau et al., 1998).

3.3. Spray-drying

Spray-drying is a scalable, well-automatized process, which employs rapid drying from solutions, emulsions, suspensions or even melts and foams into dry free-flowing powders (Cal et al., 2010). Drying occurs within seconds because of the nozzle atomizes the liquid phase into small drops to obtain a maximal surface area in contact with the drying gas. The opportunity of varying the operation parameters (inlet temperature, feed rate, aspirator or air flow) during the process enables the production of particles with controlled size and morphological aspects. One of

the most common applications of spray-drying is in the field of dry powder inhaler production (Steckel et al., 2004). The most important requirement of dry powder inhaler formulation is to produce monodisperse particles in the size range of 1-10 µm. Spray-drying is an appropriate method for this purpose. The conventional process is limited to producing particles with a characteristic size below 2 µm mainly because of the atomization technology is based on pressure or centrifugal forces, and also due to the limited collection efficiency of the cyclones (Zgoulli et al., 1999, Wan et al., 1992, Oneda et al., 2003 Palmieri et al., 1994). The production and collection of submicron particles from a solution is only possible with a piezoelectric driven vibrating mesh atomizer and a high-efficiency electrostatic dry powder collector. Owing to the fast evaporation of the solvent, gentle drying is available, which protects the product from thermic decomposition. With the correct selection of the operation parameters, heat sensitive materials can be also processed. By using spray-drying, an amorphous product with good flow properties can be produced (Vicente et al., 2013) in one operation step, which can be an intermediate before tableting or can provide better water solubility of the active substance. The high quality of the spray-dried products is due to the protection of the particles through evaporative cooling during the process. It also allows the encapsulation (Tewa-Tagne et al., 2007, Hamishehkar et al., 2010) of active agents in a biodegradable polymer or taste masking agent, thus opening a wide spectrum of opportunities in the field of particle engineering in pharmaceutical, materials and food science (Oliveira et al., 2013). Sterile spray-drying could be also applied for the preparation of stable vials, because drying takes place in a closed system and impurities can be avoided.

Spray-drying is an excellent method for the formulation of DDSs of crystalline carriers. Different carriers, e.g. sugar alcohols, are commonly applied for carrier systems (Table 1). Particle size reduction can be achieved by the formulation of microcomposites. By setting the appropriate operation parameters, micronization and even nanonization can take place in the product (Vehring et al., 2008).

Table 1 Different types of carriers produced with spray-drying

Carrier	API	Reference
PEG 4000 + lactose	—	Corrigan et al., 2002, Chidavaenzi et al., 2001
Mannitol	—	Mönckedieck et al., 2016, Maas et al., 2001,
Trehalose	—	Ógáin et al., 2011, Islam et al., 2008, Gradon et al., 2014, Maurya et al. 2005
Trehalose + sorbitol	—	Maurya et al. 2005
Trehalose + raffinose + HPβCD	—	Amaro et al., 2015
Maltodextrin + gum Arabic + waxy starch + microcrystalline cellulose	Pomegranate juice	Yousefi et al., 2011
PEG 6000 + HPMC	Itraconazole	Janssens et al., 2008
PEG 6000 + Soluplus®	Nifedipine + Sulfamethoxazole	Altamimi et al., 2016

PEG 6000	Loperamide	Weuts et al., 2005
Mannitol + Trehalose	Meloxicam	Pomázi et al., 2011
PVP	Curcumin	Paradkar et al., 2004
PVP + PVAc	Diltiazem HCl	Al-Zoubi et al., 2016
PVP + isomalt	Celecoxib	Ghanavati et al., 2017

3.4. Melt technology

Melt technology is used increasingly by technological operations in the pharmaceutical industry, whereby novel products can be produced efficiently. This green technology involves dust-free processes and elastic materials can also be used to produce the final form. There is no need for the use of extra organic solvents in the production, therefore there are no residual solvents in the product and less environmentally harmful chemical waste is generated in contrast with other conventionally used techniques. Melt technology can result in amorphous products, which may have higher dissolution rates and bioavailability than those of the corresponding crystalline forms (Domian et al., 2002, Broman et al., 2001, Six et al., 2001, Redenti et al., 1996). With a fusion method, a solid dispersion of the excipients and active agent can be prepared.

Melt granulation or thermoplastic granulation is a technique that facilitates the agglomeration of powder particles using meltable binders, which melt or soften at relatively low temperature (50–90 °C) (Shanmugam et al., 2015). Cooling of the agglomerated powder and the consequent solidification of the molten or softened binder complete the granulation process. Through a drop-melting method, pastilles can be formed, and pastillation is achieved in one step of a conventional melting process.

Melt extrusion is a process which involves a preliminary stage in which dry powders, drug and excipients are mixed by conventional blenders, followed by the addition of a liquid phase and further mixing to ensure homogeneous distribution. The wet powder mass is extruded through cylindrical dies or perforated screens with circular holes, of typically 0.5–2.0 mm diameter, to form cylindrical extrudates, followed by pellet-forming (Breitenbach et al. 2002).

In situ coating is a novel approach in melt technology developed by Ulrich et al (Wendt et al., 2014, Ulrich et al., 2014, Abouzeid et al., 2014), in which the formation of the pastille and its coating occur in the same step. Upon using a eutectic mixture of two compounds (e.g. sugars or sugar alcohols), phase separation can take place and either of the components may form a coating. As phase separation is a thermal process, the recrystallization of the amorphized components can be investigated (Patterson et al., 2005, Mah et al., 2015, Löbmann et al., 2013). The drop-melting method is a suitable technique for pastille formation, where solidification takes place at the surface of the pastilles, corresponding to the recrystallization of the components. Viscosity is a critical parameter of this technology: it influences drop size, whereas a relatively high viscosity

decreases molecular mobility, thereby hindering the recrystallization process and surface solidification (i.e. formation of the "coating" or "shell"). In case of high viscosity, seed crystals or ultrasonic agitation can be used to initiate nucleation (Wendt et al. 2014).

3.5. Dose sipping form

The dose sipping form is a novel dosage form in paediatric therapy (Tuleu et al., 2005, Breitkreutz et al., 2007, Krause et al., 2008). Sipping a single dose of preparation through a drinking straw is a novel form of drug administration in paediatric therapy (Walsh et al., 2011). Generally granules, pellets, mini tablets, micropellets or microcomposites are filled into a plastic drinking straw as drug delivery device (Ziegler et al., 2008) (Fig. 2). The controller located at the bottom of the straw acts like a filter. During sipping, the drug containing load will be transported to the top of the straw. The cap on the top of the system has two functions, to avoid the microbiological contamination of the system and to keep the solid components inside the straw. Before use, it has to be removed. The dose sipping form is a flow-through system, which depends on the entering liquid. Therefore liquids with low viscosity, e.g. tea, carbonated drinks, water are suitable, while viscose liquids like juice with pulp or milk shake can block the system. The advantages of the dose sipping form are basically related to patient compliance. Especially children often refuse to take tablets or capsules, but drinking a cup of drink through a straw is related to natural habit and the bitter taste of drugs can be well tolerated. It can be applied discreetly and the dissolved drug can pass in the mouth easily, almost unnoticed. This application form is especially suitable for patients who have problems swallowing drug products and therefore refuse to take medicine at all (e.g. pediatric or elderly patients). Difficulties with administering drugs to children are a widespread problem, which needs improvement with regard to off-label use for example (Schirm et al., 2003, Kearns et al., 2003, Standing et al., 2005). The first sipping device on the pharmaceutical market was Claroship® (Grünenthal GmbH), which contains the macrolide antibiotic clarithromycin in a micropellet form (Yoo 2008).
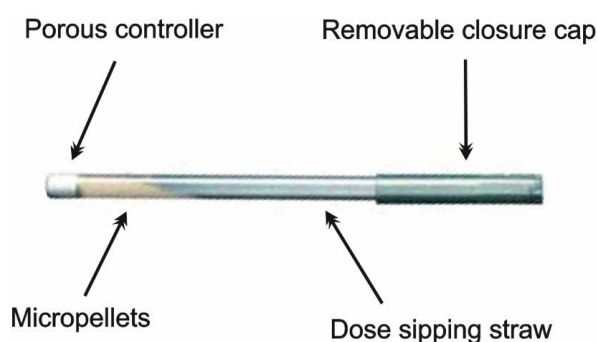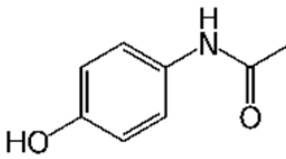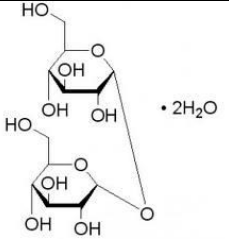

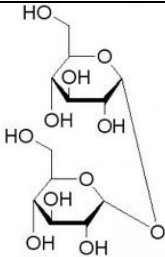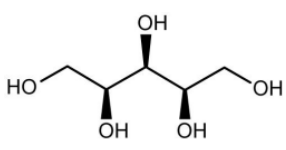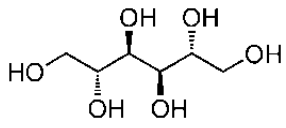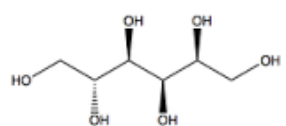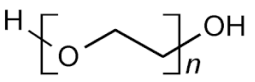**Fig. 2:** Dose sipping form

3.6. Lozenges

Lozenges or pastilles are buccal pharmaceutical preparations containing a drug along with flavouring and sweetening agents (Sastry et al., 2000, Bansal et al., 2014). They are mostly compressed tablets formulated without a disintegrant and harder than ordinary tablets so that they will dissolve slowly in the mouth. Different types of lozenges are hard candy lozenges, soft lozenges, chewable lozenges. Lozenges can be used for hospice or chemotherapy patients who often experience nausea and in paediatric therapy, e.g. Actiq® the fentanyl citrate containing oral transmucosal lozenge (Web reference 3, Sharar et al., 2002). Paediatric patients often show improved compliance with lozenges over other types of oral formulations such as tablets or capsules (Pundir et al, 2014). Although these lozenges are most often used for a localized effect in the mouth (throat lozenges), they can also be used for a systemic effect (Kishorbhai et al., 2014) if the drug is well absorbed through the buccal lining or is swallowed. Analgetics and antihistamines are commonly utilized in such formulations, which are easy to use in paediatric or geriatric therapy and the drug can be kept in contact with the oral cavity for an extended period of time. By means of buccal absorption, the disadvantages of peroral administration can be avoided, such as the hepatic first-pass metabolism or enzymatic degradation within the gastrointestinal tract, which prevent the oral administration of certain classes of drugs, particularly proteins and peptides (Sholaei et al., 1998), and additionally a lower amount of drug is needed to achieve the therapeutic effect. In the USA, a buccal pharmaceutical preparation, Meltaways® (Tylenol), containing 80 mg of PCT in dextrose carrier, is available as a chewable tablet in paediatric therapy. Such solid preparations have the aim of fast release.

4. MATERIALS AND METHODS

4.1. Materials

PCT as model drug was chosen for our experimental work; it was obtained from Sanofi Aventis (Frankfurt am Main, Germany) and TRE dihydrate (h-form) from Karl Roth GmbH+Co. KG. (Karlsruhe, Germany). This was regarded as 100% crystalline material. Anhydrous TRE (β-form) was produced by dehydration of TRE dihydrate at 85 °C during 4 h under vacuum (Nagase et al., 2002) and checked within 24 h both with DSC and XRPD. XYL, MAN, PEG 2000 and PEG 6000 were purchased from Sigma-Aldrich Chemie GmbH (Mannheim, Germany) and SORB from Molar Chemicals Ltd. (Halásztelek, Hungary) (Table 2).

Table 2 Materials applied for experimental work

Material	IUPAC name	Chemical structure	Theoretical applications	Applications in our work
Paracetamol (PCT)	N-(4-hydroxyphenyl)-acetamide		analgesic and antipyretic agent, a selective COX-2 inhibitor (Hinz et. al., 2008)	Model API in microcomposites and drop-melted pastilles
Trehalose-dihydrate (TRE dehydrate)	2R,3S,4S,5R,6R)-2-(Hydroxymethyl)-6-[(2R,3R,4S,5S,6R)-3,4, 5-trihydroxy-6-(hydroxymethyl)oxan-2-yl]oxyoxane-3,4,5-triol dehydrate		Colour adjuvant; flavour enhancer; freeze-drying agent; humectant; stabilizing agent; sweetening agent; tablet diluent; thickening agent (Rowe et al., 2009)	Carrier for PCT containing microcomposites prepared with spray-drying
Anhydrous trehalose (Anhydrous TRE)	2R,3S,4S,5R,6R)-2-(Hydroxymethyl)-6-[(2R,3R,4S,5S,6R)-3,4, 5-trihydroxy-6-(hydroxymethyl)oxan-2-yl]oxyoxane-3,4,5-triol anhydrous			
Xylitol (XYL)	(2R,3r,4S)-Pentane-1,2,3,4,5-pentol		Coating agent; diluent; emollient; humectant; sweetening agent; tablet and capsule diluent; tablet filler (Rowe et al., 2009)	Component of eutectic pastille basis
Mannitol (MAN)	(2R,3R,4R,5R)-Hexane-1,2,3,4,5,6-hexol		Diluent; plasticizer; sweetening agent; tablet and capsule diluent; therapeutic agent; tonicity agent (Rowe et al., 2009)	Component of eutectic pastille basis
Sorbitol (SORB)	(2S,3R,4R,5R)-Hexane-1,2,3,4,5,6-hexol		Humectant; plasticizer; stabilizing agent; sweetening agent; tablet and capsule diluent (Rowe et al., 2009)	Component of eutectic pastille basis
Polyethylene glycol 2000 and 6000 (PEG 2000 and 6000)	poly(oxyethylene)		Ointment base; plasticizer; solvent; suppository base; tablet and capsule lubricant (Rowe et al., 2009)	Wettability enhancer material in microcomposites and pastilles; viscosity enhancer in drop-melted pastilles

4.2. Methods

4.2.1. Preparation of formulations

4.2.1.1. Preparation of spray-dried TRE and PCT containing microcomposites

For the investigation of recrystallization, kinetic TRE dihydrate was spray-dried from 10% solutions in water (5.00 g of TRE and 45.0 g of water) using a Büchi 191 Mini Spray Dryer (Büchi, Switzerland) (Fig. 3). The aqueous solutions used for the preparation of microcomposites contained 7.5% TRE, 1.5% PCT and 1.5% PEGs. The parameters used are given in Table 3 (Moran et al., 2007). The spray-dried products were stored in a desiccator over cobalt (II) chloride contaminated silicon-dioxide (25±2 °C, 32±5% RH) until use.

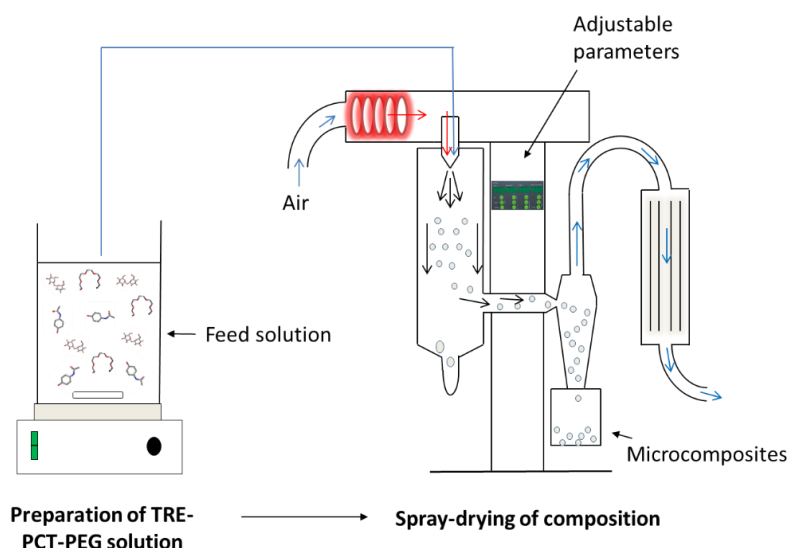**Fig. 3:** Preparation of microcomposites with BÜCHI B-191 spray-dryer

Table 3 Operation parameters for the preparation of spray-dried TRE

Operation parameters	Settings
Inlet temperature (°C)	130-140
Outlet temperature (°C)	75-92
Nozzle diameter (mm)	0.7
Feed rate (mL/min)	2
Pressure (bar)	4.8
Atomiser flow rate (normoliter/h)	600
Aspirator (%)	80

4.2.1.2. Preparation of PCT containing pastilles with in situ coating technology

For pastillation, the one-drop pastillation device developed by Kaiser Steel Belt Systems GmbH (Krefeld, Germany) was used (Fig. 4A). Physical mixtures of XYL-MAN with PEG as carrier additive were prepared and melted in a temperature-controlled double-walled vessel at 110 °C. A crank shaft moved at constant rate by an engine pressed the mixture in drop form through a valve at the bottom of the vessel onto a 25 °C thermostated cooling plate, where it solidified into a flat-bottomed pastille (Wendt et al., 2014).

Eutectic mixtures of XYL-SORB with PEGs as carrier additives were prepared and melted in a heated pipette at 110°C. PCT was dispersed in the melted carrier. The melted solid dispersion was dropped onto a 25°C thermostated cooling plate, where it solidified to form flat-bottomed pastilles (Fig. 4B) (Bülau et al., 1997). Four mixtures were studied, including (1) XYL-SORB 50–50 wt.% (referred to as XYL-SORB-EUT) without PCT, (2) XYL-SORB with PCT (14.29%) (referred to as XYL-SORB-EUT + PCT), (3) XYL–SORB with PCT and PEG 2000 (7.81%) (referred to as XYL-SORB + PCT + PEG 2000) and (4) XYL-SORB and PCT with PEG 6000 (7.81%) (referred to as XYL-SORB + PCT + PEG 6000).
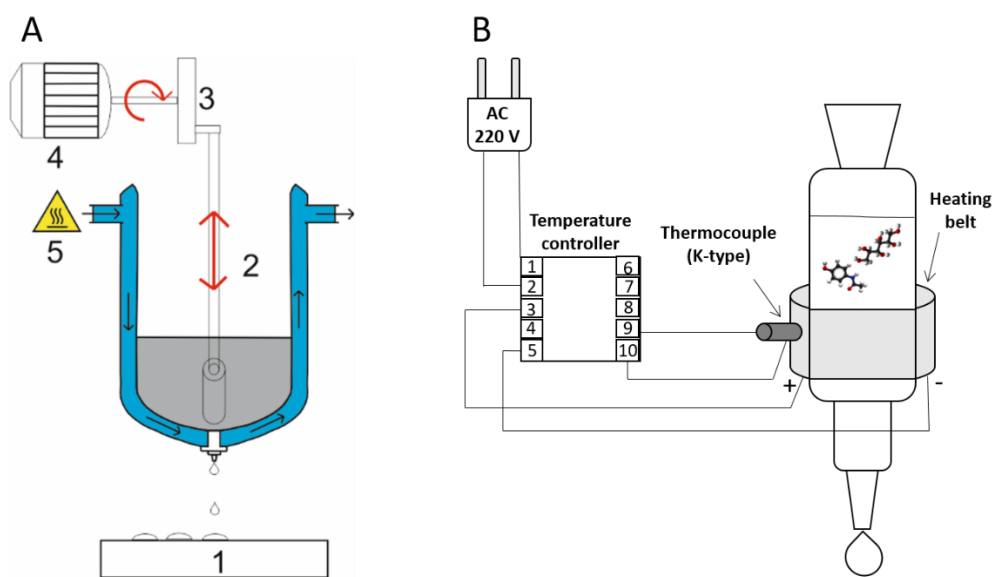

Fig. 4: One-drop pastillation device (1 - temperature controlled plate, 2 - double walled vessel, 3 - crank shaft, 4 - engine, 5 - thermostat) (A), heated pipette (B).

4.2.2. Instrumental analytical investigations applied for preformulation

4.2.2.1. X-ray powder diffraction (XRPD)

XRPD analysis was performed with a Bruker D8 Advance diffractometer (Bruker AXS GmbH, Karlsruhe, Germany) with Cu K λI radiation (λ = 1.5406 Å) and a VÅNTEC-1 detector. The samples were scanned at 40 kV and 40 mA. The angular range was 3° to 40° 2θ, at a step time of 0.1 s and a step size of 0.007° in a quartz holder, at ambient temperature and RH. All manipulations, Kα 2-stripping, background removal and smoothing of the area under the peaks of diffractograms were performed with DIFFRACTPLUS EVA software. The determination of the polymorph forms was based on the Cambridge Crystallographic Data Centre (CCDC ID: AI631510) X-ray powder diffractograms.

4.2.2.2. Differential scanning calorimetry (DSC)

DSC measurements were carried out with a Mettler-Toledo 821^e DSC instrument (Mettler-Toledo GmbH, Switzerland). Samples were crimped in aluminium pans and were examined at different temperature intervals and heating rates under a constant argon flow of 150 mL/min. Every measurement was normalized to sample size and was evaluated with STARe Software.

4.2.2.3. Viscosity measurement

Rheological measurements were carried out at 110°C using a Physica MCR101 rheometer (Anton Paar GmbH, Graz, Austria). A parallel-plate measuring device was used with a diameter of 25 mm and 0.20 mm gap height. Shear rate was increased from 0.1 to 100 1/s in a controlled rate mode. Shearing time was 300 s.

4.2.2.4. Contact angle measurement

The melted compositions were cast on a slide, where they solidified with a flat surface on which contact angle measurements were carried out. The contact angle (θ) was determined by means of the sessile drop technique, using an OCA 20 Optical Contact Angle Measuring System (Dataphysics, Filderstadt, Germany) and the method of Wu. The liquid mediums used for our contact angle measurements included bidistilled water (interfacial tension of polar component (γp) = 50.2 mN/m, interfacial tension of disperse component (γd) = 22.6 mN/m) and diidomethane (γp = 1.8 mN/m, γd = 49 mN/m). Polarity percentage was calculated from the interfacial tension of the polar component (γp) and the surface free energy (γ) values as follows:

$$Polarity\,(\%) = \left(\frac{\gamma^p}{\gamma}\right) * 100 \quad (1)$$

4.2.3. Dosage form investigations

4.2.3.1. Determination of flowability parameters

The parameters of flowability were determined with software-controlled PharmaTest PTG-1 powder testing equipment (PharmaTest, Hainburg, Germany). The powder flow was controlled by sensors and the time was measured for 100 mL of spray-dried material to flow, the angle of repose (α), the volume of the heap and the bulk density of the sample are calculated from the mass and height of the formed powder heap.

4.2.3.2. Particle size distribution (PSD)

Particle size distributions of the spray-dried powders were determined by laser diffraction using Malvern (Malvern Mastersizer Scirocco 2000; Malvern Instruments Ltd., Worcestershire, UK). Air was used as the dispersion medium for the microcomposites from the entrance to the sample cell. Approximately 500 mg of product was loaded into the feeder tray. The particle size distribution was characterized by the d(0.5), D[3,2] and D[4,3] value.

4.2.3.3. Scanning electron microscopy (SEM)

The morphology of the particles was examined by SEM (Hitachi S4700, Hitachi Scientific Ltd., Tokyo, Japan). A sputter coating apparatus (Bio-Rad SC 502, VG Microtech, Uckfield, UK) was applied to induce electric conductivity on the surface of the samples. The air pressure was 1.3–13.0 MPa. Briefly, the samples were sputter-coated with gold–palladium under an argon atmosphere, using a gold sputter module in a high-vacuum evaporator and the samples were examined at 10 kV and 10 A. The shape of PCT containing microcomposites was examined by analysing several SEM images with the ImageJ software environment.

4.2.2.4. Raman spectroscopy (Raman)

The uniformity of PCT content in the pastilles was investigated with Cobalt TRS 100 instrument (Cobalt Light Systems Ltd., Abingdon, UK) over the wavenumber range 1700-200 1/cm. Each reported spectrum is the average of at least 3 scans with an exposure time of 1 s, a laser power of 0.4 W and a laser spot size of 8 mm.

For the determination of different PCT polymorphs, a Thermo Fisher DXR Dispersive Raman instrument (Thermo Fisher Scientific. Inc., Waltham, MA, USA) equipped with a CCD camera and a diode laser operating at a wavelength of 780 nm was used. Raman measurements were carried out with a laser power of 12 mW at a slit aperture size of 25 μm on a spot size of 2 μm, with an exposure time of 6 s, for a total of 48 scans in the spectral range 1700-200 1/cm with cosmic ray and fluorescence corrections.

The PCT-containing pastilles were investigated by Raman chemical mapping to localize the different forms of PCT in the composition. A 2775 μm * 60 μm size surface were analysed with step size of 10 μm with an acquisition time of 3 sec per spectrum. The mapping was carried out with a laser power of 12 mW at 25 μm slit aperture size. The chemometric processing of vibrational chemical images was studied by multivariate curve resolution alternating least squares (MCR-ALS) chemometric method. The Raman spectra were normalized in order to eliminate the intensity deviation between the measured areas.

4.2.2.5. Geometrical parameters and hardness

The diameter and the height of 20 pastilles were measured with a screw micrometer (Starrett Co., Athol, MA, USA) and their masses were measured using an analytical scale (Mettler Toledo AX205 Delta Range analytical scale, Mettler Toledo GmbH, Greifensee, Switzerland).

The hardness of the pastilles was analysed by a Heberlein hardness tester (Heberlein & Co. AG, Switzerland). Five randomly selected pastilles were investigated to calculate the average and the standard deviation.

4.2.2.6. Drug content determination

100 mg of microcomposites and a powdered pastille plus 15 mL of methanol was shaken in a 100 mL volumetric flask until the powder got dissolved. Then 85 mL of water was added to adjust the volume to 100 mL. Next, a 1 mL aliquot was transferred to a 100 mL volumetric flask and was mixed with methanol/water 15:85 to 100 mL. The dissolved amount of PCT was analysed spectrophotometrically at 244 nm (PerkinElmer, Lambda 20 spectrophotometer, Dreieich, Germany) (Behera et al., 2012).

4.2.4.5. In vitro dissolution studies

The dissolution profile of PCT from microcomposites and pastilles of different compositions was determined according to the USP-2 paddle method (Pharmatest, Heinburg, Germany). The rotating velocity of the paddle within the dissolution vessel was 75 rpm. The dissolution studies were carried out in 100.0 mL of phosphate buffer solution at pH 6.8 ± 0.1 characteristic of the oral cavity and at normal body temperature of $37 \pm 0.5°C$, as well as in 900.0 mL of 0.1 N HCl at a gastric pH of 1.2 ± 0.1 at $37 \pm 0.5°C$ (Mashru et al., 2005, Gahel et al., 2009). At predetermined time intervals, 5 mL samples were taken and filtered immediately (using a Minisart SRP 25, Sartorius, Göttingen, Germany; pore size: 0.2 μm,), and the amount of dissolved drug was determined spectrophotometrically at 244 nm (PerkinElmer, Lambda 20 spectrophotometer, Dreieich, Germany).

5. RESULTS AND DISCUSSION

5.1. Preformulation studies of TRE based microcomposites

In the preformulation we investigated and quantified the physical changes of the spray-dried amorphous TRE through the use of various analytical techniques. The recrystallization kinetics can be followed, which is important because of the appearance of polymorphic forms. TRE was chosen for carrier because it is often used as a sweetening or taste masking agent formulated with spray-drying (Ógáin et al., 2011, Islam et al., 2008, Pomázi et al., 2011, Maurya et al., 2005, Maurya et al., 2005, Moran et al., 2007, Amaro et al., 2015) in pharmaceutical technology.

5.1.1. Determination of calibration curves with XRPD

Physical mixtures of spray-dried (amorphous) and the two different crystalline forms of TRE were prepared to achieve 0, 5, 10, 30, 50, 70, 90, 95 and 100% crystalline content by mass. The components were weighed to a total amount of 0.50 g and were mixed until homogeneous in a trituration mortar. The peak intensities of the individual components are proportional to the quantities of components in the mixture. Three characteristic peaks from each were selected from the diffractograms of TRE dihydrate (at 8.531°, 12.552° and 14.224° 2θ) and anhydrous TRE (at 6.572°, 20.351° and 24.792° 2θ). Multiple linear regression (MLR) was used to determine the calibration curve. The dependent variable was the crystallinity and the independent variables were the relative intensity values at chosen 2θ values. After the determination of the degree of crystallinity from the w/w ratio of the physical mixtures, a calibration curve was fitted. The linear regression of the data produced an $r^2 = 0.995$ and a slope of 0.990 for TRE dihydrate (Fig. 5A.). For anhydrous TRE, $r^2 = 0.997$ and the slope was 0.997 (Fig. 5B.).
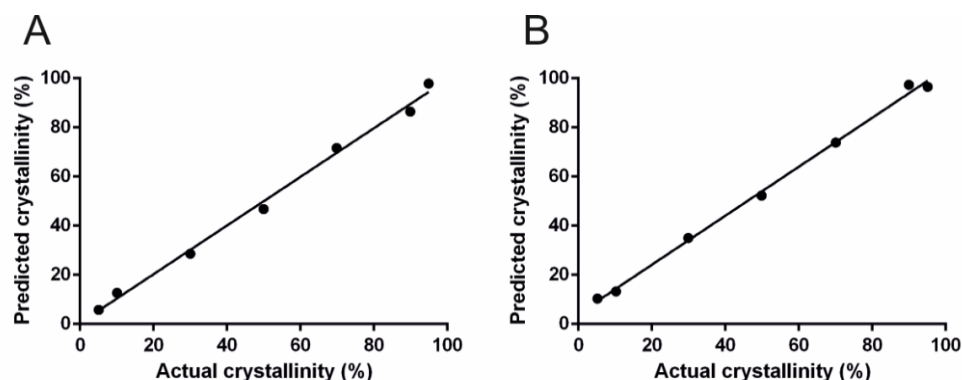

Fig. 5: Relation between predicted and actual crystallinity of physical mixtures of crystalline TRE dihydrate - amorphous form (A), anhydrous TRE - amorphous form (B) determined by conventional XRPD

Because of the well-correlating r^2 values, the degree of crystallinity can be quantified.

5.1.2. Calculation of recrystallization kinetics

The recrystallization kinetics was modelled by using the Avrami equation (Eq. 2):

$$1 - \alpha = \exp(-Kt^n) \quad (2)$$

where α is the fraction of recrystallized TRE at time t, K is the rate constant and n is the Avrami index, a parameter characteristic of the nucleation and growth mechanism of crystals.

The fraction of recrystallized TRE (α) was calculated from the area under the characteristic peaks using the following equation (Eq. 3):

$$\alpha = \frac{A_{crystalline}}{A_{crystalline} + A_{amorphous}} * 100 \quad (3)$$

where α is the crystalline fraction, A is the area of characteristic crystalline peaks and amorphous sign. The XRPD instrument was calibrated every day with corundum during the 28-day measurement to minimalize the day to day intensity changes in XRPD emission.

The Avrami parameters were obtained from the experimental data by using the double logarithmic form of Eq. (4):

$$\ln[-\ln(1 - \alpha)] = \ln K + n \ln t \quad (4)$$

The activation energy of the recrystallization was calculated by using the Arrhenius equation (Eq. 5):

$$k = k_0 \exp\left(-\frac{E_a}{RT}\right) \quad (5)$$

In the model, k is the rate constant at temperature T, k_0 is the frequency factor, R is the gas constant and E_a is the activation energy. The logarithmic form of Eq. (5) allows the determination of the activation energy (Eq. 6) (Mazzobre et al., 2001).

$$\ln k = \ln k_0 - \frac{E_a}{RT} \quad (6)$$

5.1.3. Hot-humidity stage XRPD analysis (HH-XRPD)

For the development and qualification of solid compositions, it is important to investigate and determine changes of the crystalline phases or the effect of crystallization inhibitor when materials are exposed to changing humidity and temperature. By increasing the RH in small intervals (10%) at the exact temperature, good estimation could be gained in a few hours at the exact temperature about the behaviour of the samples, which could be reflected in the results of the conventional stability test. There is no need for additional hygrostats and extra samples, the measurement takes place directly in the chamber connected to the instrument. The RH was set at

16

10, 20, 30, 40, 45, 50, 60 and 70% at 40 °C, 60 °C and 70 °C controlled temperatures, and the samples were kept in each condition for 1 h before measurement. These investigations are not only important to establish procedures for storage, production and shipment, but also emulate the digestion of the respective drug and its first interactions with the patient. In this context HH-XRPD was used to predict the tendency to recrystallization, which is presented in Table 4.

Table 4 The degree of crystallinity calculated from the HH-XRPD data (A: amorphous, h-form: dihydrate, β-form: anhydrous)

Time; RH	Form of TRE			Degree of crystallinity (%)		
(min; %)	40 °C	60 °C	70 °C	40 °C	60 °C	70 °C
0; 0	A	A	A	0	0	0
60; 10	A	A	A	0	0	0
120; 20	A	A	A	0	0	0
180; 30	A	A	h-form	0	0	11.7
240; 40	A	A	h-form	0	0	31.1
300; 45	h-form	h-form	h-form	14.8	27.2	65.2
360; 50	h-form	h-form	h-form	35.8	62.4	100
420; 60	h-form	h-form	β/h-form	70.2	78.8	100
480; 70	h-form	h-form	β/h-form	100	100	100

The samples measured at 40 and 60 °C were amorphous up to 45% RH, when recrystallization began in the TRE dihydrate polymorph. The samples measured at 70 °C were amorphous up to 30% RH, than they recrystallized to dihydrate form and up to 60% RH the anhydrous form appeared, too. The determination of the polymorph forms was based on the Cambridge Crystallographic Data Centre (CCDC ID: AI631510) X-ray powder diffractograms (Fig. 6).
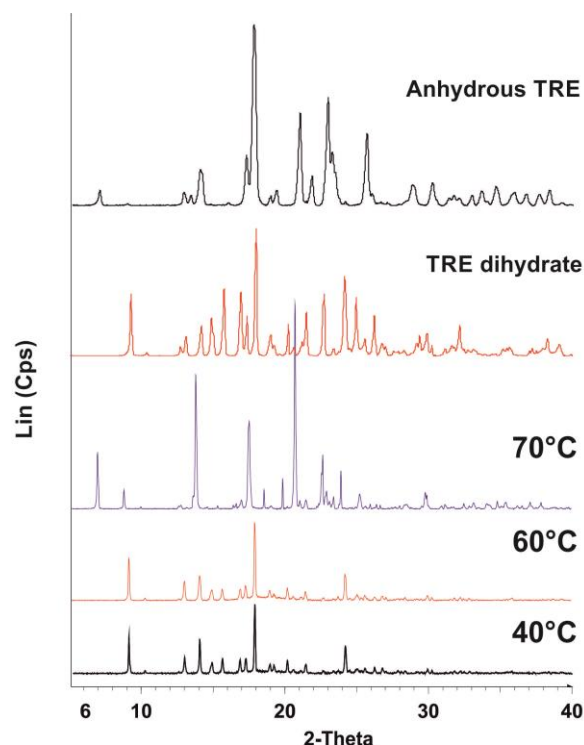
Fig. 6: The recrystallized TRE polymorphs at 40, 60 and 70 °C controlled temperatures

The diffractograms measured at 40, 60 and 70 °C showed an increasing tendency to recrystallization. The relative intensities and integrals of the peaks increased with the temperature, therefore the temperature influences the tendency of TRE to recrystallize.

To investigate the temperature dependence of recrystallization, the recrystallized fractions were plotted against time for each temperature. As the calibration showed, before XRPD the method could be used for quantitative measurements. The curves obtained by fitting the Avrami Eq. (2) were in good agreement ($r^2 > 0.992$) with the experimental points (Fig. 7).
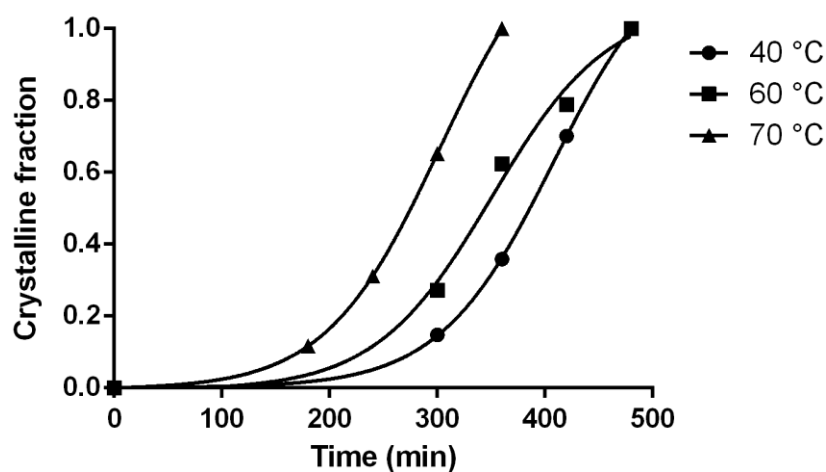

Fig. 7: Crystallization kinetics by fitting the Avrami equation to the HH-XRPD data

The sigmoidal curves showed that increased temperature accelerates the recrystallization and reduces the crystallization half-time. To acquire information about the velocity of the process and the dimensions of crystal growth, the parameters K and n were determined by using the linearized Avrami equation (Eq. 4) (Fig. 8) and the activation energy was calculated via the logarithmic form of the Arrhenius model (Eq. 6) (Table 8).
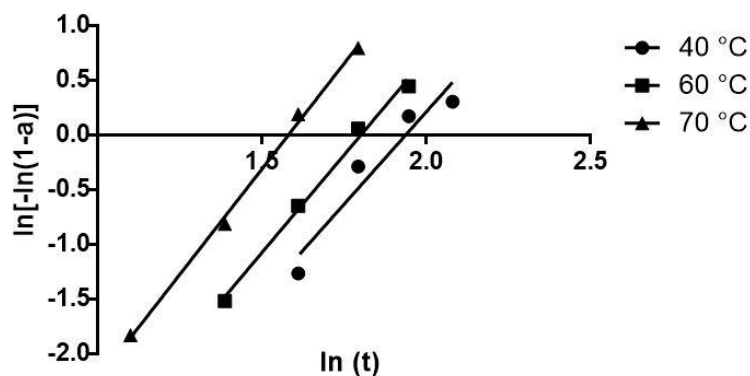

Fig. 8: Determination of the Avrami parameters n and K from HH-XRPD data

5.1.4. Analysis of samples stored in hygrostats (XRPD)

Spray-dried products were stored for 28 days at 40 °C and 60 °C, in 3-3 hygrostats, where the RH was set to 30%, 40% and 50% RH. In each desiccator and hygrostat, there was a digital humidity meter during the storage for controlling the relative humidity (Table 5). With this investigation we can get information about suitable storage conditions of spray-dried products.

Table 5 Different storage conditions of amorphous samples

Temperature (°C)	RH (%)	Storage time (day)
	30±5	28
40±2	40±5	28
	50±5	28
	30±5	28
60±2	40±5	28
	50±5	28

The fractions of recrystallized TRE were measured at different times during the 28 days of storage. The conventional XRPD analysis showed that the samples stored at 40 °C, 30% and 40% RH, and at 60 °C, 30% RH remained amorphous. The samples stored at 40 °C, 50% RH recrystallized in the dihydrate form. The storage conditions at 60 °C, 40% RH resulted in the recrystallization of the anhydrous form, and in the sample stored at 60 °C, 50% RH, both polymorphs appeared, the h-form (dihydrate) and the β-form (anhydrous) (Fig. 9).

19
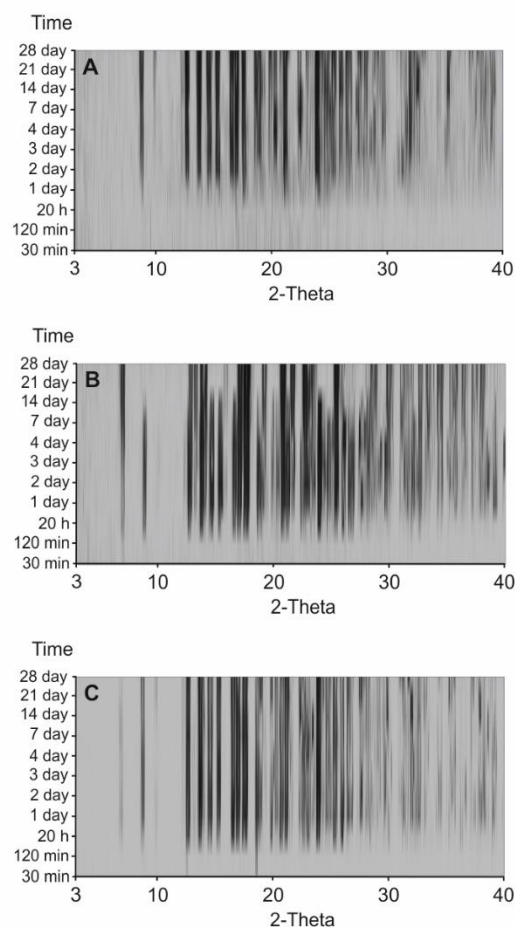
Fig. 9: Top-view pictures of XRPD investigations of samples stored for 28 days at 40 °C, 50% RH (A), 60 °C, 40% RH (B) and 60 °C, 50% RH (C)

Figure 9B shows that the stripe at 8.531° 2θ disappears after storage for 14 days, and there is a polymorph conversion of TRE dihydrate into the anhydrous form, confirmed by the characteristic thick stripe at 6.572° 2θ. Figures 9A and C do not indicate any polymorph conversion. The diffractograms measured after 28 days of storage are shown in Fig. 10.

20

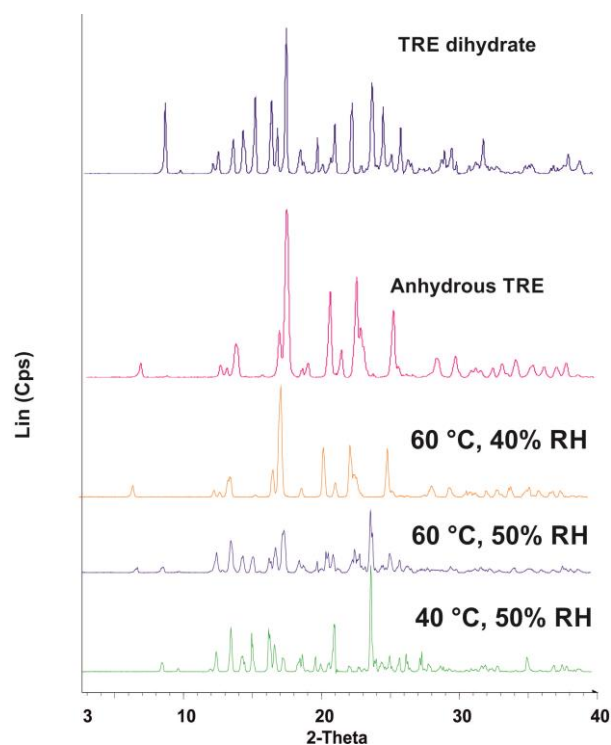**Fig. 10:** Diffractograms of samples stored for 28 days under different conditions, compared with TRE forms in CCDC

The degree of crystallinity of the recrystallized polymorphs was calculated by evaluating the diffractograms in Fig. 10 according to the MLR model. The results showed that amorphous fractions remained in the samples, but decreased at higher temperature and RH (Table 6) in comparison with diffractograms of TRE in CCDC.

Table 6 The degree of crystallinity calculated from the XRPD data after 28 days

Condition	Form of TRE			Quantity (%)		
t; RH	amorphous	dihydrate	anhydrous	amorphous	dihydrate	anhydrous
(°C; %)		(h-form)	(β-form)		(h-form)	(β-form)
40; 30	+	-	-	100	0	0
40; 40	+	-	-	100	0	0
40; 50	+	+	-	63.1	36. 9	0
60; 30	+	-	-	100	0	0
60; 40	+	-	+	25.5	0	74.5
60; 50	+	+	+	0.4	58.2	41.5

By means of the 28-day stability tests, the different recrystallized polymorph forms can be detected and quantified. The results showed that at 40 °C and 50% RH the dihydrate was detected, but the bulk of the investigated sample remained amorphous. Storage at 60 °C and 40% RH resulted in the appearance of the anhydrous form and only a minor proportion of the sample remained amorphous. At 60 °C and 50% RH, both polymorphic forms were detected and almost the whole sample recrystallized. This conventional method is often used as a long-term stability test in the development of a drug delivery system.

5.1.5. DSC investigation

Samples loaded at different RH (10, 20, 30, 40, 45, 50 and 70%) in the XRPD humidity chamber for 1 h were crimped in aluminium pans and were examined in the temperature interval 25-250 °C at a heating rate of 10 °C/min. The amount of recrystallized TRE dihydrate was calculated from the integral of the endothermic peaks at 108 °C, which is the melting point of TRE dehydrate β-form. Table 7 shows the enthalpy changes of melting and the calculated crystalline fraction at different temperatures with increasing the RH.

Table 7 Enthalpy changes (ΔH) of melting and the crystalline fraction (α) at different temperatures with increasing the RH

RH (%)	ΔH (J/g)			α (%)		
	40 °C	60 °C	70 °C	40 °C	60 °C	70 °C
30	-	-	17.1	0	0	11
40	-	-	27.3	0	0	17.6
45	44.5	33.0	128.1	28.7	21.3	82.7
50	63.8	66.0	137.6	41.2	42.6	88.8
60	130.4	123.5	141.4	84.2	79.7	91.3
70	153.5	153.0	153.8	99.1	98.8	99.3

The amount of crystalline fractions showed that the recrystallization of the amorphous sample is more significant with increasing RH and at 70% RH total recrystallization of the samples occurred at all 3 temperatures. The comparison of these results with those in Table 4 shows that DSC and HH-XRPD measurements correlate well. With this method, only the fraction of recrystallized TRE dihydrate can be determined. Since the anhydrous form has high melting point, the dihydrate

form is conversed into the anhydrous form resulting in false measurement data. However, the method can be used for fast stability testing during the preformulation.

The crystalline fractions calculated from the DSC data (Table 7) were plotted against time for each temperature with $r^2 > 0.983$ (Fig. 11).
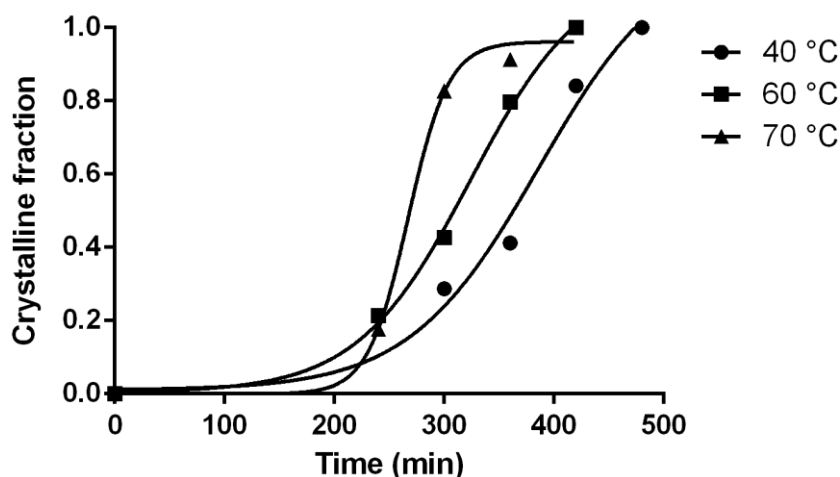

Fig. 11: Crystallization kinetics by fitting the Avrami equation to the DSC data

The sigmoidal curves showed that increased temperature accelerates the recrystallization and reduces the crystallization half-time. To acquire information about the velocity of the process and the dimensions of crystal growth, the Avrami parameters should be determined. The parameters K and n were determined by using the linearized Avrami equation (Eq. 4). A plot of ln [-ln (1-α)] against ln (t) yields a straight line with slope n and intercept ln K (Fig. 12). The activation energy was calculated via the logarithmic form of the Arrhenius model (Eq. 6). Table 8 shows the parameters of the recrystallization process.
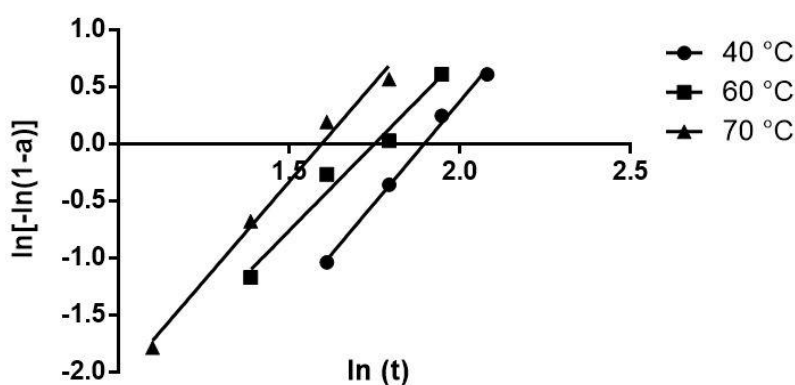

Fig. 12: Determination of Avrami parameters n and K from DSC data

Table 8 Avrami parameters and activation energy of recrystallization investigated with HH-XRPD and DSC

Method	t (°C)	n	K	E_a (kJ mol^{-1})
	40	3.373	5.79E-04	
HH-XRPD	60	3.566	1.70E-03	47.215
	70	3.934	2.84E-03	
	40	3.378	1.69E-03	
DSC	60	2.989	5.98E-03	41.645
	70	3.156	6.29E-03	

The values of rate constant K show that increasing temperature accelerates the recrystallization process. There are differences between the measurement results of the two methods, but the results correlate well. The comparison of the HH-XRPD data with the DSC measurements demonstrates that increasing temperature accelerates the recrystallization and reduces the crystallization half-time. The parameters K and n were determined by using the linearized Avrami equation (Eq. 3) (Fig. 12).

5.2. Incorporation of PCT in the microcomposites

After the preformulation studies of TRE containing carrier systems PCT was incorporated with the aim to produce microcomposites for preparation of dose sipping form. Because spray-drying results in amorphization in TRE, the dissolution time is fast enough for the liberation of the API to occur in the liquid media during application. By assuring low RH during the storage of the preparation, the amorphous form can be preserved. To reduce the adhesion of microparticles due to the electrostatic charge, PEGs were added to the formulation. After spray-drying the PCT-containing microcomposites, dosage form investigations were carried out. First, we studied the moisture content, flowability of the products, then the structure of microcomposites was checked before and after storage, finally the drug amount and the dissolution extent were measured.

5.2.1. Moisture content determination and flowability study

Analysing the moisture content of microcomposites is important because of the microbiological stability, as TRE is a good soil of microorganisms and to avoid recrystallization. That is why we tried to minimalize it in the samples. Moisture content determination was carried out with thermogravimetric analysis (Mettler-Toledo TG/DSC1) in the temperature interval 25-300 °C, at a heating rate of 10 °C/min under constant argon (150 mL/min) and nitrogen (60mL/min) flow. Another important parameter is flowability because of the filling of microcomposites in the straw. The

flowability parameters and moisture content of spray-dried PCT containing samples were determined (Table 9).

Table 9 Moisture content and flowability parameters of spray-dried samples

Sample	Flow time (s)	Angle of repose (°)	Volume (mL)	Mass (g/100 mL)	Bulk density (g/mL)	Moisture content (%)
TRE-PCT	16.5	19.6	46.6	16.65	0.167	6.24
TRE-PCT- PEG 2000	12.6	8.8	27.5	14.31	0.143	4.05
TRE-PCT- PEG 6000	9.6	6.3	20.2	12.81	0.128	2.79

It can be concluded that the PEG containing samples have shorter flow time because of the low electrostatic charge. PEG containing samples also have lower moisture content, which can predict a better microbiological stability.

5.2.2. DSC investigation of spray-dried samples

The thermal behaviour of the fresh spray-dried samples and different compositions after 3 months of storage in a desiccator (25±2 °C, 32±5% RH) was investigated with DSC (Fig. 13).
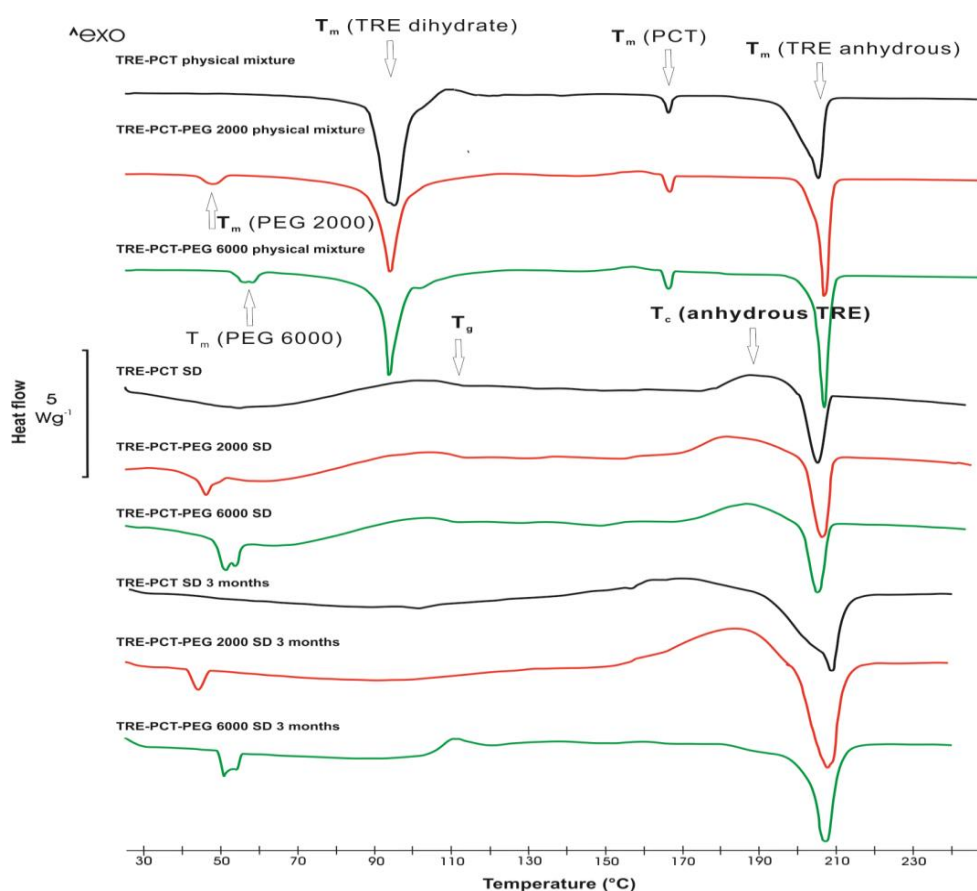

Fig. 13: DSC curves of the different compositions

25

When comparing the DSC curves of spray-dried samples to physical mixtures it can be concluded that spray-drying resulted in amorphization in the TRE-PCT-PEG samples, the glass transition temperatures (T_g) can be detected. PEGs preserved their semicrystalline form, TRE and PCT have no influence on their structures and the melting points can be detected. Each of the three compositions was stable up to 160 °C, over it the recrystallization of TRE anhydrous form took place, which confirms its melting point at 208 °C. The samples stored for 3 months remained amorphous and stable up to 160 °C.

5.2.3. XRPD investigation

The structure of the spray-dried and the stored samples was also investigated with XRPD and compared to that of the physical mixtures (Fig. 14).
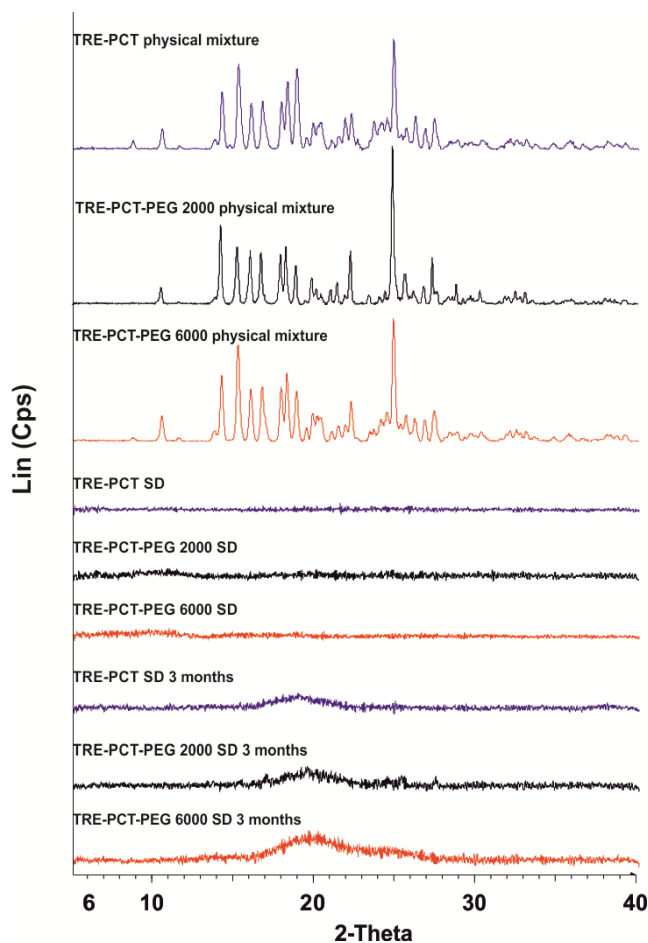

Fig. 14: XRPD diffractograms of spray-dried samples and physical mixtures

The XRPD diffractograms show spray-drying resulted in amorphization, the characteristic peaks of crystalline agents could not be observed, the samples remained amorphous after 3 months of storage.

5.2.4. PSD and SEM images

As moisture content determination and flowability studies showed that PEG containing samples have better properties, the further investigations were carried out only with these samples. The particle size (Fig. 15) and the PSD (Table 10) of spray-dried PEG containing samples were determined with laser diffraction analysis.
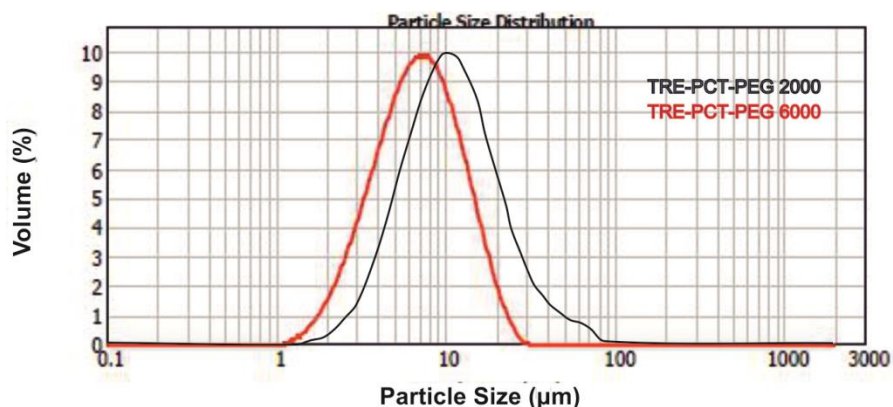

Fig. 15: PSD of TRE-PCT-PEG containing samples

Table 10 Influence of different PEGs on PSD of microcomposites

Samples	d(0.5) [µm]	D[3,2] [µm]	D[4,3] [µm]
TRE-PCT-PEG 2000	10.711	8.893	13.685
TRE-PCT-PEG 6000	6.897	5.667	7.938

Laser diffraction analysis shows the average particle size of PEG 6000 containing microcomposites is smaller than that of PEG 2000 containing ones. Spray-drying resulted in monodisperse distribution in both PEG containing compositions. Their morphology was investigated with SEM (Fig. 16).
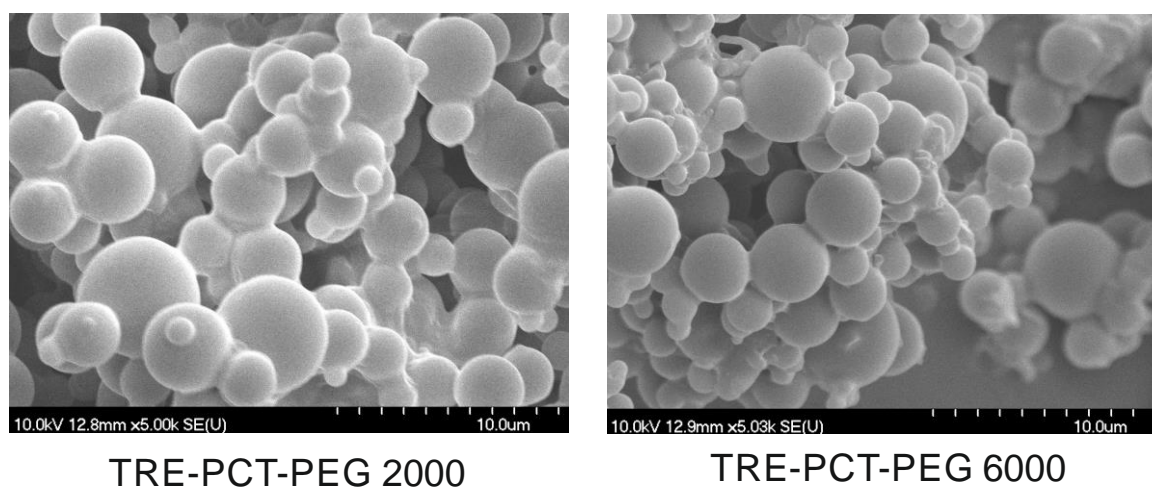

TRE-PCT-PEG 2000   TRE-PCT-PEG 6000

Fig. 16: SEM images of PEG containing samples

27

The SEM images reveal that in both cases spherical microcomposites were produced, their surface was uniform, no fracturing could be observed on it.

5.2.5. Drug content determination

Before the *in vitro* dissolution studies, the drug content of the microcomposites was determined. 100 mg from each composition (TRE-PCT, TRE-PCT- PEG 2000 and TRE-PCT-PEG 6000) was investigated. The calculated and measured PCT contents were 14.29 mg, spectrophotometrically 14.24 ± 0.71 mg, respectively.

5.2.6. In vitro dissolution

According to the drug content determination, 280.89 mg of microcomposites contains the required dose of PCT (40.0 mg). In the *in vitro* dissolution studies three parallel measurements were carried out, in which the PCT dissolutions of different PEG containing microcomposites were compared at the oral cavity pH (pH 6.8±0.1) and in the gastric juice (pH 1.2±0.1) (Figs 17 and 18).

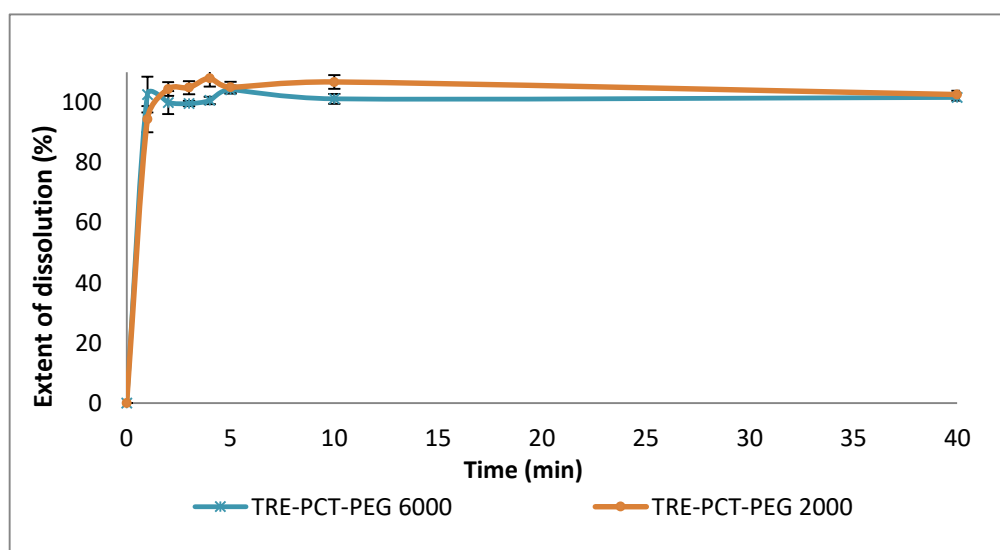**Fig. 17:** Dissolution extents of microcomposites at the oral cavity pH of 6.8±0.1 and 37±0.5 °C (average value±SD, n=3)

In both cases, the PCT was practically fully dissolved from the microcomposites in the medium of the oral cavity (pH 6.8±0.1) within 2 min. The fast dissolution kinetics can be explained with the high specific surface.
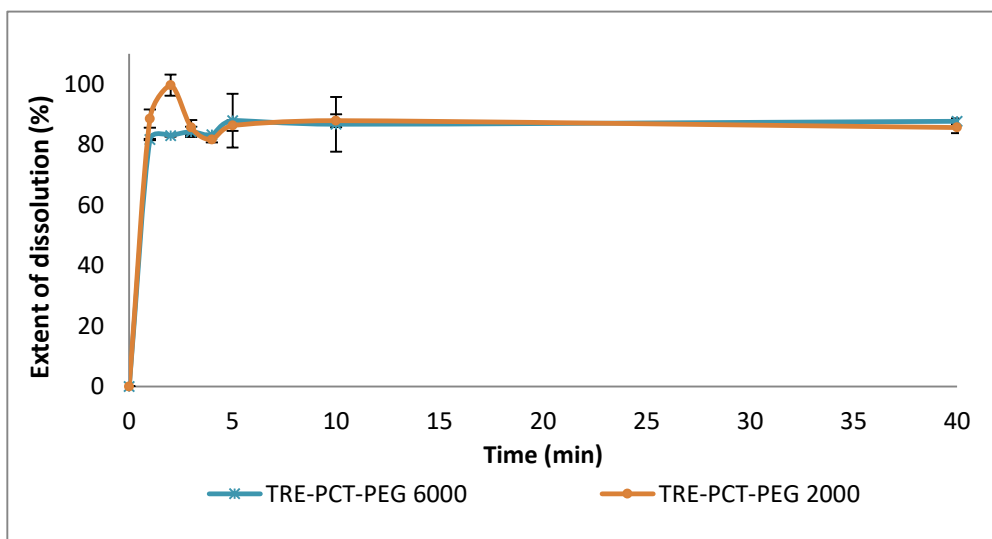
Fig. 18: Dissolution extents of microcomposites at the gastric pH of 1.2±0.1 and 37±0.5 °C (average value±S.D., n=3)

In the acidic medium (pH 1.2±0.1), the PCT also practically fully dissolved from the microcomposites within 2 min. A burst effect can be observed on the curve of the PEG 2000 containing product, which can be explained with the amorphization of the sample.

Summary

In the preformulation study of spray-dried microcomposites, the three analytical methods (HH-XRPD, XRPD, DSC) were compared to investigate the recrystallization of amorphous TRE. In this light, the suitable choice of the storage conditions can protect the amorphous TRE samples from crystallization. In view of these results, TRE is applicable for formulating API containing microcomposites with spray-drying.

After the incorporation of PCT in microcomposites it was revealed that the use of PEGs in the formulation decreased the electrostatic charge of the particles and produced good flow properties. Spray-drying resulted in amorphization in the samples (TRE, PCT), T_g could be determined, PEGs remained semicrystalline in the formulations. The amorphous compositions are stable under 160 °C, at higher temperature the recrystallization of amorphous TRE begins. After 3 months the samples remain amorphous at ambient temperature and RH. Dissolution studies showed PCT was fully dissolved in the medium after 2 min. According to these results, the two PEG containing compositions can be utilized for the formulation of dose sipping form and paediatric application.

5.3. Preformulation of PCT containing pastilles produced with melt technology

5.3.1. Phase diagrams of sugar alcohols

In the development of a carrier system (DDS) for melt technology, the physico-chemical interactions of the components should be examined in order to determine the optimum composition for pastille-forming method.

Determination of the phase diagram of XYL–MAN and XYL–SORB physical mixtures is necessary to find the eutectic melting temperature and to understand the mechanism of crystallization of the pastille. 100 mg of solid XYL–MAN and XYL–SORB dispersions of different ratios were prepared and the melting temperatures for the phase diagram were collected with DSC (Fig. 19).
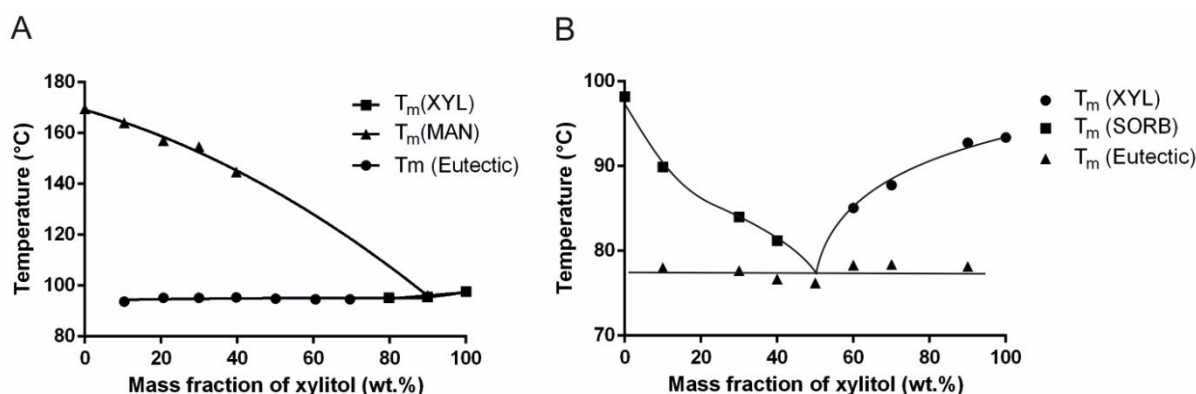

Fig. 19: Phase diagrams of the XYL–MAN (A) and XYL–SORB (B) systems by plotting the melting points of the compositions versus their different mass ratios

The point of interception of the curves on the binary phase diagrams indicated the eutectic concentration at 90 wt.% XYL–10 wt.% MAN and 50 wt.% XYL–50 wt.% SORB. The melting temperature of pure XYL was detected at 97.6°C. The melting temperature of the XYL–MAN eutectic composition dropped to 95.5 °C, of XYL-SORB eutectic composition proved to be 76.9 °C. The phase diagrams suggest that phase separation between XYL–MAN and XYL-SORB is theoretically possible. The melting temperature of pure MAN (169.5 °C) can be decreased by more than 70 °C in the eutectic mixture.

Eutectic melting enthalpy *ΔH* (J/g) values for the different XYL–MAN and XYL–SORB dispersions, as determined by the integration of the eutectic peak area, were plotted versus the mass ratio of xylitol in order to construct the Tamman's triangle showing the eutectic ratio of sugar alcohols at the maximal melting enthalpy value (Fig. 20) (Rycerz et al., 2013).
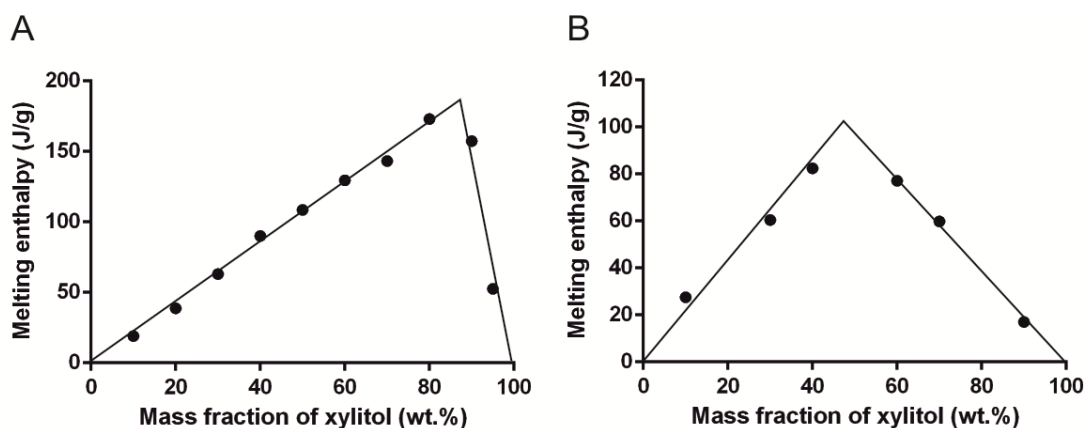
30

Fig. 20: Construction of the Tamman's triangles of XYL–MAN (A) and XYL–SORB (B) by plotting the eutectic melting enthalpies ΔH versus their different mass ratios

The enthalpy of the eutectic compositions is maximal ($\Delta H_{XYL-MAN}$ =191.2 J/g; $\Delta H_{XYL-SORB}$=101.1 J/g) and converges to zero for compositions corresponding to the pure components. These data confirm that XYL–MAN form a eutectic mixture in a 90–10 wt.% and XYL–SORB in 50–50 wt.% ratio. Because the eutectic mixture of XYL and MAN results in rapid solidification, it is necessary to apply PEG as softener material. According to the literature data, it has no influence on the recrystallization of the components (XYL, MAN and PCT) but promotes the formation of pastille dosage form (Bashiri-Shahroodi, 2007). The ternary phase diagram of xylitol, mannitol and PEG 6000 was also investigated in certain cases. 100 mg solid XYL–MAN samples in different ratios were prepared with a constant amount of PEG 6000 (7.81 %) to determine the ternary phase diagram. The melting temperatures were analysed by DSC at a heating rate of 2 °C min^{-1}. Parabolic curve fitting was applied to investigate the effect of the polymer on the eutectic concentration (Fig. 21). It turned out that, in the presence of this quantity of PEG 6000, the eutectic concentration of xylitol and mannitol was at 80 wt.% xylitol and 20 wt.% mannitol.
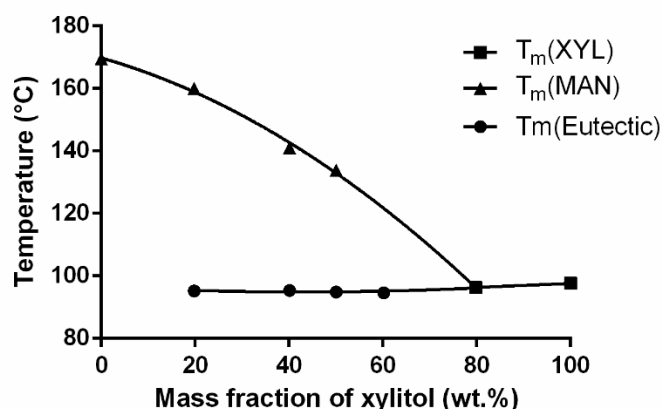

Fig. 21: The XYL–MAN phase diagram in the presence of a fixed amount of PEG (7.81 mg per 100 mg)

31

After identifying the eutectic composition of XYL–MAN in the presence of PEG 6000, we investigated the influence of PEG in the XYL–SORB composition, too. PEG 2000 (7.81%) and 6000 (7.81%) were added to the eutectic dispersions. The melting point (T_m) of the samples was examined in the temperature interval of 25-170 °C at a heating rate of 2°C/min under a constant argon flow of 150 mL/min (Fig. 22). Next, the samples were cooled to –40°C and then reheated to 110°C at a heating rate of 2°C min-1 under a constant argon flow of 150 mL/min and a nitrogen flow of 50 mL/min to study glass transition (T_g) (Table 11).
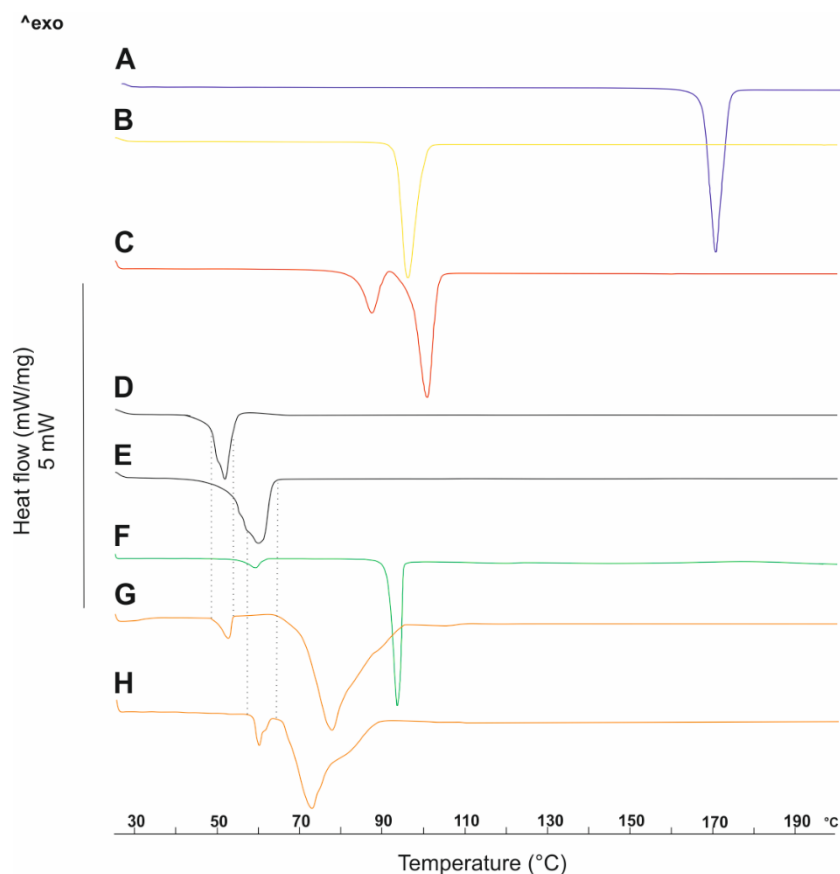
Fig. 22: DSC curves of the components, **A**: MAN, **B**: XYL, **C**: SORB, **D**: PEG 2000, **E**: PEG 6000, **F**: eutectic mixture of XYL-MAN with PEG 6000, **G**: eutectic mixture of XYL-SORB with PEG 2000, **H**: eutectic mixture of XYL-SORB with PEG 6000

It was found that during heating both PEGs melt separately from the compositions and have no influence on the eutectic composition of XYL–SORB. We suppose that the lower T_m and T_g values of the XYL–SORB–EUT+PEG 6000 mixture result from the interaction of PEG 6000 with one of the eutectic components (Table 11).

Table 11 Melting points (T_m) and glass transitions (T_g) of the XYL–SORB–PEG compositions and the pure components studied

Composition	First heating			Cooling	Second heating	
	T_m (°C)	T_{mPEG} (°C)	T_g (°C)	T_{cryst} (°C)	T_m (°C)	T_g (°C)
XYL	97.6	–	–	–	–	–19.5
MAN	166.1	–	–	114.1	166.1	–
SORB	98.2	–	–	–	–	–1.6
XYL–MAN–EUT	95.5	–	–	–	–	–16.9
XYL–MAN–EUT + PEG 6000	97.6	60.5	–	–	60.3	–16.2
XYL–SORB–EUT	76.9	–	–	–	–	–10.9
XYL–SORB–EUT + PEG 2000	77.6	51.8	–	–	51.8	–11.0
XYL–SORB–EUT + PEG 6000	72.4	60.0	–	–	60.1	–14.3

5.3.2. Optimization of eutectic formula

Our target was to develop a pastille containing 40 mg PCT. Since PEG 6000 was found to influence the eutectic concentration of XYL–MAN, a Box-Behnken experimental design was carried out to optimize the formulation as concerns the carrier. Three experimental factors (XYL, MAN and PEG 6000) were varied in the design, at 3 levels in 15 runs so as to construct the surface plot for the optimization process (Table 12) according to the recrystallization time.

Table 12 Variables and their levels in the Box-Behnken design

	Levels		
	-1	**0**	**1**
Independent variables (factors)	**Contents of components (wt.%)**		
XYL	48.13	61.25	75.94
MAN	6.88	15.31	12.31
PEG 6000	0	7.81	15.63

Recrystallization begins on the shell of the pastille and tends inwards to the core. If this process takes place too quickly, the dissolved melt components with higher melting temperatures (PCT and MAN) recrystallize first and their crystals sink to the bottom of the pastille, resulting in an inhomogeneous distribution. A composition was first sought in which recrystallization was slow enough to preserve the homogeneous distribution of the components. The experimental results

showed that each of the three components exerted a significant effect on the recrystallization. At a 95% confidence level, the coefficients differed from zero and the P-values were <0.05, the time of recrystallization depending significantly on the fractions of the components. The surface plot illustrates the recrystallization times of the different component ratios (Fig. 23).
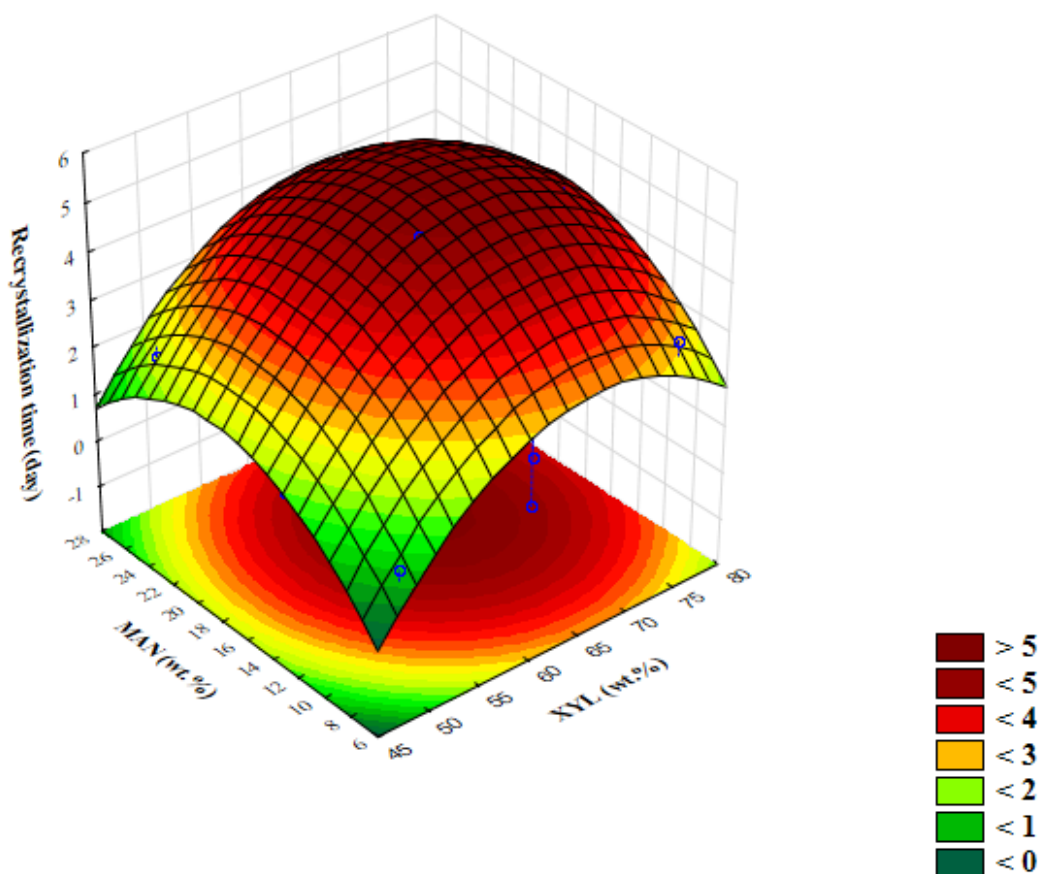

Fig. 23: Surface plot illustrating optimization of the XYL–MAN–PEG 6000 containing carrier

The surface plot depicts recrystallization times from 1 to 5 days. The maximum in the plot is observed at 61.25 wt.% XYL, 15.31 wt.% MAN, which corresponds to the eutectic composition. The composition also included 7.81 wt.% PEG 6000, and the PCT content of the pastille was 15.63 wt.%. The calculations indicated that the pastille mass should be ~256 mg containing the 40 mg of PCT. In case of XYL–SORB pastilles we used 38.28 wt.% XYL, 38.28 wt.% SORB (which corresponds to the eutectic composition), 15.63 wt.% PCT and 7.81 wt.% PEG 2000 / 6000, because PEGs had no significant influence on the eutectic concentration of sugar alcohols.

5.3.3. Viscosity measurements

The viscosity of the melted dispersions is a critical parameter for drop formation. High viscosity decreases molecular mobility, and therefore hinders recrystallization. For our viscosity measurements, all the dispersions were melted on a heated magnetic stirrer, then the melt was thermostated on the plate of the viscosity measuring device. Measurements were carried out at a constant temperature of 110°C. All measurements were performed in triplicate and the average values are shown in Table 13.

Table 13 Viscosity data of the compositions to be pastilled (n=3)

Composition	Viscosity (mPas)
XYL-MAN-EUT	347±5
XYL-MAN-EUT + PEG 6000 (7.81%)	352±6
XIL-SORB-EUT	368±3
XYL-SORB-EUT + PEG 2000 (7.81%)	370±20
XYL-SORB-EUT + PEG 6000 (7.81%)	359±13

The viscosity values of all samples were similar. The viscosity of the sample containing PEG 2000 was slightly higher than that of the one containing PEG 6000. This phenomenon was unexpected because the viscosity of pure PEGs is known to increase with their molecular weight. To clarify this behaviour of the samples, viscosity measurements were expanded using other compositions containing PEGs in different ratios (5%, 7.81%, 10%, 15%, 20%, 30%, 60%, 100%). Fig. 24 shows the viscosity of the different compositions.
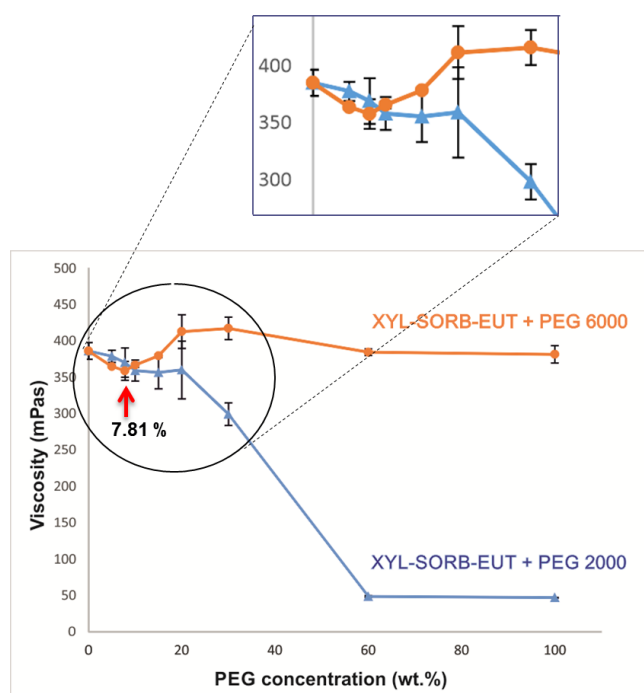

Fig. 24: Viscosity of XYL-SORB-EUT compositions containing different concentration of PEGs

35

It could be observed that the viscosity of pure XYL-SORB-EUT (368±3 mPas) and that of PEG 6000 (370±2 mPas) are almost the same. According to these results, significant changes in the viscosity of eutectic and PEG 6000 compositions could not be expected. Even so, our results showed the viscosity curve has a minimum value under 20 % PEG 6000 concentration. PEG 2000 has significantly lower viscosity than pure XYL-SORB-EUT, but the increase of the concentration of PEG 2000 in the composition led to the drastic decrease of the viscosity (Fig. 24). The viscosity changing effect of PEGs strongly depends on their molecular weight. Therefore in low PEG concentration PEG 2000 and 6000 containing samples show a similar viscosity value.

5.3.4. Contact angle measurements

The wettability of the pastilles has a significant influence on the dissolution rates and the release characteristics in oral drug delivery. Wettability is characterized by the contact angle of the liquid (water). A smaller contact angle indicates greater wettability of the pastille. To formulate an appropriately dissolving pastille, a well-wetting surface is a fundamental step. The polarity percentage can be calculated from the interfacial tension of the polar component (γ^p), the interfacial tension of disperse component (γd) and the surface free energy (γ) (Table 14).

Table 14 Contact angles (θ), surface free energies (γ) and polarities of compositions

Compositions	θ_{water} (°)	$\theta_{diiodomethane}$ (°)	γ^d (mN/m)	γ^p (mN/m)	γ (mN/m)	Polarity (%)
XYL-MAN-EUT	32.9±3.24	36.7±1.83	46.34	30.92	77.26	40.02
XYL-MAN-EUT + PEG 6000	34.7±1.79	44.3±2.58	38.21	32.47	70.68	45.94
XYL-MAN-EUT + PCT + PEG 6000	35.4±1.64	45.3±2.09	35.95	32.76	68.71	47.68
XYL-MAN-EUT + PCT	33.8±2.35	34.9±1.88	44.82	31.63	76.45	41.37
XYL-SORB-EUT	28.1±3.6	20.5±2.9	42.96	31.74	74.70	42.49
XYL-SORB-EUT + PEG 2000	17.0±1.47	29.7±1.62	39.98	36.60	76.58	47.79
XYL-SORB-EUT + PEG 6000	21.6±3.63	19.5±2.72	43.22	34.03	77.25	44.05
XYL-SORB-EUT + PCT	26.7±4.71	22.7±1.84	42.33	32.49	74.82	43.24
XYL-SORB-EUT + PCT + PEG 2000	34.0±1.82	47.9±2.91	32.41	33.17	65.58	50.58
XYL-SORB-EUT + PCT + PEG 6000	30.1±3.40	35.9±1.45	37.62	32.77	70.39	46.55

The results show that the PEGs increase the surface free energies and the polarity of the compositions without PCT. PCT dissolves in the melt of the eutectic and recrystallizes during the solidification; it has no effect on the value of γ. In the case of the compositions with PCT, the PEGs (mainly PEG 2000) decrease γ and increase the polarity, which promotes the wetting of the pastille, therefore the dissolution.

5.3.5. Pastillation of the carrier

Pastillation took place on the surface of a thermostated cooling plate at 25 °C for 24 h. Because of the relatively high viscosity of the melt, the molecular mobility was decreased and crystallization was hindered in the core. PEGs do not prevent the recrystallization of the components, they were applied as softener material to form the pastille. In order to initiate crystallization, pure XYL crystals were used as seeds (Talja et al., 2001).

After 24 h a thin XYL shell crystallized on the surface of the pastille, which gradually thickened during the storage until the whole of the pastille had solidified. After 5 days the core was fully solid as shown previously by the surface plot (Fig. 24), but after 3 days the DSC analysis demonstrated that the crystallization of the sample was still taking place. Fig. 25 presents DSC curves of samples stored for various times.
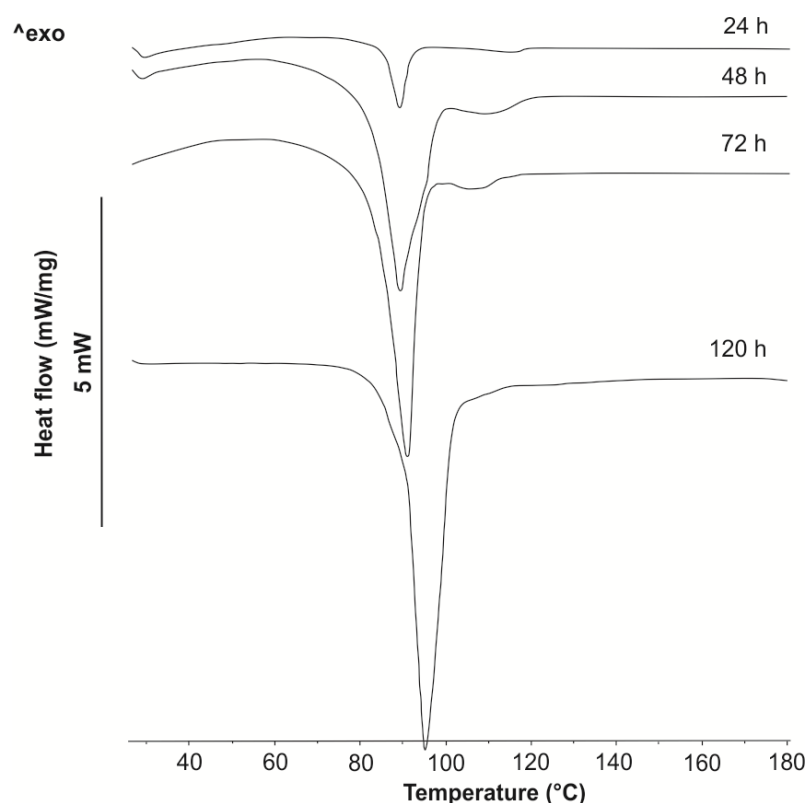

Fig. 25: Recrystallization of the XYL-MAN-EUT + PEG 6000 pastille carrier

The endotherms in the DSC curves indicate the melting temperature of XYL. The increasing area of the peaks reflects the extent of crystallization. As the crystallization progresses, the glass transition undergoes a depression. Table 15 shows the DSC data of recrystallization.

Table 15 DSC data of recrystallization compared to physical mixture

Time of measurement (h)	Melting temperature (°C)	Fusion enthalpy (J/g)
24	88.59	12.47
48	89.36	104.81
72	90.50	123.16
120	95.50	168.57
Physical mixture	95.40	168.27

We found that during the recrystallization of the XYL-MAN-EUT + PEG 6000 pastille, a phase separation occurs. A well-defined shell and core structure can be differentiated, therefore the phase separation was investigated with DSC (Fig. 26).
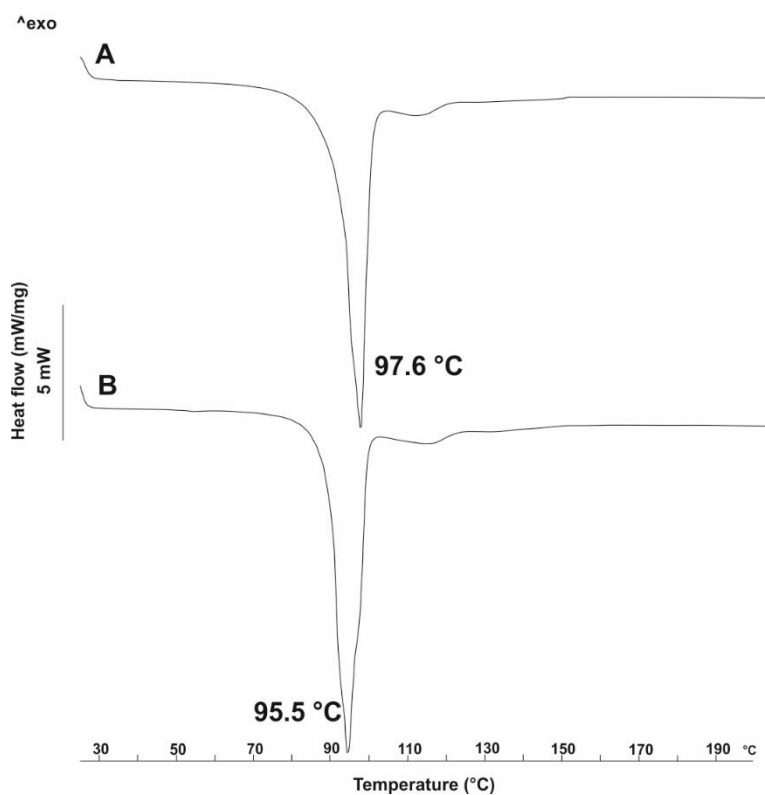

Fig. 26: DSC curves of XYL-MAN-EUT + PEG 6000 pastille shell (A) and core (B)

The melting temperatures of the core and shell of the pastille are different. The melting temperature of the shell is at 97.6 °C parallel with the melting temperature of starting XYL. The melting temperature of the core structure is at 95.5 °C, which is parallel to the eutectic temperature of XYL-MAN. It means the eutectic composition is located in the core of the pastille.

5.4. Pastillation process with PCT

On the basis of the factorial design, for XYL-MAN containing pastilles 61.25 wt.% XYL, 15.31 wt.% MAN, 7.81 wt.% PEG 6000 and 15.63 wt.% PCT (Fig. 23) were used and for XYL-SORB containing pastilles 38.28 wt.% XYL, 38.28 wt.% SORB, 15.63 wt.% PCT and 7.81 wt.% PEG 2000/6000 (Fig. 27). This gave the best pastille shape without visible pores, and a homogeneous shell texture. The PEG content resulted in an appropriate crystallization time and decreased the melting temperature of the mixture through the formation of a solid dispersion (Akiladevi et al., 2011).
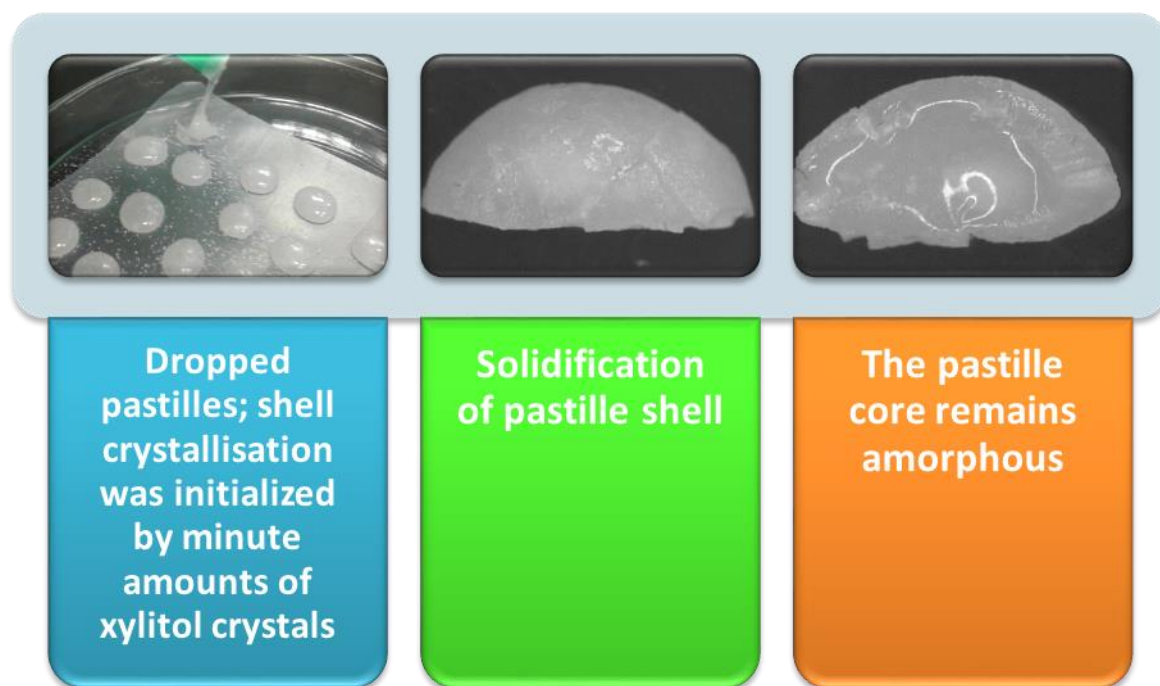

Fig. 27: Steps of pastillation process

After storage for 5 days, the pastille and the physical mixtures were investigated by DSC and compared. The DSC curves of the recrystallized pastille and the initial components can be seen in Fig. 28.
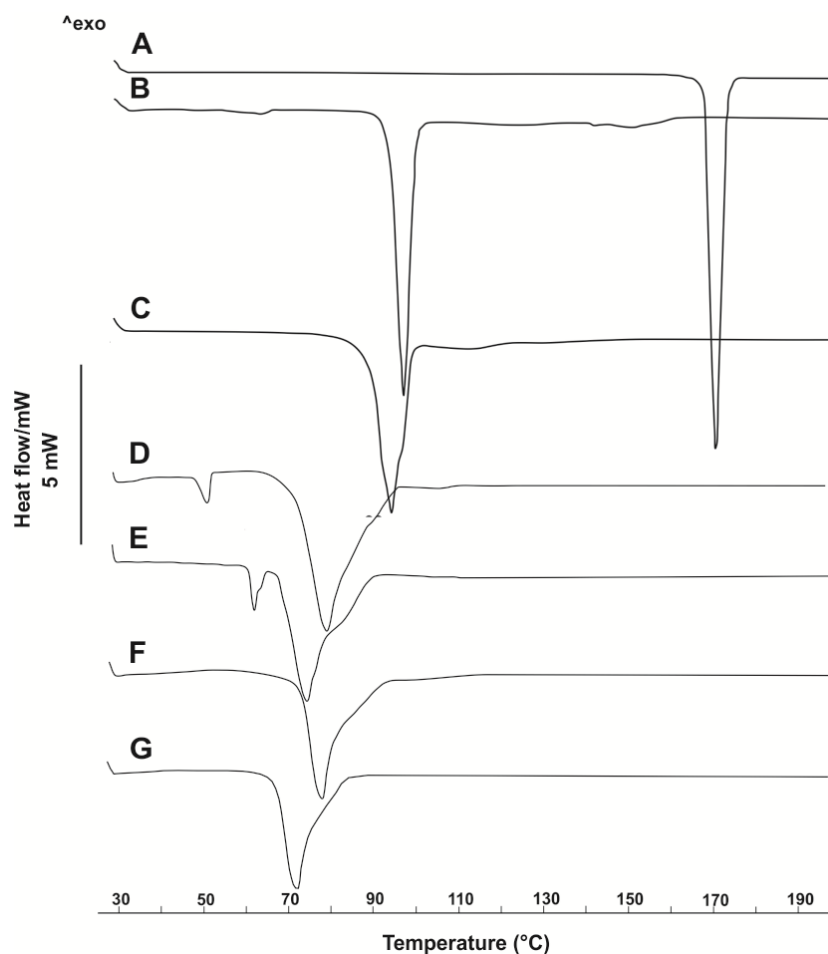
Fig. 28: DSC curves of pastilles and components, **A**: PCT, **B**: XYL-MAN-EUT + PEG 6000, **C**: XYL-MAN-EUT + PEG 6000 pastille, D: XYL-SORB-EUT + PEG 2000, E: XYL-SORB-EUT + PEG 6000, F: XYL-SORB-EUT + PEG 2000 pastille, G: XYL-SORB-EUT + PEG 6000 pastille

The DSC curves demonstrate that the high melting temperature of PCT (**A**), is not seen in the DSC curves of the physical mixture and the pastille (**B** to **G**), as a result of the PCT partly dissolving in the melt of the eutectic.

5.4.1. X-Ray powder diffraction (XRPD)

Because of the fusion of PCT in the eutectic, the possibility of polymorphic transition of the API during the recrystallization must be considered. PTC has three crystal modifications: a monoclinic form I, which has poor direct compressibility, an orthorhombic form II, and an unstable phase (form III), which can be stabilized only under certain conditions (for example, between a microscopy slide and a cover glass) (Perlovich et al., 2007). XRPD measurements were carried out to identify the polymorphic form of the PCT in the product. The comparison of the diffractogram of the starting PCT with the diffractograms of the various crystal modifications

available from the Cambridge Crystallography Data Centre (CCDC ID: AI631510) revealed that the starting PCT was in monoclinic Form I (Fig. 29A). The shell and core structures of the pastilles were investigated after 5 days by means of XRPD; the diffractograms are presented in Fig. 29B.
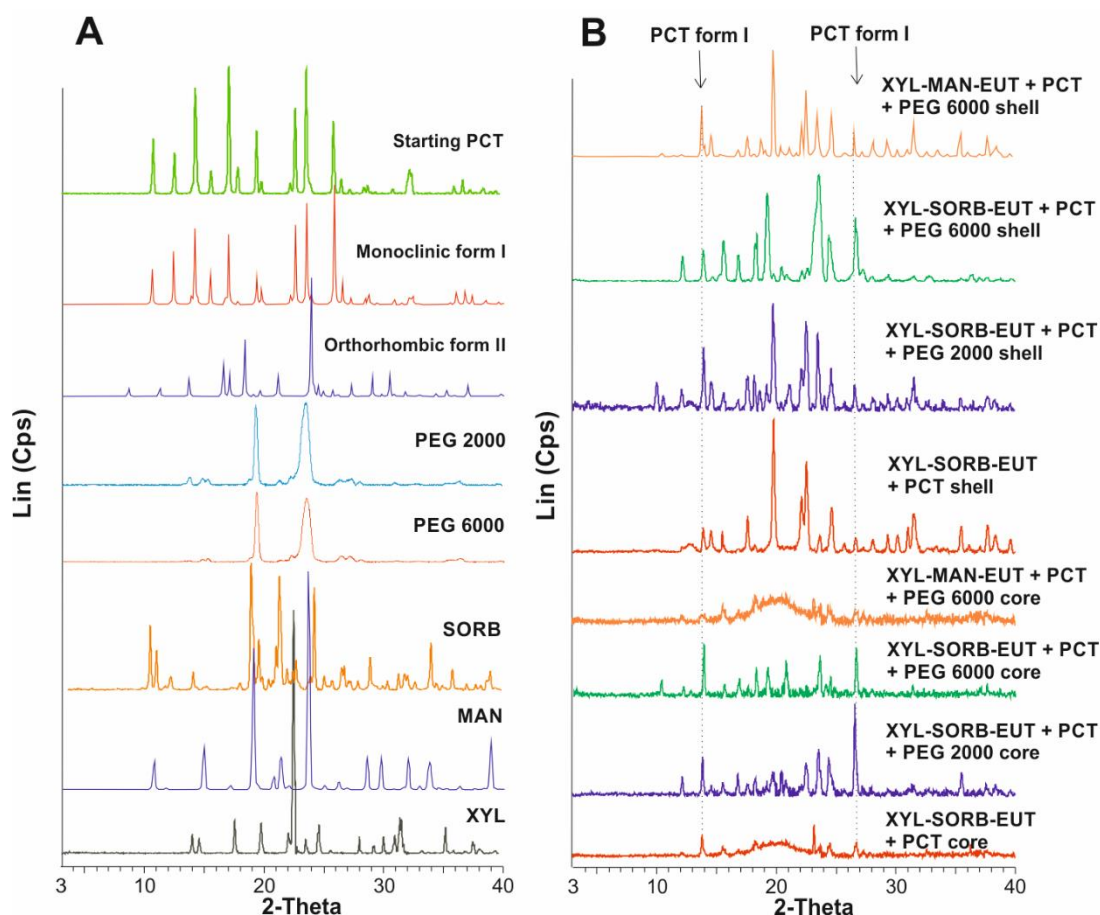

Fig. 29: Diffractograms of the polymorphic forms of PCT and the starting components (A) in comparison with shell and core structure of pastilles (B) at different locations and in the presence of different PEGs

The characteristic peaks of the components can be traced in the diffractograms of the pastille cores and shells. The characteristic peaks of the PCT in the core at 13.924° and 23.557° 2θ indicate the presence of the monoclinic form I. The XYL-MAN-EUT + PCT + PEG 6000 contains XYL, MAN and PCT, the XYL-MAN-EUT + PCT + PEG 6000 core shows amorphous signs, but contains PCT crystals. The XYL-SORB-EUT + PCT shell contains PCT and XYL, and the characteristic peaks of SORB at 10.055° and 10.595° 2θ could not be detected. The diffractogram of the XYL-SORB-EUT + PCT core shows amorphous signs, but contains PCT crystals. From these results the homogenous distribution of PCT in the pastille could be supposed.

The XYL-SORB-EUT + PCT + PEG 2000 shell and XYL-SORB-EUT + PCT + PEG 6000 shell contain PCT and xylitol, and the characteristic peaks of SORB could also be detected. The XYL-SORB-EUT + PCT + PEG 2000 core contains PCT crystals, but some amorphous signs could be detected. The diffractogram of the XYL-SORB-EUT + PCT + PEG 6000 core shows that the core structure is partly amorphous and contains SORB and PCT crystals. Since some characteristic peaks of the components overlap, we had to use Raman spectroscopy to locate the components.

5.4.2. Raman spectroscopy

Because of the slow solidification, the distribution of the PCT in the pastilles was first investigated by TRS. Figure 30 shows the transmission Raman spectra of pure PCT (**a**) and the XYL-MAN-EUT + PCT + PEG 6000 pastille shell (**b**) and core (**c**). The spectra in **b** and **c** are basically identical, the almost negligible differences involving new peaks due to the non-PCT ingredients. The pastille spectra indicated that there was no change in the crystal modification of the material in the sample tray during the measurement, with the main characteristic Raman bands of PCT in the intervals of 1660-1540, 1400-1160, 870-770 and 660-560 cm^{-1}. The identity of spectra **b** and **c** confirmed the uniform distribution of PCT throughout the pastilles.
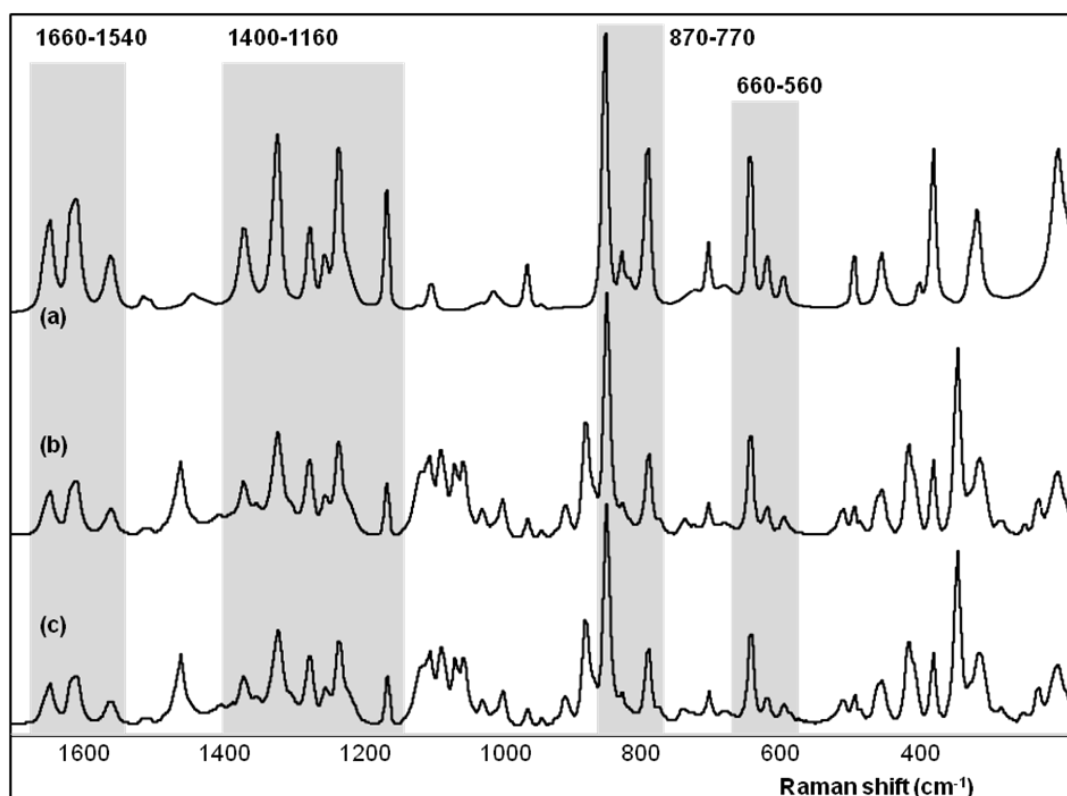

Fig. 30: Transmission Raman spectra of the starting PCT (**a**), the shell of XYL-MAN-EUT + PCT + PEG 6000 pastille (**b**) and the core of the PCT containing pastille (**c**)

To identify the polymorphic forms of the PCT after the recrystallization, DRS spectra were acquired with a DXR instrument. The DXR Raman spectra of all the PCT forms produced in various modes of the heating-cooling process were identical and were those of the metastable orthorhombic polymorph of PCT form II (not shown). The Raman spectra of PCT display strong bands at 1648, 1610, 1561, 1323, 1236, 857, 796, 650 and 390 cm^{-1}, assigned to -NH·CO·CH$_3$ stretching, C-C Ar stretching, C-N stretching / in-plane N-H bending, C-N stretching, phenyl-N and Ar C-C stretching, out-of-plane C-C skeletal deformation, C-N-C stretching and Ar =C-H out-of-plane deformation, respectively (Fig. 30a). Table 16 lists the principal Raman bands of PCT, and selected Raman bands of MAN, PEG 6000 and XYL are presented in Fig. 31. Although most of the main and characteristic Raman bands of the ingredients and PCT overlap, the differentiation of the PCT is of primary importance. The highlighted Raman bands at 1660-1540, 1168, 710 and 390 cm^{-1} were used to identify the PCT in the pastilles.

Table 16 Observed Raman peaks and their assignments for the starting PCT, form II of PCT and for the PCT-containing pastille (shell and core)

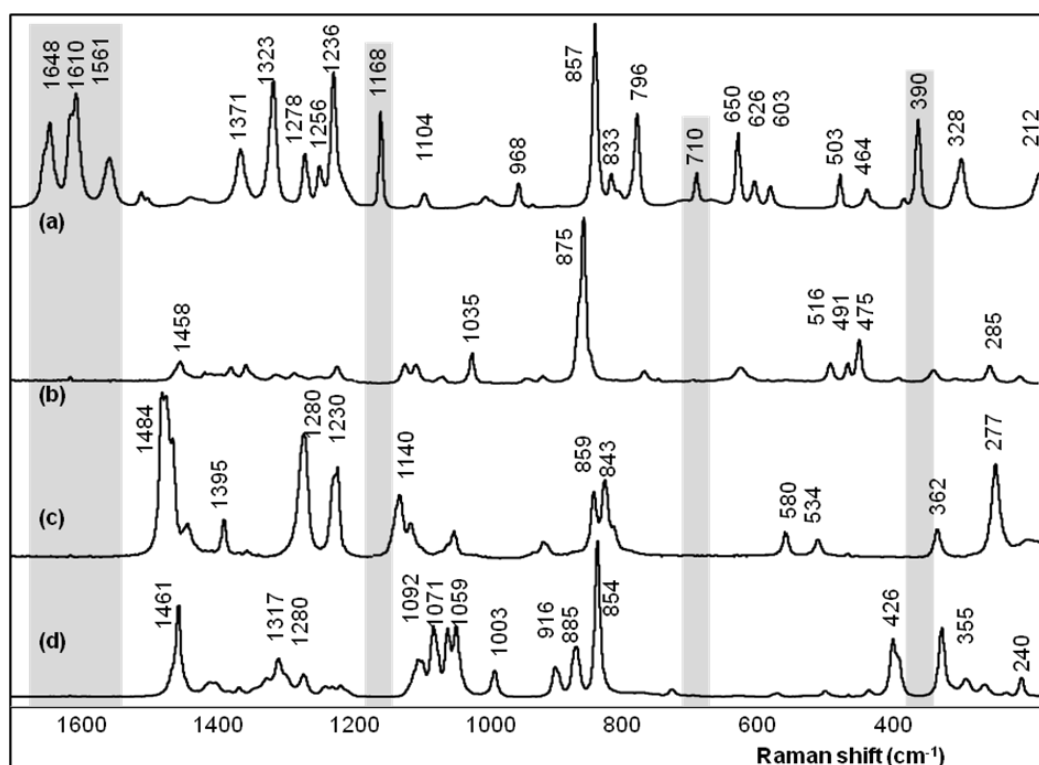| PCT	PCT form II	Pastille shell	Pastille core	Assignment
464w	453w	465w	464w	skeletal bending
503m	508w	505w	505w	Ar ring deformation
650s	650s	652m	652m	Ar =C-H out-of-plane deformation
710m	709w	711w	711w	out-of-plane CN-H and phenyl deformation
796s	798m	798m	798m	phenyl-N bending and out-of-plane p-substituted Ar ring deformation
857vs	860s	858s	857s	out-of-plane C-C skeletal deformation
968w	966w	969w	970w	C-C stretching
1104w	1106w	1105w	1109w	CH$_3$ rocking
1236s	1219m	1237s	1238m	phenyl-N and Ar C-C stretching
1256w	1244w	1257w	1257w	symmetrical CH$_3$ deformation
1323s	1326vs	1324s	1324s	C-N stretching
1515w	1510w	1515w	1517w	secondary amine deformation
1561m	1560w-sh	1561m	1562w	C-N stretching and in-plane N-H bending
-	1575m	-	-	amide N-H deformation
1610s	1608s	1610s	1611s	C-C Ar stretching
1617vw-sh	1623s	1619sh	1619sh	asymmetrical C=C Ar stretching, C-N stretching
1648s	1648m	1648s	1648m	-NH·CO·CH$_3$ stretching

Fig. 31: DXR spectra of the starting PCT (**a**) and the components as MAN (**b**), PEG 6000 (**c**) and XYL (**d**)

Fig. 32 presents DXR spectra of the starting PCT, form II and the PCT in the pastille shell and the core. The most marked differences between the two polymorphic PCT forms are to be seen in the highlighted regions, i.e. the intense Raman double peak at 1617-1610 cm^{-1} was split into two peaks at 1623 and 1608 cm^{-1} and one new peak appeared at 1575 cm^{-1}, in parallel with a - decrease in the intensity of the peak at 1560 cm^{-1}. The PCT form II spectrum exhibits the characteristic peaks of the starting PCT, but shifted to higher wavenumber: as 1561→1575, 1371→1374, 1323→1326, 857→860, 833→837, 503→508 and 328→330 cm^{-1}. This indicates that the corresponding chemical bonds are in a higher energy state. Table 16 lists the principal Raman bands of PCT form II, the metastable physical state of this, having a higher energy state than that of the starting PCT, which is consistent with the reported data. The exceptions (1256→1244, 1236→1219 and 464→453 cm^{-1}), are attributed to the symmetric CH$_3$ deformation, the phenyl-N and aromatic C-C stretching and the skeletal bending of PCT. The presence of PCT in the pastilles was not associated with the formation of the metastable PCT, form II. These data confirm the PCT is in the thermodynamically stable monoclinic form.
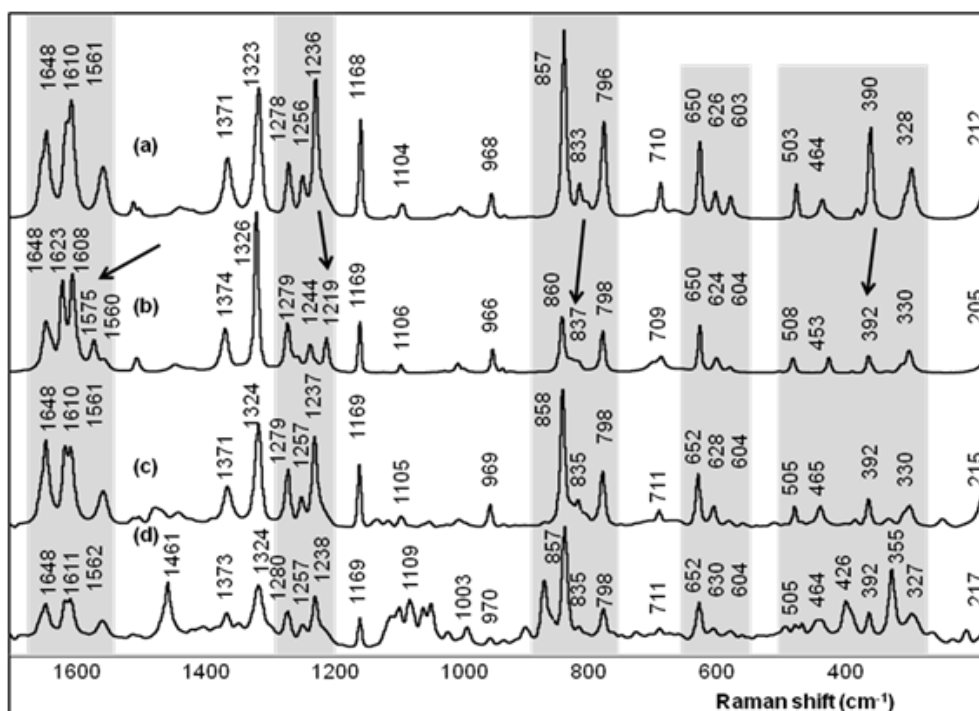
44

Fig. 32: DXR spectra of the starting PCT (**a**), form II of PCT (**b**), the shell of XYL-MAN-EUT + PCT + PEG 6000 pastille (**c**) and core of the pastille (**d**)

Fig. 33 shows the distribution map of different forms of PCT and XYL in one pastille at 10* magnification. In order to confirm the homogeneity of PCT, the pastille mapping has been resolved. The characteristic bands obtained for different PCT polymorphs presented in Fig. 32 as highlighted regions have been used to visualize the spatial distribution of PCT from Raman chemical mapping. The resolution of the chemical map and therefore the identification of the ingredients present can be produced using multivariate curve resolution – alternating least squares (MCR-ALS) chemometric method. This method allows for the recovery of the response profiles of different components in complex samples, and provides information about the composition. Furthermore, this method is an enhancement over simple surface mapping analysis, since the qualitative and quantitative information are calculated at the same time. Unlike the principal components resulting from principal component analysis (PCA), the component spectra from MCR-ALS method can be compared directly to spectral databases. The purpose of the analysis was to confirm the homogeneous distribution of the PCT and xylitol in the pastille. According to the chemical mapping, in fact, PCT can be found in well-defined packages inside the pastilles, properly to the stratification of the pastille inner structure. The higher xylitol (marked in green colour) concentration of the pastille's outer shell was also confirmed by Raman mapping.
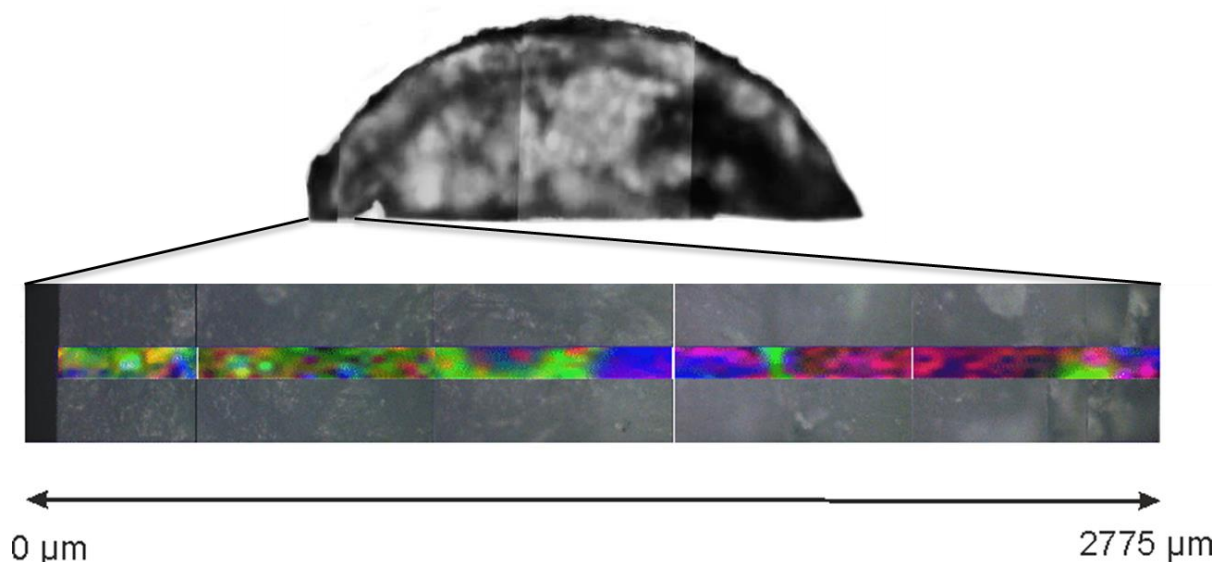
Fig. 33: Raman distribution map of two PCT polymorphs (monoclinic PCT-blue, orthorhombic PCT-red) and xylitol (green) in one whole pastille (at 10* magnification).

5.4.3. Geometrical parameters and hardness

The diameter and the height of 20 pastilles were measured with a screw micrometer and their mass with analytical scales. The average diameter of the pastilles was 10.60±0.31 mm, the height was 3.11±0.23 mm and the mass was 279±2 mg mg. Fig. 34 illustrates the top view (**A**) and the largest vertical cross-section (**B**) of the drop-melted pastille.

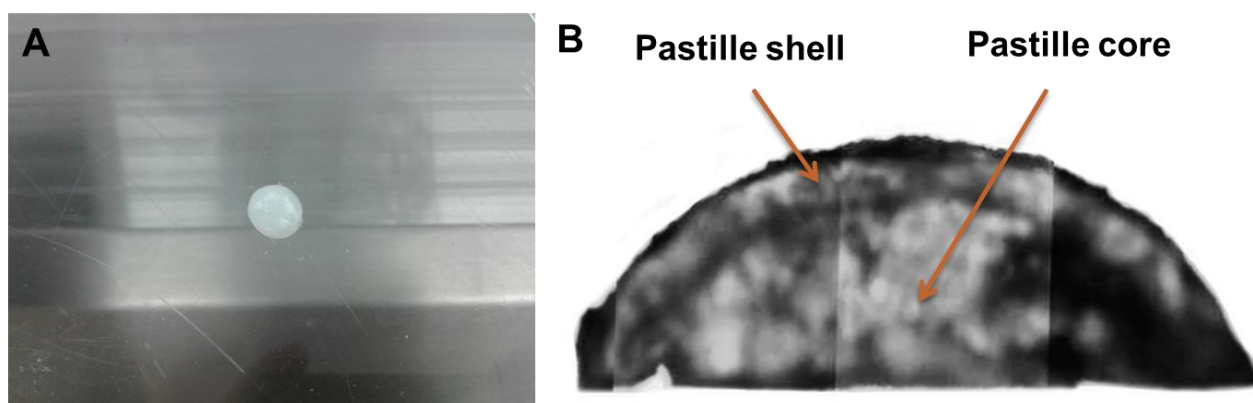**Fig. 34:** The top view (**A**) and the largest vertical cross-section (**B**) of the drop-melted pastilles

The braking hardness of 5 pastilles was measured. The average hardness of the pastilles made from XYL-MAN-EUT + PCT + PEG 6000 was 25±5 N, that from XYL-SORB-EUT + PCT was 29±5 N, that from XYL-SORB-EUT + PCT + PEG 2000 was 27 ±6 N and that from XYL-SORB-EUT + PCT + PEG 6000 was 27±4 N.

5.4.4. Drug content determination

Before the *in vitro* dissolution studies, the drug content of the pastilles was determined. Three different batches from each composition were investigated. The calculated and measured PCT contents of the pastilles were 40.19 mg, spectrophotometrically 40.12 ± 0.31 mg, respectively.

5.4.5. In vitro dissolution studies

In vitro dissolution studies of PCT containing pastilles after the total recrystallization (5 days) were carried out. In three parallel measurements, the PCT dissolutions of the pastilles produced from different compositions were compared at the oral cavity pH (pH 6.8±0.1) and in the gastric juice (pH 1.2±0.1) (Figs 35 and 36).
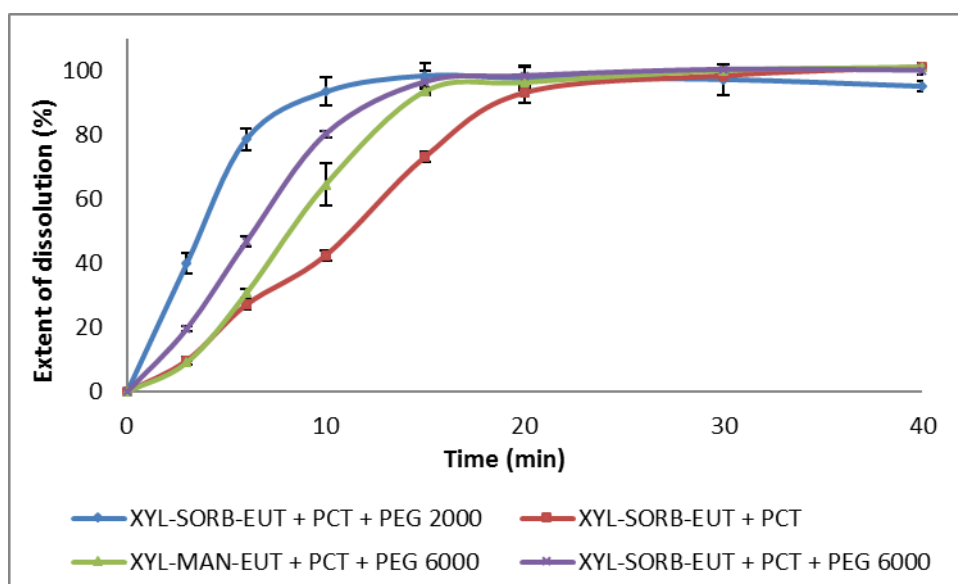

Fig. 35: Dissolution extents of drop-melted pastilles at the oral cavity pH of 6.8±0.1 and 37±0.5 °C (average value±SD, n=3).

In all cases, the PCT was practically fully dissolved from the pastilles in the medium of the oral cavity (pH 6.8±0.1) within 20 min.
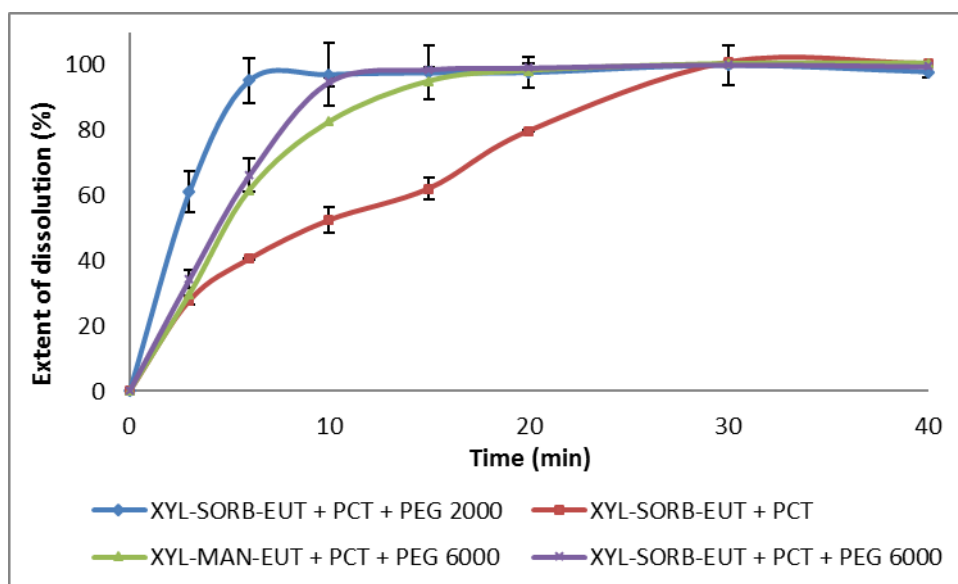
Fig. 36: Dissolution extents of drop-melted pastilles at the gastric pH of 1.2±0.1 and 37±0.5 °C (average value±S.D., n=3).

In the acidic medium (pH 1.2±0.1) the PCT also practically fully dissolved within 20 min in the case of the PEG-containing pastilles. The pastille without PEG dissolved only after 30 min. The differences in the extents of dissolution can be explained by the different surface free energies of the pastilles. The lower surface free energy of the (PEG)-containing pastilles resulted in higher polarity and faster dissolution than in the case of the pastille without PEG. When the pastille is swallowed, the liberation of PCT also occurs, but 5 min longer is required than in the mouth. It could be concluded that, by using PEGs, the wettability and therefore the dissolution time of the pastilles were improved, which justified this dosage form.

Summary

This part of experimental work discusses the application of developed carrier system and the melt technology to have a PCT containing pastille as new lozenge dosage form for children therapy. The eutectic composition of XYL-MAN and XYL-SORB was first determined by constructing the binary phase diagram and the Tamman triangle from the DSC data. As a component of the carrier, PEG as a softener agent did not inhibit the recrystallization of the components but the solidification would be slower, which promoted the pastille forming. Contact angle measurements showed that wettability can be improved by using PEGs in the formulations. The viscosity changing effect of PEGs strongly depends on the molecular weight. It was revealed that solidification occurred in the pastilles and the shell especially consisted of XYL. The Raman measurement showed the homogenous distribution of components in the pastille.

6. CONCLUSIONS

The aim of our research work was to apply conventional technologies such as spray-drying and melt technologies with new approaches to research and develop innovative PCT containing solid DDSs for paediatric administration. The spray-drying process was applied to prepare microcomposites for dose sipping form and the melt process was suitable to formulate pastilles with "*in situ* coating" technology as lozenge.

I.   First we surveyed the literature background of innovative forms used in paediatric therapy with conventional technologies, spray-drying and melt technology. In this part of work, the possibilities of innovation, the viewpoints of development of paediatrics, preparation methods and two innovative dosage forms were surveyed. Examples related to spray-drying and melt technology were collected. Finally, the pros and cons of the dose sipping form and lozenges were collected as "value added" preparations for "unmet medical need".

II.   In the experimental part, two conventional technologies were applied to formulate different innovative DDSs in an organic solvent free manner for oral administration. One of the formulations was microcomposites produced with spray-drying, which can be applied as a dose sipping form. The other drug delivery systems were lozenges formulated with *in situ* coating technology. These formulations did not contain any colouring agents or preservatives.

III.   The spray-dried TRE carrier was investigated with different screening methods. The investigation of spray-dried TRE suggested a method which is sensitive and rapid to predict the recrystallization process in the preformulation study. In this light, the suitable choice of the storage conditions can protect the amorphous TRE samples from crystallization. It could be concluded that HH-XRPD is faster than other conventional techniques and a good prediction for the recrystallization of amorphous compounds during preformulation, moreover, the physical changes could be studied on one sample. In view of these results, TRE was applicable for formulating API containing microcomposites with spray-drying.

Melt technology was the development of such crystalline drug carrier/basis for pastilles which consists of two-two well-recrystallized sugar alcohols and PEG as poor crystallization inhibitor. This carrier system is suitable for use in melt technology to formulate pastilles containing recrystallized PCT.

IV.   After the incorporation of a low amount of PCT in the forms, dosage form investigations were carried out. The investigation of microcomposites showed that the use of PEGs in the formulation decreased the electrostatic charge of the particles and produced good flow properties. Spray-drying resulted in amorphization in the samples (TRE, PCT), T_g could be determined, PEGs remained semicrystalline in the formulations. After 3 months the samples remain amorphous at ambient temperature and RH. In the pastilles solidification occurred after 5 days

and the shell consisted of mainly xylitol. The Raman measurement justified the homogenous distribution of the components in the pastille. The *in vitro* dissolution studies showed in the presence of PEGs the extent of PCT dissolution was higher than from the pure eutectic because of its lower surface free energy and higher polarity.

V.   All in all, we can conclude spray-drying and melt technology can be utilized in the industry for producing dosage forms without any organic solvents, colouring agents and preservatives, using natural excipients, which can be well tolerated e.g. in children's therapy.

Practical relevance and new approaches of this research work are the followings:

1. Spray-drying and melt technology as conventional technologies are suitable to formulate different innovative DDSs in an organic solvent free manner, without any colouring- or preservative agents, avoiding lactose and sucrose, meeting the requirements of paediatric therapy.
2. TRE based microcomposites made by spray-drying technology can be successful in development of amorphous DDS.
3. Two sugar alcohols and PEG based DDSs result in new compositions for melt technology (*in situ* coating process).
4. Suggested new formulations may be the PCT containing dose sipping form and pastilles as lozenge, which can be utilized in the industry for paediatric preparations.

7. REFERENCES

- Abouzeid A., Petersen S., Ulrich J., Utilizing melt crystallization fundamentals in the development of a new tableting technology. *Front. Chem. Sci. Eng.* (2014) 8, 346-352.
- Aguiar J. P., Fernandes T. A., Nese C., Fernandes A. I., Pinto J. F. Production and characterization of spray-dried theophylline powders prepared from fresh milk for potential use in paediatrics. *J. Pharm. Pharmacol.* (2016) DOI: 10.1111/jphp.12612
- Akiladevi D, Shanmugapandiyan P, Jebashingh D, Basak S, Preparation and evaluation of paracetamol by solid dispersion technique. *Int. J. Pharm. Sci.* (2011) 1, 188-191.
- Alpar H. O., Somavarapu S., Atuah K. N., Bramwell V. W. Biodegradable mucoadhesive particulates for nasal and pulmonary antigen and DNA delivery. *Adv. Drug. Deliv. Rev.* (2005) 57, 411–30.
- Altamimi M. A., Neau S. H. Investigation of the in vitro performance difference of drug-Soluplus® and drug-PEG 6000 dispersions when prepared using spray drying or lyophilization. *Saudi. Pharm. J.* (2017) 25, 419-439.
- Al-Zoubi N., Al-obaidi G., Tashtoush B., Malamataris S. Sustained release of diltiazem HCl tableted after co-spray drying and physical mixing with PVAc and PVP. *Drug. Dev. Ind. Pharm.* (2016) 42, 270-279.
- Amaro M. I., Tajber L., Corrigan O. I., Healy A. M. Co-spray dried carbohydrate microparticles: crystallization delay/inhibition and improved aerosolization characteristics, through the incorporation of hydroxypropyl-β-cyclodextrin with amorphous raffinose or trehalose. *Pharm. Res.* (2015) 32, 180-195.
- Bansal M., Singh S. K., Gulati M. Lozenges as delivery system for upper respiratory catarrh medication. *Recent. Pat. Drug. Deliv. Formul.* (2014) 8, 92-100.
- Bashiri-Shahroodi A, Dropping method as a new possibility in preparation of solid dispersions. *Doctoral dissertation*, Szeged, 2007
- Behera S., Ghanty S., Ahmad F., Santra S., Banarjee S. UV-visible spectrophotometric method development and validation of assay of paracetamol tablet formulation. *J. Anal. Bioanal. Techniques.* (2012) 6, 1000151.
- Boxall A, Rudd M, Brooks B, Caldwell D, Choi K, Hickmann S. Pharmaceuticals and personal care products in the environment: what are the big questions? *Environ. Health. Perspect.* (2012) 120, 1221-1229.
- Breitenbach J. Melt extrusion: from process to drug delivery technology. *Eur. J. Pharm. Biopharm.* (2002) 54, 107-117.
- Breitkreutz J., Boos J. Paediatric and geriatric drug delivery. *Expert. Opin. Drug. Deliv.* (2007) 4, 37-45.
- Broman E, Khoo C, Taylor R. L. A comparison of alternative polymer excipient and processing methods for making solid dispersions of poorly water soluble drug. *Int. J. Pharm.* (2001) 222, 139-151.
- Bülau H. C., Ulrich J. Parameters influencing the properties of drop-formed pastilles, CGOM. *Shaker Verlag*, Aachen, (1997), 123–130.

- Cal K., Sollohub K. Spray drying technique. I: Hardware and process parameters. *J. Pharm. Sci.* (2010) 99, 575-586.

- Chidavaenzi O. C., Buckton G., Koosha F. The effect of co-spray drying with polyethylene glycol 4000 on the crystallinity and physical form of lactose. *Int. J. Pharm.* (2001) 216, 43-49.

- Claus S., Schoenbrodt T., Weiler C., Friess W. Novel dry powder inhalation system based on dispersion of lyophilisates *Eur. J. Pharm. Sci.* (2011) 43, 32-40.

- Corrigan D. O., Healy A. M., Corrigan O. I. The effect of spray drying solutions of polyethylene glycol (PEG) and lactose/PEG on their physicochemical properties. *Int. J. Pharm.* (2002) 235, 193-205.

- Crowe J.H., Tablin F., Wolkers W. F., Gousset K., Tsvetkova N. M., Ricker J. Stabilization of membranes in human platelets freeze-dried with trehalose. *Chem. Phys. Lipids.* (2003) 122, 41-52.

- de Zwart L. L., Haenen H. E., Versantvoort C. H., Wolterink G., van Engelen J. G., Sips A. J., Role of biokinetics in risk assessment of drugs and chemicals in children. *Regul. Toxicol. Pharmacol.* (2004) 39, 282–309.

- Dixit R. P., Puthli S. P. Oral strip technology: overview and future potential. *J. Control. Release.* (2009) 139, 94-107.

- Farkas G., Ropp M., Fraser F. C. Artificial sweeteners and fatal malformations: negative experimental evidence. *Pediatrics* (1971) 48, 337-337.

- Gahel M. C., Parikh P. P., Aghora P. P., Nagari S. A., Delvadia R. R., Dabhi M. Application of simple lattice designe and desirability function for the formulation development of mouth dissolving film of salbutamol sulphate. *Curr. Drug. Deliv.* (2009) 6, 486-494.

- Ghanavati R., Taheri A., Homayouni A. Anomalous dissolution behavior of celecoxib in PVP/Isomalt solid dispersions prepared using spray drier. *Mater. Sci. Eng. C.* (2017) 72, 501-511.

- Gradon L., Sosnowski T. R. Formation of particles for dry powder inhalers. *Adv. Powder Technol.* (2014) 25, 43-55.

- Hamishehkar H., Emami J., Najafabadi A. R., Gilani K., Minaiyan M., Mahdavi H., Nokhodchi A. Effect of carrier morphology and surface characteristics on the develpement of respirable PLGA microcapsules for sustained-release pulmonary delivery of insulin. *Int. J. Pharm.* (2010) 389, 74-85.

- Heyman M. B. Lactose intolerance in infants, children, and adolescents. *Pediatrics* (2006) 118, 1279-1286.

- Hinz B., Cheremina O., Brune K. Acetaminophen (paracetamol) is a selective cyclooxygenase-2 inhibitor in man. *FASEB J.* (2008) 22, 383-390.

- Hutteau F., Mathlouthi M., Portmann M. O., Kilcast D. Physicochemical and psychophysical characteristics of binary mixtures of bulk and intense sweeteners, *Food Chem.* (1998) 63, 9–16.

- Islam N., Gladki E. Dry powder inhalers (DPIs)—A review of device reliability and innovation. *Int. J. Pharm.* (2008) 360, 1–11.

- Janssens S., De Armas H. N., Roberts C. J., Van den Mooter G. Characterization of ternary solid dispersions of itraconazole, PEG 6000, and HPMC 2910 E5. *J. Pharm. Sci.* (2008) 97, 2110-2120.

- Kaushik D., Dureja H. Taste masking of bitter pharmaceuticals by spray drying technique. *J. Chem. Pharm. Res.* (2015) 7, 950-956.

- Kearns G. L., Abdel-Rahman S. M., Alander S. W., Blowey D. L., Leeder J. S., Kauffman R. E. Developmental pharmacology - Drug disposition, action, and therapy in infants and children. *New. Engl. J. Med.* (2003) 349, 1157-1167.

- Krause J., Breitkreutz J. Improving drug delivery in paediatric medicine. *Pharm. Med.* (2008) 22, 41-50.

- Krause J., Thommes M., Breitkreutz J. Immediate release pellets with lipid binders obtained by solvent-free cold extrusion. *Eur. J. Pharm. Biopharm.* (2009) 71, 138-144.

- Kümmerer K. Sustainable from the very beginning: rational design of molecules by life cycle engineering as an important approach for green pharmacy and green chemistry. *Green Chem.* (2007) 9, 899-907.

- Löbmann K., Laitinen R., Grohganz H., Strachan C., Rades T., Gordon K. C. A theoretical and spectroscopic study of co-amorphous naproxen and indomethacin. *Int. J. Pharm.* (2013) 453, 80-87.

- Maas S. G., Schaldach G., Littringer E. M., Mescher A., Griesser U. J., Braun D. E., Walzel P. E., Urbanetz N. A. The impact of spray drying outlet temperature on the particle morphology of mannitol. *Powder Technol.* (2011) 213, 27-35.

- Mah P. T., Laaksonen T., Rades T., Peltonen L., Strachan C. J. Differential scanning calorimetry predicts the critical quality attributes of amorphous glibenclamide. *Eur. J. Pharm. Sci.* (2015) 80, 74-81.

- Mäkinen K. K. Sugar alcohol sweeteners as alternatives to sugar with special consideration of xylitol. *Med. Princ. Pract.* (2011) 20, 303-320.

- Mashru R. C., Sutariya V. B., Sankalia M. G., Parikh P. P. Development and evaluation of fast-dissolving film of salbutamol sulphate. *Drug. Deliv. Ind. Pharm.* (2005) 31, 25-34.

- Maurya M., Murphyb K., Kumarb S., Mauerera A., Lee G. Spray-drying of proteins: effects of sorbitol and trehalose on aggregation and FT-IR amide I spectrum of an immunoglobulin G. *Eur. J. Pharm. Biopharm.* (2005) 59, 251–261.

- Maurya M., Murphyb K., Kumarb S., Shib L., Lee G. Effects of process variables on the powder yield of spray-dried trehalose on a laboratory spray-dryer. *Eur. J. Pharm. Biopharm.* (2005) 59, 565–573.

- Mazzobre M. F., Soto G., Aguilera J. M., Buera M. P. Crystallization kinetics of lactose in systems co-lyofilized with trehalose. Analysis by differential scanning calorimetry. *Food Res. Int.* (2001) 34, 903-911.

- Mennella J. A., Beauchamp G. K. Optimizing oral medications for children, *Clin. Ther.* (2008) 30, 2120–2132.

- Mönckedieck M., Kamplade J., Littringer E. M., Mescher A., Gopireddy S., Hertel M., Steckel H. Spray Drying Tailored Mannitol Carrier Particles for Dry Powder Inhalation with Differently Shaped Active Pharmaceutical Ingredients. *Springer International Publishing*. In Process-Spray (2016) 517-566.

- Moran A., Buckton G. Adjusting and understanding the properties and crystallisation behaviour of amorphous trehalose as a function of spray drying feed concentration. *Int. J. Pharm.* (2007) 343, 12-17.
- Moreton R. C., Armstrong N. A. The effect of film composition on the diffusion of ethanol through soft gelatine films. *Int. J. Pharm.* (1998) 161, 123-131.
- Nagase H., Endo T., Ueda H., Nakagaki M. An anhydrous polymorphic form of trehalose. *Carbohydr. Res.* (2002) 337, 167-173.
- Nataha M. C. Lack of pediatric drug formulations. *Pediatrics* (1999) 104, 607-609.
- Ógáin O. N., Li J., Tajber L., Corrigan O. I., Healy A. M. Particle engineering of materials for oral inhalation by dry powder inhalers. I-Particles of sugar excipients (trehalose and raffinose) for protein delivery. *Int. J. Pharm.* (2011) 405, 23–35.
- Oliveira A. M., Guimarães K. L., Cerize N. N. P., Tunussi A. S., Poço J. G. R. Nano spray drying as an innovative technology for encapsulating hydrophilic active pharmaceutical ingredients (API). *J. Nanomed. Nanotechnol.* (2013) 4, 1000186.
- Oneda F., Re M. I. The effect of formulation variables on the dissolution and physical properties of spray-dried microspheres containing organic salts. *Powder Technol.* (2003) 130, 377-384.
- Palmieri G. F., Wehrle P., Stamm A. Evaluation of spray drying as a method to prepare microparticles for controlled drug release. *Drug. Dev. Ind. Pharm.* (1994) 20, 2859-2879.
- Paradkar A., Ambike A. A., Jadhav B. K., Mahadik K. R. Characterization of curcumin–PVP solid dispersion obtained by spray drying. *Int. J. Pharm.* (2007) 271, 281-286.
- Patterson J. E., James M. B., Forster A. H., Lancaster R. W., Butler J. M., Rades T. The influence of thermal and mechanical preparative techniques on the amorphous state of four poorly soluble compounds. *J. Pharm. Sci.* (2005) 94, 1998-2012.
- Perlovich G. L., Volkova T. V., Bauer-Brandl A. Relative stability of the monoclinic and orthorhombic phase revisited by sublimation and solution calorimetry. *J. Therm. Anal. Cal.* (2007) 89, 767-774.
- Phaemachud T., Tuntarawongsa S. Clotrimazol soft lozenges fabricated with melting and mold technique. *Res. J. Pharm. Biol. Chem. Sci.* (2010) 1, 579-586.
- Pomázi A., Ambrus R., Sipos P., Szabó-Révész P. Analysis of co-spray-dried meloxicam–mannitol systems containing crystalline microcomposites. *J. Pharm. Biomed. Anal.* (2011) 56, 183-190.
- Pomázi A., Buttini F., Ambrus R., Colombo P., Szabó-Révész P. Effect of polymers for aerolization properties of mannitol-based microcomposites containing meloxicam. Eur. Polym. J. (2013) 49, 2518-2527.
- Redenti E., Peveri T., Zanol M., Ventura P., Gnappi G., Montenero A. A study on the differentation between amorphous piroxicam: beta-cyclodextrin complex and a mixture of the two amorphous components. *Int. J. Pharm.* (1996) 129, 289-294.
- Reti-Nagy K., Malanga M., Fenyvesi E., Szente L., Vámosi G., Váradi J., Bácskay I., Fehér P., Ujhelyi Z., Róka E., Vecsernyés M., Balogh G., Vasvári G., Fenyvesi F. Endocytosis of fluorescent cyclodextrins by intestinal Caco-2 cells and its role in paclitaxel drug delivery. *Int. J. Pharm.* (2015) 496, 509-517.

- Róka E., Ujhelyi Z., Deli M., Bocsik A., Fenyvesi É., Szente L., Fenyvesi F., Vecsernyés M., Váradi J., Fehér P., Gesztelyi R., Félix C., Perret F., Bácskay I. K. Evaluation of the cytotoxicity of α-cyclodextrin derivatives on Caco-2 cell line and human erythrocytes. *Molecules* (2015) 20, 20269-20285.
- Rowe R. C., Sheskey P. J., Quinn M. E. Handbook of pharmaceutical excipients 6th edition, *RPS publishing* (2009) 746-747.
- Rycerz L. Practical remarks concerning phase diagrams determination on the basis of differential scanning calorimetry measurements. *J. Therm. Anal. Calorim.* (2013) 113, 231-238.
- Sastry S. V., Nyshdham J. R., Fix J. A. Recent technological advances in oral drug delivery - a review. *Pharm. Sci. Technolo. Today.* (2000) 3, 138-45.
- Schirm E., Tobi H., de Vries T. W., Choonara I., De Jong-van den Berg L. T. W. Lack of appropriate formulations of medicines for children in the community. *Acta Paediatr,* (2003) 92, 1486-1489.
- Shanmugam S. Granulation techniques and technologies: recent progresses. *BioImpacts: BI,* (2015) 5, 55.
- Sharar S. R., Carrougher G. J., Selzer K. L., O'donnell F., Vavilala M. S., Lee L. A. A comparison of oral transmucosal fentanyl citrate and oral oxycodone for pediatric outpatient wound care. *J.Burn. Care. Res.* (2002) 23, 27-31.
- Sholaei A.H. Buccal mucosa as a route for systemic drug delivery. *J. Pharm. Pharmaceut. Sci.* (1998) 1, 15-30.
- Six K., Verreck G., Peeters J., Augustijns P., Kinget R., Van den Mooter G. Characterization of glassy itraconazole: a comperative study of its molecular mobility below Tg with that of structural analgues using MTDSC. *Int. J. Pharm.* (2001) 213, 163-173.
- Standing J.F., Tuleu C. Paediatric formulations - Getting to the heart of the problem. *Int. J. Pharm.* (2005) 300, 56-66.
- Steckel H., Brandes H. G. A novel spray-drying technique to produce low density particles for pulmonary delivery. *Int. J. Pharm.* (2004) 278, 187–195.
- Szepes A., Fiebig A., Ulrich J., Szabó-Révész P. Structural study of a-lactose monohydrate subjected to microwave irradiation. *J. Therm. Anal. Cal.* (2007) 89, 757-760.
- Szepes A., Hasznos-Nezdei M., Kovács J., Funke Z., Ulrich J., Szabó-Révész P. Microwave processing of natural biopolymers – studies on the properties of different starches. *Int. J. Pharm.* (2005), 302, 166-171.
- Szűts A., Láng P., Ambrus R., Kiss L., Deli M. A., Szabó-Révész P. Applicability of sucrose laurate as surfactant in solid dispersions prepared by melt technology. *Int. J. Pharm.* (2011) 410, 107-110.
- Talja R. A., Roos Y. H. Phase and state transition effect on dielectric, mechanical and thermal properties of polyols. *Thermochim. Acta,* (2001) 380, 109-121.
- Tewa-Tagne P., Briançon S., Fessi H. Preparation of redispersible dry nanocapsules by means of spray-drying: development and characterisation. *Eur. J. Pharm. Sci.* (2007) 30, 124-135.

- Thi T. H. H., Morel S., Ayouni F., Flament M. P. Development and evaluation of taste-masked drug for paediatric medicines–Application to acetaminophen. *Int. J. Pharm.* (2012) 434, 235-242.
- Tuleu C., An overview of paediatric drug delivery. *Drug. Deliv. Rep.* (2005) Autumn/Winter 19-21.
- Ulrich J., Abouzeid A., Hartwig A., Petersen S., Wendt K., Geht es nicht einfacher? In situ Coating – Beschichtung direkt aus der Schmelze. *CIT plus* (2015) 3, 44-45.
- Van Arnum P. "Green Drug Delivery: Spray-dried solid amorphous dispersions with a cellulosic exicpient." *Pharm. Technol.* (2010) 34, 43.
- Vehring R. Pharmaceutical particle engineering via spray drying. *Pharm. Res.* (2008) 25, 999-1022.
- Vicente J., Pinto J., Menezes J., Gaspar F. Fundamental analysis of particle formation in spray drying. *Powder Technol.* (2013) 247, 1-7.
- Walsh J., Bickmann D., Breitkreutz J., Chariot-Goulet M., EuPFI. Delivery devices for the administration of paediatric formulations: overview of current practice, challenges and recent developments. *Int. J. Pharm.* (2011) 415, 221-231.
- Wan L. C. S., Heng P. W. S., Chia C. G. H. Spray drying as a process for microencapsulation and the effect of different coating polymers. *Drug. Dev. Ind. Pharm.* (1992) 18, 997-1011.
- Web reference 1 http://www.fda.gov/downloads/drugs/guidances/ucm070305.pdf
- Web reference 2 http://www.ema.europa.eu/ema/index.jsp?curl=pages/about_us/general/general_content_000265.jsp
- Web reference 3 http://www.actiq.com/
- Wendt K., Petersen S., Ulrich J. Application of in situ coating on a two-compound system. *Chem. Eng. Technol.* (2014) 37, 1408-1412.
- Weuts I., Kempen D., Verreck G., Decorte A., Heymans K., Peeters J., Van den Mooter G. Study of the physicochemical properties and stability of solid dispersions of loperamide and PEG6000 prepared by spray drying. *Eur. J. Pharm. Biopharm.* (2005) 59, 119-126.
- Yoo A. κ-carrageenan micropellets: production and dissolution behaviour, *Doctoral dissertation*, Düsseldorf, 2008.
- Yousefi S., Emam-Djomeh Z., Mousavi S. M. Effect of carrier type and spray drying on the physicochemical properties of powdered and reconstituted pomegranate juice (Punica Granatum L.). *Food Sci. Technol.* (2011) 48, 677-684.
- Zgoulli S., Grek V., Barre G., Goffinet G., Thonart P. Microencapsulation of erythromycin and clarithromycin using a spray-drying technique. *J. Microencapsul.* (1999) 16, 565-571.
- Ziegler I. M. Dose Sipping Technology—A Novel Dosage Form for the Administration of Drugs. In Modified-Release Drug Delivery Technology, *CRC Press*, Second Edition (2008) 217-229.

ACKNOWLEDGEMENTS

ANNEX

I.

A trehalóz, mint amorfizálódásra hajlamos segédanyag, rekrisztallizációjának vizsgálata

KATONA GÁBOR, JÓJÁRTNÉ LACZKOVICH ORSOLYA ÉS SZABÓNÉ RÉVÉSZ PIROSKA*

Szegedi Tudományegyetem, Gyógyszertechnológiai Intézet, Szeged, Eötvös u. 6. – 6720
*Kapcsolattartó email címe: revesz@pharm.u-szeged.hu

Summary

Katona, G., Jójárt-Laczkovich, O., Szabó-Révész, P.*: Investigation of the recrystallization of trehalose as a good glass-former excipient

An amorphous form of trehalose is easy to prepare by using a solvent method. The recrystallization kinetics can be followed well, which is important because of the occurrence of polymorphic forms of trehalose. This is especially significant in the case of dry powder inhalers. Spray-drying was used as a preparation method this being one of the most efficient technologies with which to obtain an amorphous form. This method can result in the required particle size and a monodisperse distribution with excellent flowability and with moreover considerable amorphization. In our work, trehalose was applied as a technological auxiliary agent, and literature data relating to the spray-drying technology of trehalose were collected. Studies were made of the influence of the spraying process on the amorphization of trehalose and on the recrystallization of amorphous trehalose during storage. Amorphous samples were investigated under 3 different conditions during 3 months. The recrystallization process was followed by differential scanning calorimetry and X-ray powder diffraction. The results demonstrated the perfect amorphization of trehalose during the spray-drying process. The glass transition temperature was well measurable in the samples and proved to be the same as the literature data. Recrystallization under normal conditions was very slow but at high relative humidity the process was accelerated greatly. Amorphous trehalose gave rise to dihydrate forms (γ- and h-trehaloses) during recrystallization, and β-trehalose was also identified as an anhydrous form.

Keywords: trehalose, amorphous form, spray-drying, recrystallization, polymorphism.

Összefoglalás

A trehalóz oldószeres eljárással könnyen amorfizálható anyag. A rekrisztallizáció folyamata jól nyomon követhető, vizsgálata pedig indokolt a spontán amorfizálódás következtében megjelenő különböző polimorf módosulatok miatt. Ennek különösen a porinhalációs készítményeknél van jelentősége. Oldószeres eljárásként a porlasztva szárítást alkalmaztuk, amivel kívánt szemcseméretű, kiváló folyási tulajdonsággal rendelkező monodiszperz rendszer állítható elő, valamint nagymértékű amorfizálódás következhet be. A kísérletes munka előzményeként bemutatjuk a trehalózt, mint a gyógyászatban alkalmazott segédanyagot és annak legfontosabb tulajdonságait, illetve porlasztva szárítással történő feldolgozásának irodalmi hátterét. Arra kerestük a választ, hogy porlasztva szárítással előállítható-e amorf trehalóz, s különböző körülmények között tárolva (3 hónap), milyen változásokat tapasztalunk. Analitikai módszerként a differenciális pásztázó kalorimetriát és a porröntgen diffrakciós módszert alkalmaztuk. Megállapítottuk, hogy a porlasztva szárítás nagymértékű amorfizálódást okoz a mintákban. Az üvegesedési hőmérséklet mérhető és az irodalmi értékkel megegyező tartományba esik. Továbbá megállapításra került, hogy magas páratartalmú közegben a trehalóz túlnyomórészt dihidrát formában (γ- és h-trehalóz) kristályosodik vissza, és a rekrisztallizáció üteme lényegesen felgyorsul. A rekrisztallizáció során egyéb polimorf módosulatot is azonosítottunk (anhidrát β-trehalóz).

Kulcsszavak: trehalóz, amorf forma, porlasztva szárítás, rekrisztallizáció, polimorfia

Bevezetés

A gyógyszerformák tervezésénél a hatóanyagok mellett a segédanyagok is kulcsfontosságú szerepet töltenek be. A helyes segédanyag megválasztásával jobb oldódási profil, nagyobb stabilitás, módosított hatóanyag leadás és jobb préselhetőség érhető el [1]. Az iparban általában kristályos formában dolgozzák fel a ható- és segédanyagokat a formulálás során, azonban egyes esetekben kedve-

zőbb tulajdonságok érhetőek el az amorf forma alkalmazásával. Ezen tulajdonságok közé tartozik a jobb vízoldékonyság, jobb préselhetőség, ismételt szabadalmaztathatóság és a polimorf módosulatok egymásba alakulásának megakadályozása [2].

A száraz porinhalációs készítményeket (*Dry Powder Inhaler* – DPI) leggyakrabban porlasztva- vagy fagyasztva szárítással állítják elő. Ezekkel az eljárásokkal kívánt szemcseméretű, valamint kivá-

ló folyási tulajdonsággal rendelkező monodiszperz rendszer állítható elő, viszont nagymértékű amorfizálódást is eredményezhet. A folyamatot, amikor az anyag valamely gyártásközi művelet, esetleg a tárolás során részben vagy egészben amorfizálódik, „indirekt amorfizálásnak", vagy amorfizálódásnak nevezzük. A kristályos és az amorf forma aránya a porinhalációs készítmények alkalmazhatóságát jelentősen befolyásolja, így folyamatos kontrollálást igényel mind a gyártás, mind pedig a felhasználásig történő tárolás során.

A kísérletes munka modell segédanyaga

A kísérletes munka modell anyagának a trehalózt választottuk, mint amorfizálódásra hajlamos segédanyagot, mivel a feldolgozás során könnyen amorfizálódhat. A trehalóz α-D-glükopiranozil-α-D-glükopiranozid–dihidrát (α,α-trehalóz–dihidrát) vagy mikóz, ami egy természetes alfa-kötésű diszacharid, amelyet két α-glükózegység alkot α 1→1 glikozidos kötéssel (*1. ábra*). Fehér, vagy csaknem fehér kristályos por, amely vízben bőségesen, metanolban alig és etanolban gyakorlatilag nem oldódik.

A trehalóz a természetben is előforduló anyag. Gombák (ebből adódik egyik szinoním neve, a mikóz = „gomba cukor"), növények és gerinctelen állatok is bioszintetizálják. Széles körben alkalmazzák segédanyagként az ipar több területén is, mint például a kozmetikai-, mezőgazdasági-, élelmiszer- és a gyógyszeriparban. Az iparban a keményítő enzimatikus átalakításával állítják elő. Más diszacharidoktól eltérően, az előállítás folyamán nem lép kémiai reakcióba aminosavakkal vagy fehérjékkel, és ez megakadályozza a termék barnulását (Maillard reakció). A trehalóz egy nem reaktív cukor. Erős stabilitása a két glükopiranóz gyűrűt összekötő glikozidos kötés kis energiájának (1 kcal/mol) köszönhető. Nem disszociál két

1. ábra: Trehalóz (D(+)-trehalóz-dihidrát) szerkezeti képlete

redukáló monoszacharid alkotórészre, csak extrém hidrolitikus körülmények között vagy trehalóz enzim hatására (amelyet a gombák és az emberi szervezet is szintetizál).

Szerepet játszik a növények és állatok anhidrobiózisában, vagyis abban a tulajdonságukban, hogy hosszú ideig képesek életben maradni víz nél-

kül. Nagy víztartó képességét a kozmetikai- és élelmiszeriparban is hasznosítják.

A biomolekula stabilizációjának mechanizmusát először Fourier-transzformációs infravörös spektroszkópia (FT-IR) alkalmazásával vizsgálták a fehérjék és cukrok közötti kölcsönhatások jellemzésének céljából. Ezt követően infravörös (IR) és Raman-spektroszkópia segítségével kimutatták, hogy a trehalóz legjelentősebb funkciója, hogy koncentrálja azt a kis mennyiségű vizet a fehérje közelében, amely a funkció megtartásához szükséges. A trehalóz fehérjestabilizáló képességét az ipar számos területén hasznosíthatják; például a kozmetikai iparban hidratáló készítményekben, vagy a gyógyszeriparban liposzóma stabilizálására.

Az élelmiszeriparban szintén alkalmazott segédanyag. Itt édesítő- és stabilizáló szerként egyaránt használják. Édessége a szacharóz 45%-ával egyezik meg.

A gyógyászatban hatóanyagként is felhasználásra kerül. „Chaperone" elnevezésű anyagként használják, amely segítséget nyújt a Creutzfeld–Jacob kórt, cisztás fibrózist és amiloid rendellenességeket okozó fehérje aggregációjának megelőzésében.

A trehalóz segédanyagként való legfontosabb alkalmazási területei gyógyszerészeti szempontból az oltóanyagok stabilizálása szobahőmérsékleten való tárolás céljára, enzimek tartósítása, illetve emlős sejtek liofilizálás alatti károsodástól való védelme. Mivel koncentrálja a fehérje közelében a vizet, így az a liofilizálás után vissza tud rendeződni natív szerkezetébe és visszanyeri funkcióját. Fejlődő országokban a járványos gyermekbénulás ellen alkalmazott orális oltóanyagok előállításánál azt tapasztalták, hogy trehalóz jelenlétében 45 °C-on szárítva azok stabilak maradtak, összehasonlítva a 4 °C-on lefagyasztott folyékony oldattal [3]. A trehalóz másik fontos alkalmazási területe a DPI formában történő hordozóanyagként való felhasználása [4-6].

A trehalóz is, mint nagyon sok más a gyógyszertechnológiában alkalmazott ható- és segédanyag, polimorfiára hajlamos. A segédanyagok polimorfiájának nagy jelentősége van a gyógyszeriparban, hiszen ez alapvetően meghatározza az adott forma olvadáspontját, oldékonyságát, fizikai és kémiai stabilitását. A trehalóznak 4 polimorf módosulata ismeretes, amelyek különböző olvadásponttal rendelkeznek (*I. táblázat*) [7].

A fent említett példák azt támasztják alá, hogy a trehalóz, mint gyógyszertechnológiai segédanyag, számtalanszor kerül feldolgozásra porlasztva- [4, 8-10] és fagyasztvaszárítással [11-13]. Mivel ezek
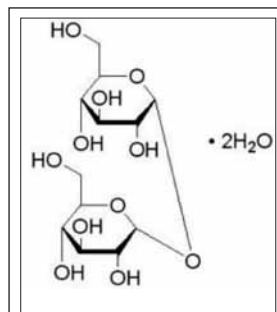
A trehalóz polimorf módosulatainak olvadáspontja [7]

Polimorf módosulat neve	Olvadáspont (°C)
α-trehalóz	126
β-trehalóz	215
γ-trehalóz	118-122
h-trehalóz	100-110

az eljárások gyakran okoznak amorfizálódást, ezért a segédanyag ilyen szempontból történő vizsgálata igen érdekes lehet. Forgalomban lévő liofilezéssel formulált védjegyzett készítmény például az ADVATE®, amelyben a hatóanyagot, a rekombináns VIII-as véralvadási faktort, a trehalóz stabilizálja [14]. Továbbá a 4 polimorf módosulat létezése a rekrisztallizáció követését is indokolja.

Az amorfizálás technológiai megvalósítása

Az amorf anyagok kialakulására / kialakítására három technológia alkalmazható: *olvadék technológia*, *őrléses* és *oldószeres eljárások* [15]. Olvadék technológiával két úton lehet amorf anyagot előállítani. Az egyik művelet során a kristályos anyagot megolvasztjuk, majd ezt az olvadékot hirtelen dermesztjük. A másik művelet során a kristályos anyagot a segédanyag olvadékában diszpergáljuk, majd ezt az olvadékot szintén dermesztjük [16]. Dezintegráló műveletek közül őrléssel is előállíthatunk amorf anyagot. Őrlés során olyan mértékű mechanikai erőt fejtünk ki a kristályrácsra, amekkorát az az elasztikus határok közt nem képes tolerálni, így megváltozik a szerkezete. A keletkező hő hatására a lokális olvadások miatt is amorfizálódhat az anyag [17]. Az oldószeres eljárások között három csoportot különíthetünk el: hőmérsékletemeléssel történő dehidráció, nyomáscsökkentéssel történő szárítás (liofilezés) [18], porlasztásos technológia [19]. Jelen munka az oldószeres megoldások témakörét, azon belül is a porlasztva szárítást érinti.

Porinhalációs készítmények formuláláshoz alkalmazott segédanyagok gyógyszertechnológiai vonatkozásai

A porlasztva szárítás egyik jelentős felhasználási területe a por inhalációs készítmények előállítása. A porinhalációs rendszerek pulmonális gyógyszerbevitelre alkalmas szilárd fázisú készítmények. Fő előnyük, hogy nagy koncentrációjú hatóanyagot juttathatunk célzottan a tüdőbe és minimális az extrapulmonális veszteség. Kiválthatunk

vele helyi illetve szisztémás hatást, valamint kedvező a biológiai hasznosíthatósága. Ennek a gyógyszerformának a fejlesztése, relatíve kevés segédanyaggal megoldható, a hatóanyag stabilitásának biztosítása egyszerű. Nincs hajtógáz, csupán egy adagolócsavar, melynek kattanásig történő tekerésével a „*unit dose*" adagolás biztosított, így nem kell tartani a túladagolástól sem [20]. A szemcseméretnek 1-5 μm-es mérettartományba kell esnie, mivel az ennél nagyobb szemcsék nem jutnak át a légutakon az alkalmazás helyére, az ennél kisebbek pedig a kilégzéssel távoznak. Ahhoz viszont, hogy a por jó folyási tulajdonságokkal rendelkezzen, ne legyen kohezív és jól lehessen dozírozni, segédanyagokra van szükség. Ezeket az anyagokat, amelyek a hatóanyagot célba juttatják, hordozóanyagnak hívjuk. Erre általában α-laktóz-monohidrátot alkalmaznak, de az új készítményekben már más segédanyagokkal is helyettesíthetik a laktózt. Ennek egyik oka a TSE (átadható spongiform enkefalopátiás betegségek) elkerülése, a másik pedig, hogy a laktóz reakcióba léphet az amino csoporttal, így fehérje és peptid készítmény nem formulálható vele. Ebben az esetben a laktózt többek között trehalózzal helyettesítik. Lehetőség van még a raffinóz és a szukróz alkalmazására is. Ezeknek a nem redukáló cukroknak van egy olyan közös kedvező tulajdonsága, hogy porlasztva szárítás során megvédik a fehérjéket vagy peptideket a különböző stresszhatásokkal szemben. Helyettesítik a hidrogén kötéseket, amelyeket normál esetben a víz tesz, valamint viszkózus keveréket alkotnak a fehérjével, melynek következményeként magas üvegesedési hőmérsékletű termék keletkezik [21].

Kísérletes munka

A kísérletes munkánk arra világít rá, hogy a polimorfiára hajlamos amorfizált vagy amorfizálódott segédanyagok a hőmérséklet és a relatív páratartalom viszonyának változására különböző polimorf módosulatok formájában kristályosodhatnak vissza és ennek nagy jelentősége van a feldolgozás, valamint az alkalmazás során. Mivel a Szegedi Tudományegyetem Gyógyszertechnológiai Intézetében már van tudományos előzménye az anyagok amorfizálhatóságának [15, 22-26], így azt a célt tűztük ki magunk elé, hogy a porinhalációs készítmények egyik fontos komponensének a trehalóznak, az amorfizálódását és az amorf forma tárolás során bekövetkezett rekrisztallizációját, polimorf módosulatait tanulmányozzuk.

Kiindulási segédanyag

A kiindulási anyag a D(+)-trehalóz-dihidrát volt (Carl. Roth. GmbH + Co. KG. 76185 Karlsruhe). Ezt tekintettük 100%-os kristályos anyagnak. Víztartalma 9,5±0,5%, szulfáttartalma pedig kevesebb, mint 0,5% volt. Fajlagos forgatóképessége: 178±2°.

Minták előállítása

A kísérletes munkánk során két mintát állítottunk elő, azonos körülmények között. Mindkét esetben a trehalózból tisztított vízzel 10%-os oldatot készítettünk mágneses keverő segítségével, és ezt az oldatot BÜCHI B-191 Mini Spray Dryer (Büchi, Svájc) készülékkel porlasztottuk a **II. táblázatban** megadott paraméterek mellett [10]. Az így nyert terméket szobahőmérsékleten (25±2 °C) exszikkátorban tároltuk 32±5%-os relatív páratartalmú (RH) légtérben a vizsgálatok indításáig.

Tárolási körülmények

A mintákat 3 hónapig tároltuk, különböző körülmények (hőmérséklet, relatív páratartalom-RH) befolyását vizsgálva [27]. Az első porlasztott mintát (**I**) normál körülmények közt tároltuk, míg a másodikat (**II**) két részre osztottuk, egyik felét a gyorsított stabilitási vizsgálatoknak (**IIa**), másik felét pedig ennél intenzívebb terhelésnek (**IIb**) vetettük alá, a következők szerint:
- normál körülmények között (**I**), exszikkátorban, 25±2 °C és 32±5% RH,
- a gyorsított stabilitási vizsgálat körülményei között (**IIa**), 40±2 °C, 75±5% RH [26],
- intenzíven terhelt kondíciók között (**IIb**), 60±2 °C, 90±5%.

Utóbbi kettőnél mi állítottunk elő különböző koncentrációjú kénsav tartalmú higrosztát tölteteket és termosztátba helyeztük azokat. A tárolási körülményeket folyamatosan kontrolláltuk.

Porlasztási paraméterek

Paraméterek	Beállítás
Bemenő hőmérséklet (°C)	130-140
Kimenő hőmérséklet (°C)	75-92
Pumpaáramlás (ml/min)	2
Sűrített levegő nyomása (bar)	4,8
Atomiser pumpaáramlás (normoliter/h)	600
Aspirátor (%)	80
Pumpa áramlása (%)	2

Vizsgáló módszerek

A mintákat METTLER Toledo 821e DSC (Mettler-Toledo GmbH., Gießen, Németország) segítségével vizsgáltuk. Ennek a módszernek a segítségével igazoltuk a trehalóz amorf formájának létét és az amorf forma üvegesedési hőmérsékletét (T_g) is követni tudtuk a rekrisztallizációs folyamat során. A mérés során 5±0,2 mg mintát mértünk alumínium tégelybe analitikai mérleg segítségével, majd a tégelyt lezártuk és behelyeztük a kemencébe. A kemencét 25 °C-tól 250 °C-ig fűtöttük fel 10 °C/min fűtési sebességgel és mértük a mintában lejátszódó termikus változásokat. Az eredményeket STAR^e szoftver segítségével értékeltük ki.

A visszakristályosodás folyamatának meghatározásához porröntgen diffrakciós vizsgálatokat is végeztünk. Erre Bruker D8 Advance diffraktométerrel (Bruker AXS GmbH., Karlsruhe, Németország) berendezést használtunk. Sugárforrásként Cu KλI sugárzást (λ= 1.5406 Å) alkalmaztunk. A minták vizsgálata 40 kV feszültség és 40 mA áramerősség alkalmazása mellett 3°-tól 40°-ig (2θ) történt. A szkennelési sebesség 0,1°/min, a lépésköz pedig 0,010° volt. A műszer kalibrálása korund segítségével történt. Az eredmények kiértékelésére pedig DIFFRACTplus EVA szoftvert alkalmaztunk. A diffraktogramokat Kα2-vel korrigáltuk, simítottuk és az alapvonal korrekcióját is elvégeztük. A termékek azonosítására a Cambridge-i Krisztallográfiai Adatbázist (CCDC ID: AI631510) használtuk.

Differenciális pásztázó kalorimetriás vizsgálatok (DSC)

A trehalóz T_g–je kísérletes úton, DSC vizsgálattal meghatározható. A mintát felfűtöttük olvadáspontja fölé, majd visszahűtöttük szobahőmérsékletre és megismételtük a fűtést ugyanazzal a fűtési sebességgel. A következőket tapasztaltuk:
- a második melegítés során eltűnt a karakterisztikus olvadáspont,
- a fűtési folyamat során nem érzékeltünk bomlásra utaló jelet,
- a Tg láthatóvá vált a görbén (2. ábra).

Az átmenet 109,3-130,0 °C-ig tart, középértéke 115,4 °C-nál található. A trehalóz irodalomból ismert T_g-je szintén ebben a tartományban található [7].

Irodalomból ismeretes, hogy az üvegesedési hőmérséklet és az olvadáspont hányadosa előrevetítheti az anyag amorfizálhatóságát [25]. A **3. ábrán** látható, hogy a kiindulási trehalóz három poli-

2. ábra: A trehalóz üvegesedési hőmérsékletének (T_g) meghatározása DSC módszerrel
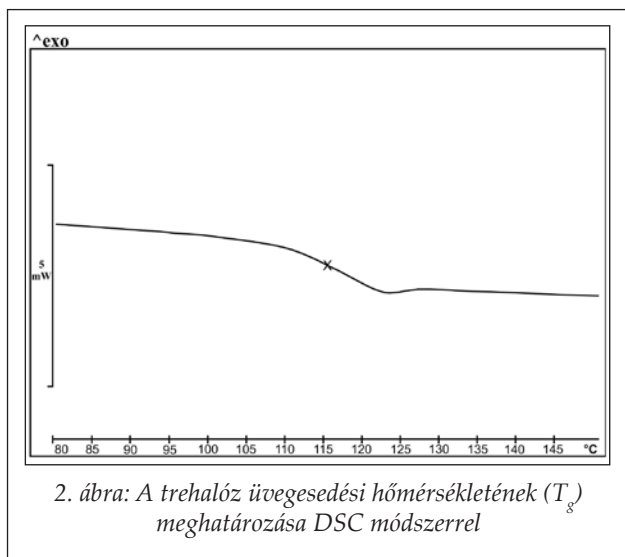
morf keveréke (A görbe). A görbe alatti terület arányos az egyes módosulatok mennyiségével. Legnagyobb arányban a h-trehalóz található meg és ez a legjobban amorfizálható módosulat, T_g/T_m (K/K) értéke 1,03. Szintén jól amorfizálható a legkisebb mennyiségben előforduló γ-trehalóz, T_g/T_m (K/K) értéke 0,98. A legkisebb T_g/T_m (K/K) értékkel a β-trehalóz rendelkezik (0,71), de még ez a polimorf is a jól amorfizálható kategóriába esik. Ezen előrvizsgálatok alapján tehát megállapítható, hogy a trehalóz amorf formája állítható elő porlasztva szárítással és igazolást nyert az is, hogy a trehalóz valóban jól amorfizálható segédanyag.

Az első porlasztásból (**I**) származó minta vizsgálati eredményeit szintén a *3. ábra* szemlélteti. Az *A görbén* a kiindulási kristályos trehalóz látható, három polimorf módosulat különíthető el rajta.
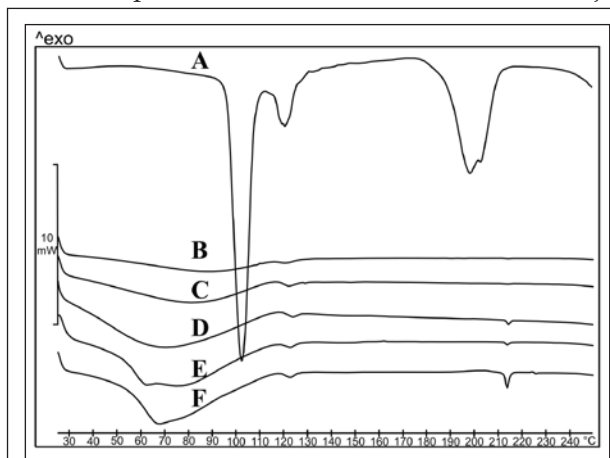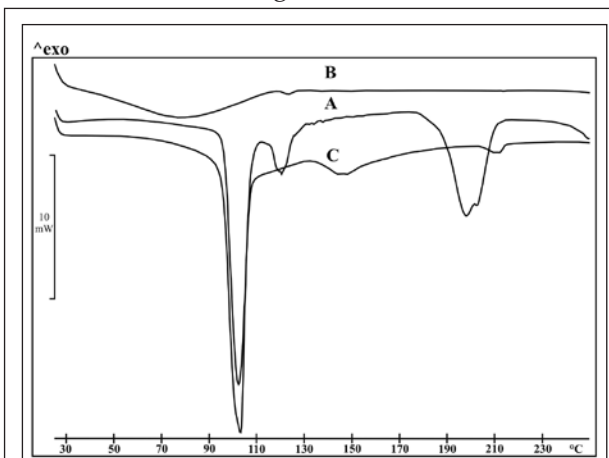
A három csúcs tehát a különböző polimorf módosulatok olvadáspontja. A többi, *B, C, D, E és F görbék* pedig a porlasztott minta DSC görbéi időrendi sorrendben. A mintákat normál körülmények között tároltuk (25±2 °C, 32±5% RH), és másfél hónapon keresztül vizsgáltuk. A *B görbén* a frissen porlasztott minta látható. Megállapítható, hogy a porlasztás nem eredményezett 100%-ban amorf terméket, a minta némi kristályos frakciót tartalmazott, mégpedig a γ-trehalóz (dihidrát) polimorf módosulatot, amelynek 122 °C-nál van az olvadáspontja. Két nappal később vizsgálva láttuk a *C görbén*, hogy a kristályos frakció nőtt, azaz megindult egy lassú rekrisztallizációs folyamat. Tizennégy nappal a porlasztás után azt tapasztaltuk a *D görbén*, hogy megjelent egy másik polimorf módosulat, a β-trehalóz (anhidrát), melynek 215 °C-nál van az olvadáspontja. Harminc (*E*), majd negyvenkét (*F*) nappal a porlasztás után azt a következtetést vontuk le, hogy mindkét polimorf módosulathoz tartozó csúcs alatti terület nőtt, azaz nőtt a kristályos frakció mennyisége.

Újabb sarzsot porlasztottunk (**II**) azonos körülmények között a trehalóz vizes oldatából. Az ezen porlasztásból származó minták vizsgálati eredményeit mutatja a *4.* és az *5. ábra*.

A *4. ábrán* az *A görbe* a kiindulási kristályos trehalóz DSC görbéje. A *B és C görbe* pedig a friss és tárolt porlasztott mintáé. Látható, hogy nem eredményezett 100%-ban amorf terméket a második porlasztás sem, a γ-trehalóz (dihidrát) polimorf módosulat megtalálható benne, olvadáspontja 123 °C-nál található. A minták egyik felét 40±2 °C, 75±5% RH higrosztát töltetben tároltuk és

3. ábra: Porlasztva szárított trehalóz rekrisztallizációjának DSC vizsgálata (I minta, tárolási körülmények: 25±2° C, 32±5% RH). A: kiindulási kristályos trehalóz, B: friss porlasztott minta, C: két napos minta, D: tizennégy napos minta, E: harminc napos minta, F: negyvenkét napos minta.
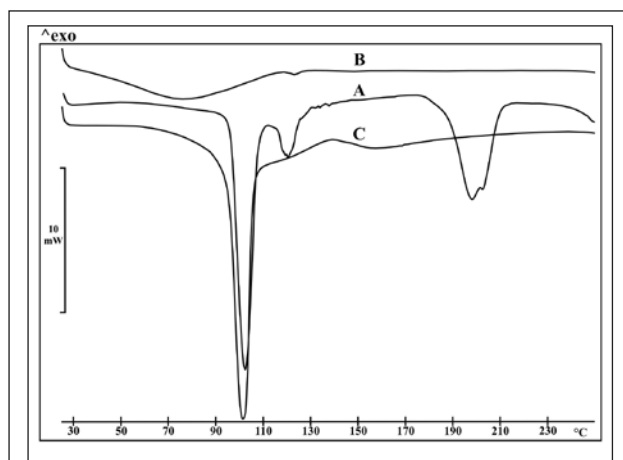

4. ábra: Kiindulási, frissen porlasztott és tárolt minták DSC görbéje: a gyorsított stabilitási vizsgálatok (IIa) körülményeinek (40±2 °C, 75±5% RH) hatása az amorf trehalózra. A: kiindulási kristályos trehalóz, B: friss porlasztott minta, C: tárolt minta 7 nap után.

hét nap után vizsgáltuk. A *C görbén* látható, hogy egy új polimorf módosulat jelent meg a β-trehalóz (anhidrát), 212 °C-nál. Következtetésként levontuk, hogy a gyorsított stabilitási vizsgálat körülményeinek hatására a minták 100%-ban visszakristályosodtak, mégpedig a h-trehalóz (dihidrát) polimorf módosulatába, melynek olvadáspontja 102 °C-nál található.
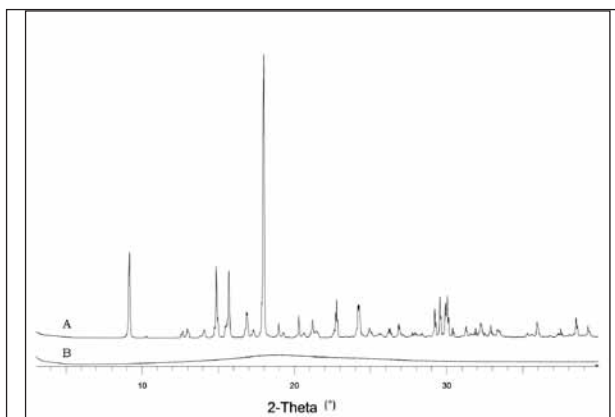
A *5. ábra* mutatja a porlasztott minta rekrisztallizációs viselkedését szélsőséges körülmények között. Az *A, B, C görbék* szintén a kiindulási kristályos trehalóz és a friss és a tárolt porlasztott minták DSC görbéi. A tárolási körülmények ennél a vizsgálatnál a következőképpen alakultak: 60±2 °C-on, 90±5% RH, tárolási idő: 7 nap. Ugyanazt tapasztaltuk, a kiindulási kevés kristályos frakciót tartalmazó amorf mintánk hét nap elteltével az agresszív tárolási körülmények hatására 100%-ban visszakristályosodott a h-trehalóz (dihidrát) polimorf módosulatába.

A DSC vizsgálatok eredményeit a ***III. táblázat*** foglalja össze. Megjelöltük, hogy a vizsgálatok során az irodalomban fellelhető trehalóz polimorf módosulatok közül, melyeket találtunk meg a mintákban. A DSC vizsgálatokból nyerhető adatok alapján, a minták adott polimorfra vetített kristályosságát is kiszámoltuk és jelöltük a táblázatban. Ez az eredmény félkvantitatívnak tekinthető, de a rekrisztallizációs tendencia leírására alkalmas. A vizsgálatok végén tapasztalt 100% fölötti értékek csupán a módszer félkvantitatív jellegére utalnak.
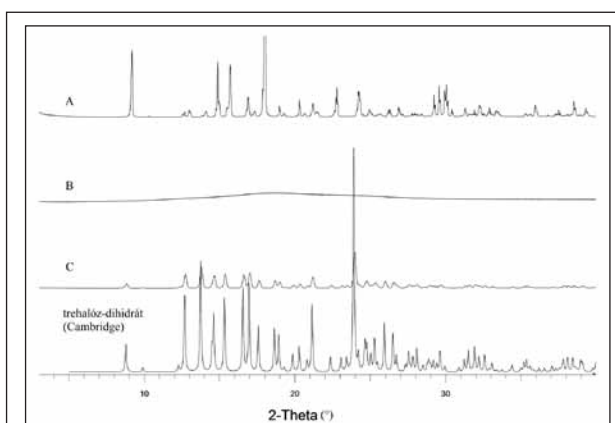
Porröntgen diffrakciós vizsgálatok (XRPD)

6. ábra: Kiindulási anyag és porlasztva szárított termék porröntgen diffraktogramjai: **A:** kiindulási kristályos trehalóz, **B:** friss porlasztott minta.

A porröntgen diffrakciós vizsgálatok eredményei összhangban vannak a DSC mérésekkel, amelyek a *6. ábrán* lévő diffraktogramokon jól követhetők. Az ábra jól mutatja, hogy az *A* jelzésű kiindulási trehalóz kristályos termék, a *B* pedig az porlasztva szárítás során képződött *I. minta*, amely röntgen amorfnak tekinthető.

Az újabb *(II. minta)* XRPD eredményeit a ***7. ábra*** szemlélteti. Az *A* diffraktogram a kiindulási kristályos trehalóz, a *B* a frissen porlasztott amorf minta és a *C* pedig a tárolt minta diffraktogramja. A *B görbe* kisimult, a jellemző intenzitás értékek eltűntek, azaz röntgen amorf terméket eredményezett a porlasztás. A visszakristályosodó mintában (*C*) kezdenek megjelenni a karakterisztikus csúcsok, összehasonlítva a Cambridge-i Krisztallográfiai Adatbázisban lévő trehalóz dihidrát polimorf módosulat diffraktogramjával, látható, hogy

5. ábra: Kiindulási, frissen porlasztott és tárolt minták DSC görbéi: szélsőségesen (**IIb**) terhelt (60±2 °C, 90±5% RH) körülmények hatása az amorf trehalózra. **A:** kiindulási kristályos trehalóz, **B:** friss porlasztott minta, **C:** tárolt minta 7 nap után.

7. ábra: A kiindulási és porlasztással előállított minták porröntgen diffraktogramjai: amorf trehalóz rekrisztallizációja és a visszanyert anyag azonosítása. **A:** kiindulási kristályos trehalóz, **B:** frissen porlasztott minta, **C:** normál körülmények között (25±2 °C és 32±5% RH) tárolt 1 napos minta.

III. táblázat

Tárolási körülmények hatására megjelenő polimorf módosulatok (3-5. ábra adatai alapján)

Porlasztott minta	Körülmények			Polimorf módosulat			
	Tárolási idő (nap)	Hőmérséklet (°C)	Páratartalom (RH%)	α	β (%)	γ (%)	h (%)
kiindulási trehalóz				-	42,93	6,84	50,23
I	0			-	-	4,47	-
I	2			-	-	6,44	-
I	14	25±2	32±5	-	0,39	5,74	-
I	30			-	0,21	5,92	-
I	42			-	1,62	6,11	-
IIa	0	40±2	75±5	-	-	5,12	-
IIa	7			-	3,29	-	101,9
IIb	0	60±2	90±5	-	-	5,12	-
IIb	7			-	-	-	104,28

a jellemző csúcsok egybeesnek. A porlasztott termék tehát a trehalóz-dihidrát polimorf módosulatba kristályosodik vissza. A kiindulási kristályos trehalózról (*A*) pedig megállapítható, hogy több polimorf módosulat keveréke, a módosulatok reflexiói megjelennek a diffraktogramon.

Összefoglalás

A kísérletes munka során porlasztva szárítással állítottunk elő trehalóz oldatból amorf szilárd fázisú terméket, majd vizsgáltuk a rekrisztallizáció folyamatát különböző körülményeket alkalmazva a tárolás során. Megállapítottuk, hogy a trehalóz porlasztva szárítással amorfizálódik (kevés kristályos frakció marad a rendszerben). A T_g mérhető a mintákban és megegyezik az irodalmi értékkel. Láthattuk, hogy viszonylag alacsony páratartalom mellett megindul a rekrisztallizáció, de a teljes folyamat igen lassú, időtartama hónapokban mérhető. Intenzívebb körülmények hatására viszont robbanásszerűen megindult a visszakristályosodás. A trehalóznál a dihidrát forma (γ- és h-trehalóz) a meghatározó a rekrisztallizáció során, de anhidrát forma (β-trehalóz) is detektálható. Megfelelően hosszú idő után a kiindulásival megegyező polimorf módosulatok keveréke nyerhető vissza. Ez

azt támasztja alá, hogy azoknál a porinhalációs készítményeknél, ahol trehalóz a hordozó, különös figyelmet kell fordítani a megfelelő tárolási körülmények megválasztására.

IRODALOM

1. *Pifferi, G.; Santoro, P.; Pedrani, M.*: Il Farmaco *54*, 1–14 (*1999*).
2. *L. Yu.*: Adv. Drug Deliver. Rev. *48*, 27-42 (*2001*).
3. http://www.omikk.bme.hu/collections/mgi_fulltext/bio/2003/06/0602.pdf [2013.06.13.] Molnár, K.: Élelmiszeripari biotechnológiák: A trehalóztermelés új gazdaságosabb eljárásai (2003).
4. *Ógáin, O. N., Li, J., Tajber, L., Corrigan, O. I., Healy, A. M.*: Int. J. Pharm. *405*, 23–35 (*2011*).
5. *Islam, N., Gladki, E.*: Int. J. Pharm. *360*, 1–11 (*2008*).
6. *Gradon, L., Sosnowski, T. R.*: Adv. Powder Technol. DOI: http://dx.doi.org/10.1016/j.apt.2013.09.012. (2013).
7. *F. Sussich, A. Cesáro.*: Carbohydr. Res. *343*, 2667-2674 (*2008*).
8. *Maurya, M., Murphyb, K., Kumarb, S., Shib, L., Lee, G.*: Eur. J. Pharm. Biopharm. *59*, 565–573 (*2005*).
9. *Maurya, M., Murphyb, K., Kumarb, S., Mauerera, A., Lee, G.*: Eur. J. Pharm. Biopharm. *59*, 251–261 (*2005*).

10. *Moran, A., Buckton, G.:* Int. J. Pharm. *343,* 12-17 (*2007*).
11. *Murugappan, S., Patil, H. P., Kanojia, G., ter Veer, W., Meijerhof, T., Frijlink, H. W., Huckriede, A., Hinrichs, W. L. J.:* Eur. J. Pharm. Biopharm *85,* 3, A, 716-725 (*2013*).
12. *Nakamura, T., Sekiyama, E., Takaoka, M., Bentley, A. J., Yokoi, N., Fullwood, N. J., Kinoshita, S.:* Biomaterials *29,* 3729–3737 (*2008*).
13. *Crowe, J. H., Tablin, F., Wolkers, W. F., Gousset, K., Tsvetkova, N. M., Ricker, J.:* Chem. Phys. Lipids *122,* 41-52 (*2003*).
14. *Parti, R., Schoppmann, A., Lee, H., Yang, L.:* Haemophilia *11,* 492-496 (*2005*).
15. *Jójárt-Laczkovich, O., Szabó-Révész, P.:* Drug Dev. Ind. Pharm., (2011).
16. *Kim,M. S., Jin, S. J., Park, H. J., Song, H. S., Hwang, S. J.:* Eur. J. Pharm. Biopharm. *69,* 454-465 (*2008*).
17. *Vollenbroek, J., Hebbink, G. A., Ziffels, S., Steckel, H.:* Int. J. Pharm. *395,* 62-70 (*2010*).
18. *DiNuzio J. C., Brough C., Hughey J. R., Miller, D. A., Williams III, R. O., McGinty, J. W.:* Eur. J. Pharm. Biopharm. *74,* 340-351 (*2010*).
19. *Chieng, N., Rades, T., Saville, D.:* Eur. J. Pharm. Biopharm. *68,* 771-780 (*2008*).
20. *Szakonyi, G., Zelkó, R.:* Acta Pharm. Hung. *80,* 121-127 (*2010*).
21. *Maas, S. G., Schaldach, G., Littringer, E. M., Mescher, A., Griesser, U.J., Braun, D. E., Walzel, P. E., Urbanetz, N. A.:* Powder Technol. *213,* 1-3, 27-35 (*2011*).
22. *Jójárt-Laczkovich, O., Szabó-Révész, P.:* J. Therm. Anal. Calorim. *102,* 243-247 (*2010*).
23. *Szabóné-Révész P., Laczkovich O., Erős I.:* Acta Pharm. Hung. *74,* 39-44 (*2004*).
24. *Jójártné Laczkovich O., Szabóné Révész P.:* Magy. Kém. Foly. *116,* 101-104 (*2010*).
25. *Mártha Cs., Jójártné Laczkovich O., Szabóné Révész P.:* Acta Pharm. Hung. *81,* 37-42 (*2011*).
26. *Mártha, Cs., Kürti, L., Farkas, G., Jójárt-Laczkovich, O., Szalontai, B. Glässer, E., Deli, M. A., Szabó-Révész, P.:* Eur. Polym. J. *49,* 2426-2432 (*2013*).
27. http://www.ich.org/products/guidelines/quality/article/quality-guidelines.html [2013.12.02] ICH Q1A(R2) International Conference on Harminization Q1A(R2) Stability Testing of New Drug Substances and Products (2003).

II.

CrossMark

Study of paracetamol-containing pastilles produced by melt technology

Gábor Katona[1,3] · Péter Sipos[1] · Patrick Frohberg[2] · Joachim Ulrich[2] ·
Piroska Szabó-Révész[1] · Orsolya Jójárt-Laczkovich[1]

Abstract The focus of this work was to apply melt technology for the formulation of a pastille containing paracetamol (PCT) in a solid dispersion with two sugar alcohols (xylitol and mannitol) and polyethylene glycol 6000 (PEG) as the carrier system components. Optimization of the pastillization was performed both statistically by using the Box–Behnken design and experimentally by determining the phase diagrams. For the latter and recrystallization of the components, differential scanning calorimetry detection was utilized. The developed pastilles consisted of a eutectic mixture of xylitol (61.25 %) and mannitol (15.31 %) with PEG (7.81 %) as carrier system together with PCT (15.63 %). The components of the pastilles underwent recrystallization at different rates for 5 days. Transmission Raman spectroscopy revealed the homogeneous distribution of the PCT in the pastille. X-ray powder diffractometry showed that the recrystallization of the PCT resulted in its monoclinic form I, while dispersive Raman spectroscopy detected both the monoclinic and orthorhombic forms. The drop-melted pastilles displayed relatively high hardness, and the PCT dissolved within 15 min. It is concluded that pastillization can be achieved through melt technology and the structure and the technological parameters of the pastille are suitable for the development of lozenges as a solid dosage form for children therapy.

Introduction

Melt technology is an increasingly used technological operation in the pharmaceutical industry, whereby novel products can be produced efficiently. This is a green technology, involving dust-free processes, and elastic materials can also be used to produce the final form. There is no need for the use of extra organic solvents in the production, and there are therefore no residual solvents in the product and less environmentally harmful chemical waste, in contrast with other conventionally used techniques. Melt technology can result in amorphous products, which may have higher dissolution rates and bioavailability than those of the corresponding crystalline forms [1–5]. With a fusion method, a solid dispersion of the excipients and active agent can be prepared. Through a drop-melting method, pastilles can be formed, and pastillization is achieved in one step of a conventional melting process. New approach in this topic is a coating process during the pastillization developed by Ulrich et al. [6–8], which means the formation of a "coating material" via the phase separation of a eutectic mixture.

In the USA, a buccal pharmaceutical preparation, Meltaways® (Tylenol), containing 80 mg of paracetamol (PCT), is available as a chewable tablet in paediatric therapy. Such solid preparations have the aim of fast release. Although they are most often used for a localized effect in the mouth, they can also be used for a systemic

✉ Piroska Szabó-Révész
  revesz@pharm.u-szeged.hu

1 Department of Pharmaceutical Technology, University of Szeged, Eötvös 6, Szeged 6720, Hungary

2 Centre of Engineering Science, Thermal Process Engineering, Martin Luther University Halle-Wittenberg, 06099 Halle, Germany

3 Richter Gedeon Plc., Budapest, Gyömrői 19-21, Budapest 1103, Hungary

Springer

effect if the drug is well absorbed through the buccal lining or is swallowed. Analgetics and antihistamines are commonly utilized in such formulations, which are easy to use in paediatric or geriatric therapy, and the drug can be kept in contact with the oral cavity for an extended period of time. By means of buccal absorption, the disadvantages of peroral administration can be avoided, such as the hepatic first-pass metabolism or enzymatic degradation within the gastrointestinal tract, which prevent the oral administration of certain classes of drugs, particularly proteins and peptides [9], and additionally, a lower amount of drug is needed to achieve the therapeutic effect.

During hot-melt techniques, pharmaceutical auxiliary agents such as polyethylene glycols (PEGs) or polyvinylpyrrolidone [10] have often been applied as meltable carriers [11, 12]. Besides PEGs, sugar alcohols are also commonly used to prepare solid dispersions [13]. Sugar alcohols have a number of beneficial properties: they often increase the dissolution of the dosage form, they serve as masking agents, and they are suitable for diabetic patients in view of their low glycaemic indices. β-D-Mannitol and D-xylitol are sugar alcohols that are often used in the pharmaceutical industry. Both are stable and inert compounds suitable for tableting, freeze-drying, capsulizing, granulating and grinding [14, 15] and as carriers in pulmonary drug delivery systems [16].

Sugars and sugar alcohols form eutectic mixtures with each other in certain ratios, resulting in a system with a lower melting temperature than that of either of the components [17]. The literature examples of this type include mannitol–sorbitol [18], xylitol–isomalt [6] and xylitol–sorbitol [19]. For xylitol–mannitol, we found eutectic melting temperature [21], but the literature has not any experimental work with this composition. Eutectics are commonly used in drug designing and delivery processes. Simple eutectic mixtures are solid dispersions involving one or more active pharmaceutical ingredients in an inert carrier or matrix in the solid state, prepared by a fusion method [20]. They are produced by the rapid solidification of the fused melt of the components. Thermodynamically, this system is a physical mixture of the crystalline components.

The aim of our work was to apply melt technology to develop a pastille as lozenge solid dosage form, which has fast dissolution rate of PCT (within 15 min). To find pastille basis, the eutectic mixture of xylitol and mannitol was investigated and the effect of PEG as softener material was controlled on the eutectic formation and the recrystallization of PCT. The thermal behaviour of the components and the product was investigated by means of differential scanning calorimetry (DSC), and the polymorph modifications were checked with X-ray powder diffractometry (XRPD) and dispersive Raman spectroscopy (DRS). The distribution of PCT in the pastille was analysed by using transmission Raman spectroscopy (TRS). The hardness of pastilles was determined with a Heberlein hardness tester, and the in vitro dissolution of PCT was investigated.

Materials and methods

Materials

D-Xylitol ((2R,3R,4S)-pentane-1,2,3,4,5-pentol) was purchased from Carl Roth GmbH & Co. KG (Karlsruhe, Germany), and β-D-mannitol ((2R,3R,4R,5R)-hexane-1,2,3,4,5,6-hexol) was from Sigma-Aldrich Chemie GmbH (Mannheim, Germany). The monoclinic form of PCT (N-(4-hydroxyphenyl)acetamide) was chosen as model material for the experimental work; it was obtained from Sanofi Aventis (Frankfurt am Main, Germany) and PEG 6000 from FERAK Laborat (Berlin, Germany).

Differential scanning calorimetry (DSC)

DSC measurements were taken to identify the eutectic mixture of xylitol and mannitol, to investigate the role of PEG and to study the recrystallization. The data were recorded with a Netzsch DSC-204 instrument (Selb, Germany) under a constant nitrogen flow of 30 mL min^{-1}. Solid xylitol–mannitol samples with xylitol contents of 10, 20, 30, 40, 50, 60, 70, 80 and 90 mass% were prepared in a trituration mortar. 7 ± 0.2 mg samples were crimped in aluminium pans with two holes and were examined in the temperature interval 25–170 °C at a heating rate of 2 °C min^{-1}. The melting temperatures for the phase diagram were taken from the endset temperatures of the DSC curves [6, 22]. Each measurement was baseline-corrected. To estimate the eutectic concentration, parabolic curve fitting was used.

Pastillization process

For pastillization, the one-drop pastillization device developed by Kaiser Steel Belt Systems GmbH (Krefeld, Germany) was used (Fig. 1).

Physical mixtures of xylitol and mannitol with PEG as carrier were prepared and melted in a temperature-controlled double-walled vessel at 110 °C. PCT was dispersed in the melted carrier. A crank shaft moved at constant rate by an engine pressed the mixture in drop form through a valve at the bottom of the vessel onto a 25 °C thermostated cooling plate, where it solidified into a flat-bottomed pastille [6].
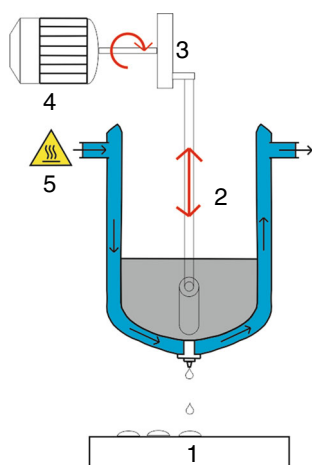
Fig. 1 Pastillization device (*1*—temperature-controlled plate, *2*—double-walled vessel, *3*—crank shaft, *4*—engine, *5*—thermostat) [6]

X-ray powder diffraction (XRPD)

XRPD analysis of the pastille was performed with a Bruker D8 Advance diffractometer (Bruker AXS GmbH, Karlruhe, Germany) with Cu K λI radiation ($\lambda = 1.5406$ Å) and a VÅNTEC-1 detector. The samples were scanned at 40 kV and 40 mA. The angular range was 3°–40° 2θ, in steps of 0.1 s at a step size of 0.007°. The sample was placed on a quartz holder and measured at ambient temperature and humidity. All manipulations, Kα 2-stripping, background removal and smoothing of the area under the diffractogram peaks were performed with DIFFRAC^{PLUS} EVA software.

Raman spectroscopy

PCT-containing pastilles were scanned first with a Cobalt TRS 100 instrument (Cobalt Light Systems Ltd., Abingdon, UK). The TRS technique is a fast, non-destructive measurement with high sampling volume, which provides data about the uniformity of the PCT content. The starting PCT material and the PCT-containing pastilles were scanned by TRS over the wavenumber range 1700–200 cm^{-1}. Each reported spectrum is the average of at least 3 scans with an exposure time of 1 s, a laser power of 0.4 W and a laser spot size of 8 mm.

To investigate the difference between the different forms of PCT and the pastilles, Raman spectra were acquired with a Thermo Fisher DXR Dispersive Raman instrument (Thermo Fisher Scientific. Inc., Waltham, MA, USA) equipped with a CCD camera and a diode laser operating at a wavelength of 780 nm. Raman measurements were taken with a laser power of 12 mW at a slit aperture size of 25 μm on a spot size of 2 μm. The spectra of the individual PEG, mannitol and xylitol were collected with an exposure time of 6 s, for a total of 48 scans in the spectral range 1700–200 cm^{-1} with cosmic ray and fluorescence corrections.

Technological parameters of the pastilles

Geometrical parameters and hardness

The diameter and the height of 20 pastilles were measured with a screw micrometer (Starrett Co., Athol, MA, USA), and their masses were measured with analytical scales.

The hardness of pastilles was determined with a Heberlein hardness tester (Heberlein & Co. AG, Switzerland). Five pastilles were investigated to calculate the average and standard deviation.

Drug content determination

A powdered pastille was taken in a 100-mL volumetric flask, 15 mL of methanol was added, and the mixture was shaken well to dissolve the powder. 85 mL of water was then added to adjust the volume to 100 mL. 1 mL of solution was next withdrawn and transferred to a 100-mL volumetric flask. The volume was adjusted with methanol to 100 mL. The dissolved PCT was investigated spectrophotometrically at 244 nm [23].

In vitro dissolution studies

The dissolution of PCT from pastilles and from comprimates of physical mixtures was determined according to the European Pharmacopoeia (8th Edition) paddle method (Pharmatest Heinburg, Germany). The paddle was rotating in the dissolution vessel at 100 rpm. The dissolution medium was 900.0 mL of purified water (pH 7.25 ± 0.1) at 37 ± 0.5 °C. At predetermined time intervals, 5 mL samples were withdrawn and immediately filtered (cut-off 0.2 μm, Minisart SRP 25, Sartorius, Göttingen, Germany), and the amount of dissolved drug was determined spectrophotometrically at 244 nm.

Results and discussion

Phase diagram of sugar alcohols

In the development of a carrier system for melt technology, the physico-chemical interactions of the components should be examined in order to determine the optimum composition for pastille-forming method.

Determination of the phase diagram of xylitol–mannitol physical mixtures is necessary to find the eutectic melting temperature and to understand the mechanism of crystallization of the pastille (Fig. 2).

We collected the melting temperatures for the phase diagram. The point of interception of the two curves indicated the eutectic concentration at 90 mass% xylitol and 10 mass% mannitol. The melting temperature of pure xylitol was detected to be 97.6 °C. The melting temperature of the eutectic composition dropped to 95.5 °C. The phase diagram suggests that phase separation between xylitol and mannitol is theoretically possible. The melting temperature of pure mannitol (169.5 °C) can be decreased by more than 70 °C in the eutectic mixture.

We found that during the recrystallization of the pastille, a phase separation occurs. A well-defined shell and core structure can be differentiated; therefore, the phase separation was investigated with DSC (Fig. 3).

The melting temperatures of the core and shell of the pastille are different. The melting temperature of the shell is 97.6 °C, parallel with the melting temperature of starting

xylitol. The melting temperature of core structure is 95.5 °C, which is parallel to the eutectic temperature. It means the eutectic composition located in the core of the pastille.

Because the eutectic mixture of xylitol and mannitol results in rapid solidification, therefore it is necessary to apply PEG, as softener material. According to the literature data, it has no influence on the recrystallization of the components (xylitol, mannitol and PCT) but promotes the formation of pastille dosage form [5]. The ternary phase diagram of the xylitol, mannitol and PEG was also investigated in certain cases. 100 mg solid xylitol–mannitol samples in different ratios were prepared with constant amount of PEG (7.81 %) to determine the ternary phase diagram. The melting temperatures were analysed by DSC at a heating rate of 2 °C min^{-1}. Parabolic curve fitting was applied to investigate the effect of the polymer on the eutectic concentration (Fig. 4). It turned out that, in the presence of this quantity of PEG, the eutectic concentration of xylitol and mannitol was at 80 mass% xylitol and 20 mass% mannitol.

Optimization of eutectic formula

Our target was to develop a pastille containing 40 mg PCT. Since PEG was found to influence the eutectic concentration, a Box–Behnken experimental design was carried out to optimize the formulation as concerns the carrier. Three experimental factors (xylitol, mannitol and PEG) were varied in the design, at 3 levels in 15 runs, so as to construct the surface plot for the optimization process (Table 1) according to the recrystallization time.

Recrystallization began on the shell of the pastille and tends inwards to the core. If this process takes place too quickly, the dissolved melt components with higher melting temperatures (PCT and mannitol) recrystallize first and their crystals sink to the bottom of the pastille, resulting in an inhomogeneous distribution. A composition was first
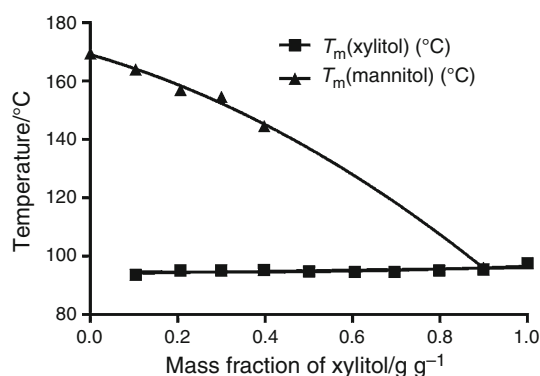
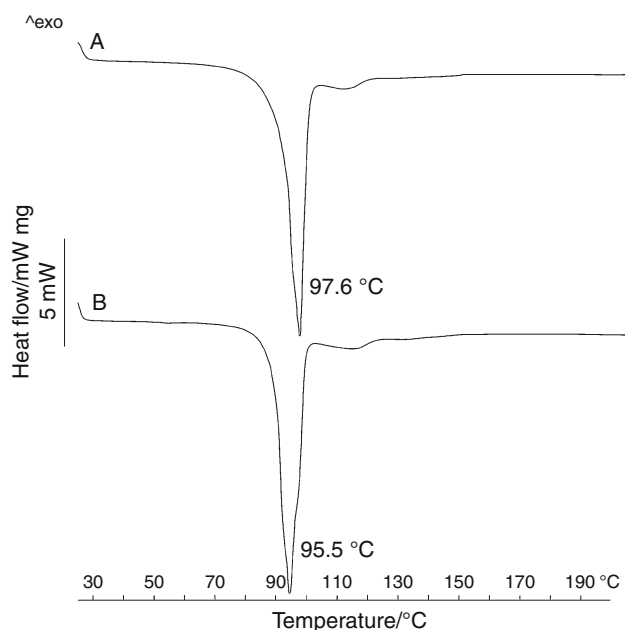Fig. 2 Phase diagram of the xylitol–mannitol system

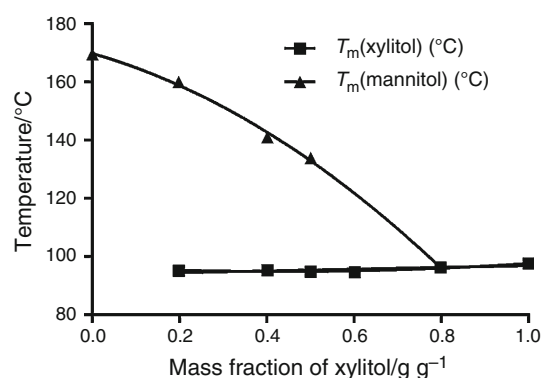Fig. 3 DSC curves of pastille shell (a) and core (b)

Fig. 4 The xylitol–mannitol phase diagram in the presence of a fixed amount of PEG (7.81 mg per 100 mg)

sought at which recrystallization was slow enough to preserve the homogeneous distribution of the components. The experimental results showed that each of the three components exerted a significant effect on the recrystallization. At a 95 % confidence level, the coefficients differed from zero and the P values were <0.05, the time of recrystallization depending significantly on the fractions of the components. The surface plot illustrates the recrystallization times of the different component ratios (Fig. 5).

The surface plot depicts recrystallization times from 1 to 5 days. The maximum in the plot is observed at 61.25 mass% xylitol, 15.31 mass% mannitol, which corresponds to the eutectic composition. The composition also included 7.81 mass% PEG, and the PCT content of the pastille was 15.63 mass%. The calculations indicated that the pastille mass should be ~256 mg containing the 40 mg of PCT.

Pastillization of the carrier

Pastillization took place on the surface of a thermostated cooling plate at 25 °C for 24 h. Because of the relatively high viscosity of the melt, the molecular mobility was decreased and crystallization was hindered in the core. PEG does not prevent the recrystallization of the components as poor crystallization inhibitor to form the pastille. In order to initiate crystallization, pure xylitol crystals were used as seeds [24].

After 24 h, a thin xylitol shell crystallized on the surface of the pastille, which gradually thickened during the storage until the whole of the pastille had solidified. After 5 days, the core was fully solid as shown previously by the surface plot (Fig. 5), but after 3 days, the DSC analysis demonstrated that the crystallization of the sample was still taking place. Figure 6 presents DSC curves of samples stored for various times.

The endotherms in the DSC curves indicate the melting temperature of xylitol. The increasing area of the peaks reflects the extent of crystallization. As the crystallization progresses, the glass transition undergoes a depression. Table 2 shows the DSC data of recrystallization.

Table 1 Variables and their levels in the Box–Behnken design

	Levels		
	−1	0	1
Independent variables/factors	Contents of components/mass%		
Xylitol	48.13	61.25	75.94
Mannitol	6.88	15.31	25.31
PEG	0	7.81	15.63
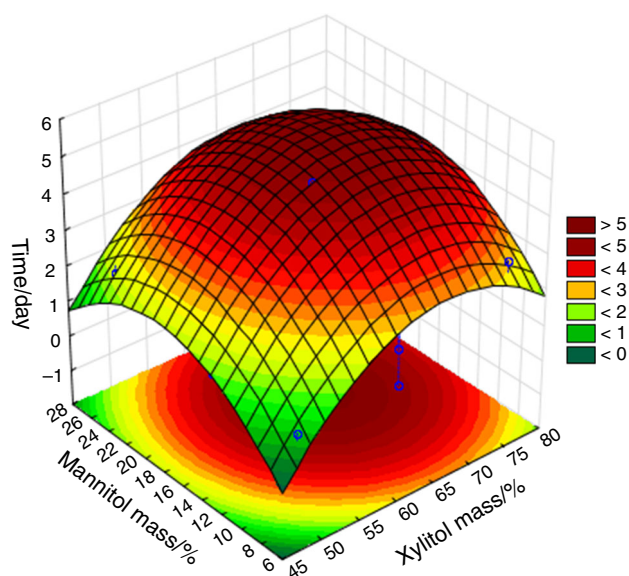
Fig. 5 Surface plot illustrating optimization of the xylitol–mannitol–PEG-containing carrier
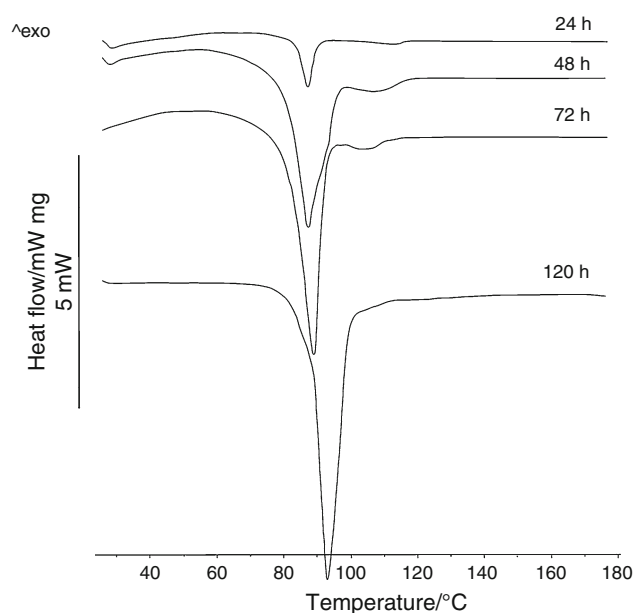

Fig. 6 Recrystallization of the pastille carrier

Table 2 DSC data of recrystallization compared to physical mixture

Time of measurement/h	Melting temperature/°C	Fusion enthalpy/ J g^{-1}
24	88.59	12.47
48	89.36	104.81
72	90.50	123.16
120	95.50	168.57
Physical mixture	95.40	168.27

Pastillization process with PCT

The aim of our work was to formulate a pastille containing PCT and sugar alcohols. This has the advantage that pastillization occurs in a single step. On the basis of the factorial design, for pastillization 61.25 mass% xylitol, 15.31 mass% mannitol, 7.81 mass% PEG and 15.63 mass% PCT were used, as indicated in Fig. 5. This gave the best pastille shape without visible pores and with a homogeneous shell texture. The PEG content resulted in an appropriate crystallization time and decreased the melting temperature of the mixture through the formation of a solid dispersion [25]. DSC curves of the components are presented in Fig. 7. The DSC curves show that the melting temperature of mannitol is not seen at the eutectic composition (compare A and E). The melting temperature of xylitol can still be observed at the eutectic compositions, but much less strongly (compare B and E). The endotherm of PEG is greatly reduced in the eutectic mixture (compare C and E).

After storage of 5 days, the pastille and the physical mixture were investigated by DSC and compared. The DSC curves of the recrystallized pastille and initial components are shown in Fig. 8.

The DSC curves demonstrate that the high melting temperature of PCT (A) is not seen in the DSC curves of the physical mixture and the pastille (B and C), as a result of the PCT partly dissolving in the melt of the eutectic.
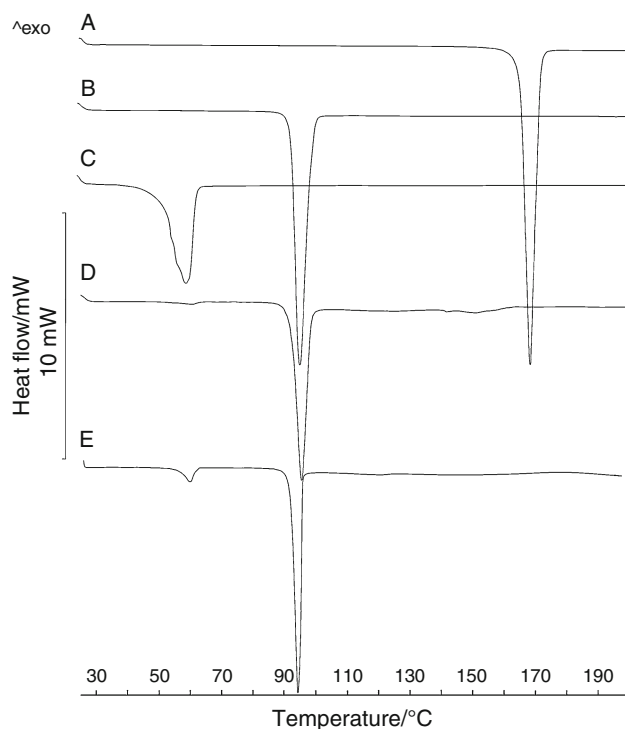
X-ray powder diffraction (XRPD)

Because of the fusion of PCT in the eutectic, the possibility of polymorphic transition of the API during the recrystallization must be considered. PCT has three crystal modifications: a monoclinic form I, which has poor direct compressibility, an orthorhombic form II, and an unstable phase (form III), which can be stabilized only under certain conditions (for example, between a microscopy slide and a cover glass) [26]. XRPD measurements were taken to identify the polymorphic form of the PCT in the product. Comparison of the diffractogram of the starting PCT with the diffractograms of the various crystal modifications available from the Cambridge Crystallography Data Centre (CCDC ID: AI631510) revealed that the starting PCT was in monoclinic form I (Fig. 9).

The core structure of the pastille was investigated after 5 days by means of XRPD; the diffractograms are presented in Fig. 10.

The characteristic peaks of the components can be traced in the diffractogram of the pastille core. The characteristic peaks of the PCT in the core at 13.924° and 23.557° 2θ indicate the presence of the monoclinic form I. Since the peaks of orthorhombic form II are overlapped, we had to use Raman spectroscopy to prove its presence.

Raman spectroscopy

Because of the slow solidification, the distribution of the PCT in the pastilles was first investigated by TRS. The transmission Raman spectra of pure PCT (a) and the PCT-containing pastille shell (b) and core (c) are shown in Fig. 11. The spectra in b and c are basically identical, the almost negligible differences involving new peaks due to the non-PCT ingredients. The pastille spectra indicated that

Fig. 7 DSC curves of the components, the eutectic and the physical mixture: *a* mannitol, *b* xylitol, *c* PEG, *d* physical mixture, *e* eutectic mixture of xylitol and mannitol with PEG
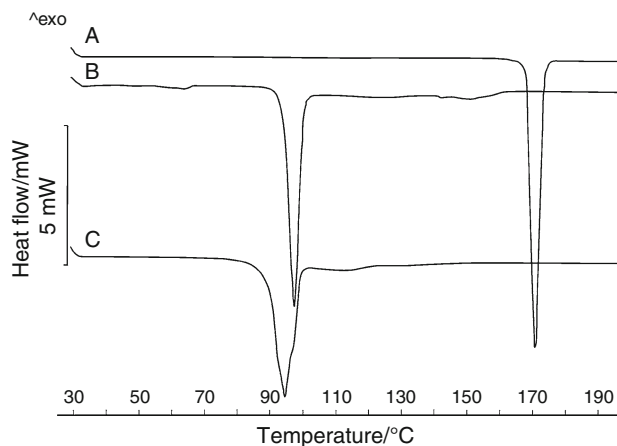

Fig. 8 DSC curves of PCT and xylitol–mannitol–PEG–PCT physical mixture and pastille: *a* PCT, *b* the physical mixture of components, *c* pastille
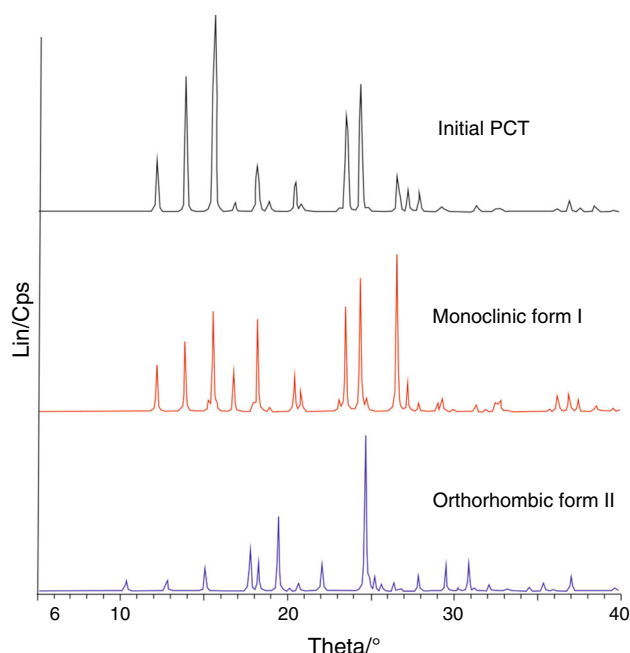
Fig. 9 Diffractograms of the polymorphic forms of PCT and the starting PCT
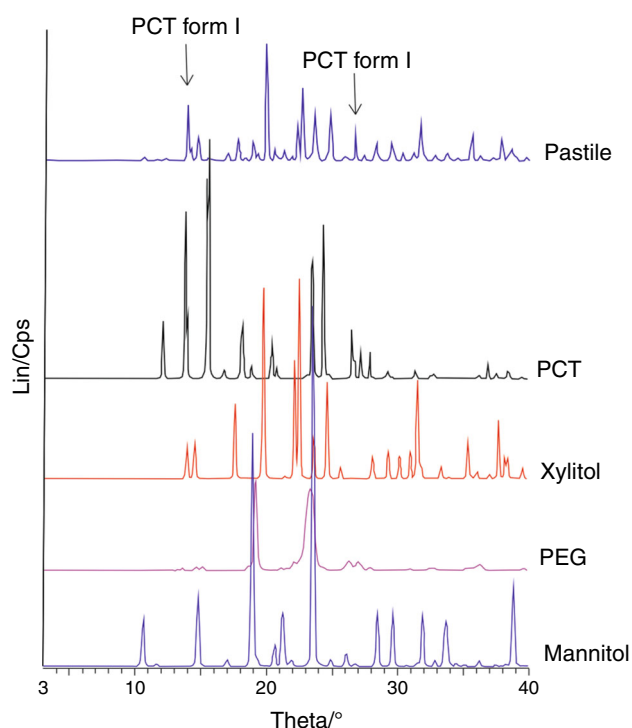

Fig. 10 Diffractograms of the pastille and the components

there was no change in the crystal modification of the material in the sample tray during the measurement, the main characteristic Raman bands of PCT in the intervals of 1660–1540, 1400–1160, 870–770 and 660–560 cm^{-1}. The

identity of spectra b and c confirmed the uniform distribution of PCT throughout the pastilles.

To identify the polymorphic forms of the PCT after the recrystallization, DRS spectra were acquired with a DXR instrument. The DXR Raman spectra of all the PCT forms produced in various modes of the heating–cooling process were identical and were those of the metastable orthorhombic polymorph of PCT form II (not shown). The Raman spectrum of PCT displays strong bands at 1648, 1610, 1561, 1323, 1236, 857, 796, 650 and 390 cm^{-1}, assigned to –NH·CO·CH$_3$ stretching, C–C Ar stretching, C–N stretching/in-plane N–H bending, C–N stretching, phenyl-N and Ar C–C stretching, out-of-plane C–C skeletal deformation, C–N–C stretching and Ar=C–H out-of-plane deformation, respectively (Fig. 11a). Table 3 lists the principal Raman bands of PCT, and selected Raman bands of mannitol, PEG and xylitol are presented in Fig. 12. Though most of the main and characteristic Raman bands of the ingredients and PCT overlap, differentiation of the PCT is of primary importance. The highlighted Raman bands at 1660–1540, 1168, 710 and 390 cm^{-1} were used to identify the PCT in the pastilles.

Figure 13 presents DXR spectra of the starting PCT, form II, and the PCT in the pastille shell and the core. The most marked differences between the two polymorphic PCT forms are to be seen in the highlighted regions, i.e. the intense Raman double peak at 1617–1610 cm^{-1} was split into two peaks at 1623 and 1608 cm^{-1} and one new peak appeared at 1575 cm^{-1}, in parallel with a decrease in intensity of the peak at 1560 cm^{-1}. The PCT form II spectrum exhibits the characteristic peaks of the starting PCT, but shifted to higher wavenumber as: 1561 → 1575, 1371 → 1374, 1323 → 1326, 857 → 860, 833 → 837, 503 → 508 and 328 → 330 cm^{-1}. This indicates that the corresponding chemical bonds are in a higher energy state. Table 3 lists the principal Raman bands of PCT form II, the metastable physical state, having a higher energy state than that of the starting PCT which is consistent with the reported data. The exceptions (1256 → 1244, 1236 → 1219 and 464 → 453 cm^{-1}) are attributed to the symmetrical CH$_3$ deformation, the phenyl-N and aromatic C–C stretching and the skeletal bending of PCT. The presence of PCT in the pastilles was not associated with the formation of the metastable PCT, form II. These data confirm the PCT is in the thermodynamically stable monoclinic form. It should be mentioned that the core of the pastille (d) contains more xylitol than the outer shell (c), e.g. the characteristic weak or moderate Raman bands of xylitol are not present at 1461, 1092, 1071, 1059 and 426 cm^{-1} in the spectrum of the pastille shell. The higher xylitol concentration in the pastille core was confirmed by the presence of the characteristic Raman peaks of xylitol at 1461, 1003, 426 and 355 cm^{-1} (Fig. 13d), which were absent from the Raman spectrum of the pastille shell (Fig. 13c).

Fig. 11 Transmission Raman spectra of the starting PCT (*a*), the shell of the PCT-containing pastille (*b*) and the core of the PCT-containing pastille (*c*)
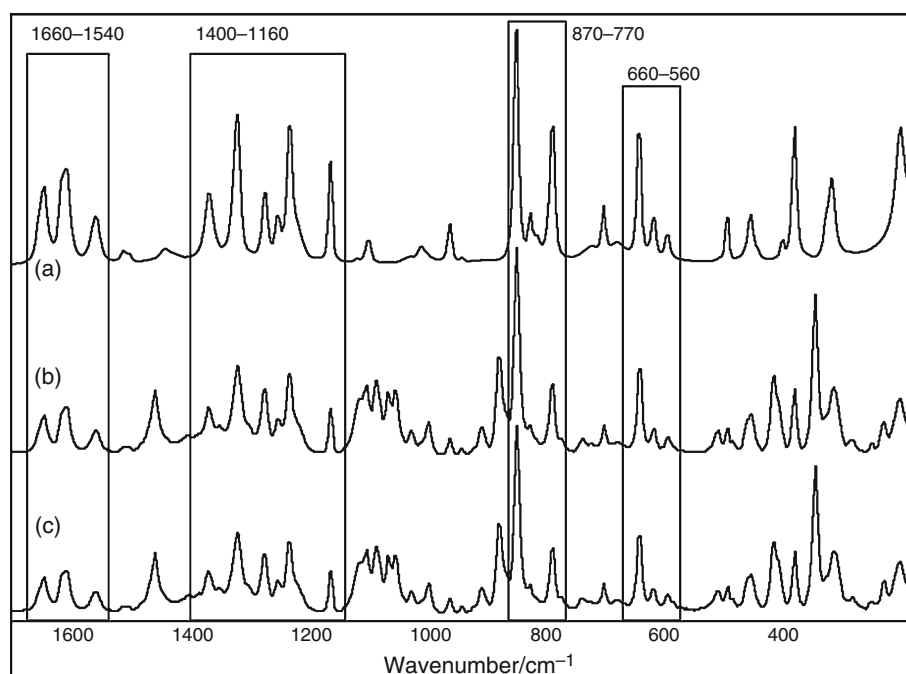

Table 3 Observed Raman peaks and their assignments for the starting PCT, form II of PCT and the PCT-containing pastille/shell and core

PCT	PCT form II	Pastille shell	Pastille base	Assignment
464w	453w	465w	464w	Skeletal bending
503m	508w	505w	505w	Ar ring deformation
650s	650s	652m	652m	Ar=C–H out-of-plane deformation
710m	709w	711w	711w	Out-of-plane CN–H and phenyl deformation
796s	798m	798m	798m	Phenyl-N bending and out-of-plane *p*-substituted Ar ring deformation
857vs	860s	858s	857s	Out-of-plane C–C skeletal deformation
968w	966w	969w	970w	C–C stretching
1104w	1106w	1105w	1109w	CH_3 rocking
1236s	1219m	1237s	1238m	Phenyl-N and Ar C–C stretching
1256w	1244w	1257w	1257w	Symmetrical CH_3 deformation
1323s	1326vs	1324s	1324s	C–N stretching
1515w	1510w	1515w	1517w	Secondary amine deformation
1561m	1560w-sh	1561m	1562w	C–N stretching and in-plane N–H bending
–	1575m	–	–	Amide N–H deformation
1610s	1608s	1610s	1611s	C–C Ar stretching
1617vw-sh	1623s	1619sh	1619sh	Asymmetrical C=C Ar stretching, C–N stretching
1648s	1648m	1648s	1648m	–NH·CO·CH_3 stretching

Technological parameters of pastille

Geometrical parameters and hardness

The diameter and the height of 20 pastilles were measured with a screw micrometer and their mass with analytical scales. The average diameter of the pastilles was 10.60 ± 0.31 mm, the height was 3.11 ± 0.23 mm, and the mass was 256.68 ± 1.99 mg. Figure 14 illustrates the top view (A) and the largest vertical cross section (B) of the drop-melted pastille.

The breaking hardness of 5 pastilles was measured. The average hardness of the pastilles was 125 ± 5 N, which is corresponded to the requirements of dosage form.

Fig. 12 DXR spectra of the starting PCT (*a*) and the components mannitol (*b*), PEG (*c*) and xylitol (*d*)
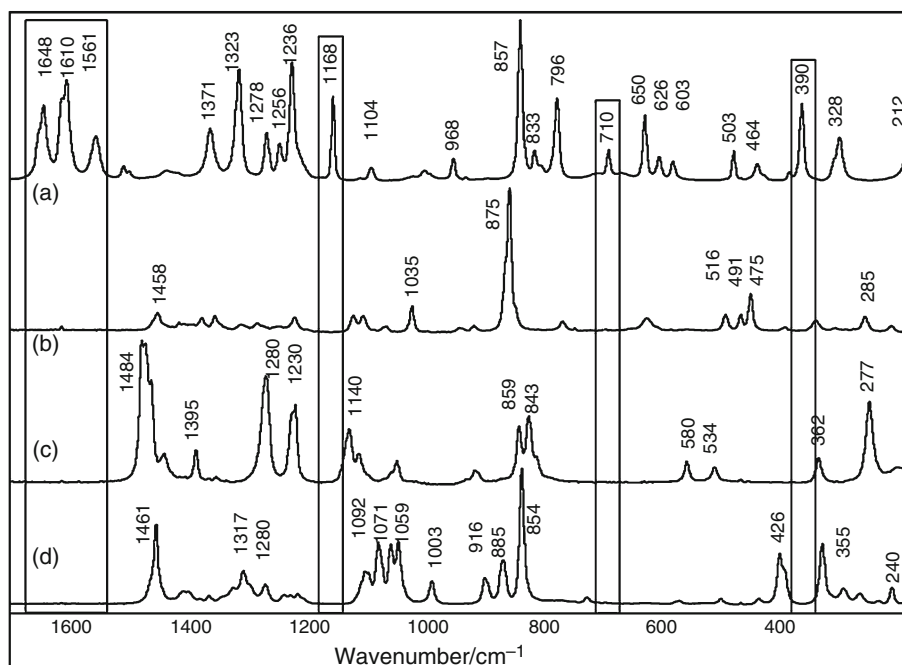
Fig. 13 DXR spectra of the starting PCT (*a*), form II of PCT (*b*), the shell of the PCT-containing pastille (*c*) and core of the PCT-containing pastille (*d*)
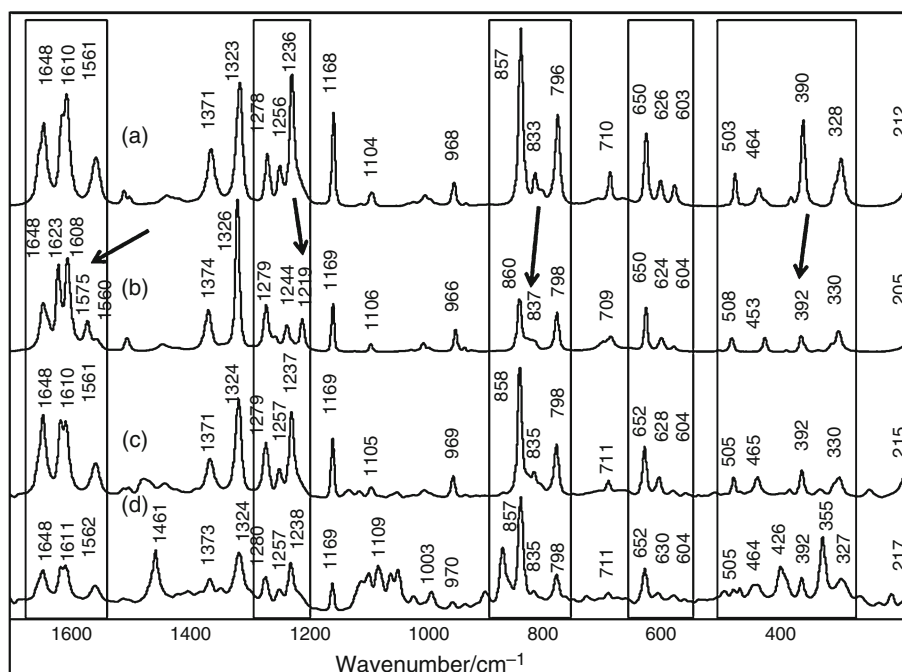
Drug content determination

Before the in vitro dissolution studies, the drug content of the pastilles was determined. Three different batches were investigated. The calculated and spectrophotometrically measured PCT contents of the pastilles were 40.19 mg and 40.12 ± 0.31 mg, respectively.

In vitro dissolution studies

In three parallel measurements, the dissolution of the pastilles was compared to that of the pure PCT crystals. In both case, the PCT was practically fully dissolved in the medium after 15 min (Fig. 15). Because of the relatively low porosity and surface area of the drop-melted pastille,

Fig. 14 The *top view* (**a**) and the *largest vertical cross section* (**b**) of the drop-melted pastille

Fig. 15 Dissolution profiles of pure PCT and drop-melted pastille

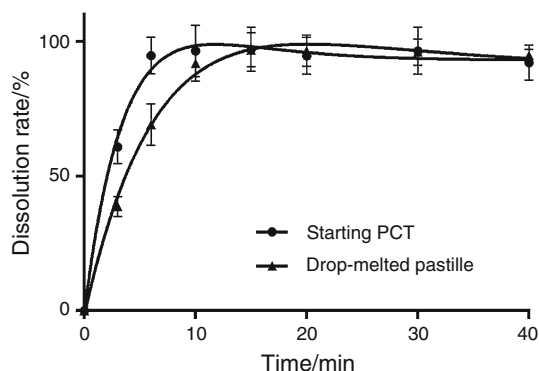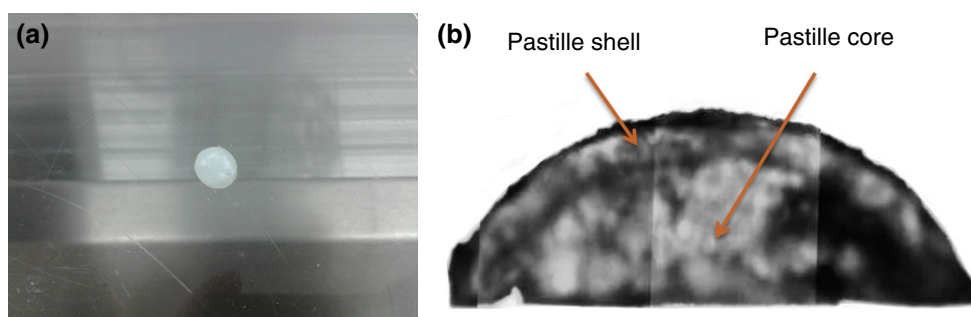they dissolved more slowly than the starting PCT crystals in the media (and would behave similarly in the mouth).

Discussion

In this study, the xylitol–mannitol–PEG eutectic mixture was successfully applied to produce a PCT-containing pastille. New finding in this work is the development of a crystalline carrier/basis for pastilles which consist of two well-recrystallized sugar alcohols as poor glass formers and the PEG as poor crystallization inhibitor. This carrier system is suitable to use a melt technology to formulate of a pastilles containing crystalline PCT. These are important viewpoints to the stability of the final product. The melt technology is an innovative technology because there is no need for the use of extra organic solvents, it is a dust-free process, and the formation of the product is in one process step.

Determining the phase diagrams, we obtained the eutectic mixture of xylitol and mannitol confirmed by DSC (90 mass% xylitol and 10 mass% mannitol with the melting temperature of 95.5 °C), which coincides with data of Detherm database [21]. Investigating the pastille shell and core structure, we found a phase separation with the eutectic composition of xylitol and mannitol located in the core (Fig. 3). The phase separation in the pastille form was

first described by Ulrich et al. [6]. As a component of the carrier, PEG served as a softener agent and did not inhibit the recrystallization of the components (xylitol, mannitol and PCT), but the solidification would be slower which promoted the pastille forming.

The pastillization was optimized both statistically with a Box–Behnken design and experimentally via the phase diagrams. The factorial design led to a carrier containing a eutectic mixture of xylitol (61.25 %) and mannitol (15.31 %) with 7.81 % of PEG. The components of the pastilles containing 15.63 % PCT recrystallized completely after 5 days. The relatively appropriate distribution of PCT was confirmed by TRS, which revealed the homogeneous distribution of the PCT both in the shell and in the core of the pastille. The DSC curves indicated that the PCT dissolved in the melted mixture of sugar alcohols and PEG, and the polymorphism of PCT during the recrystallization was therefore investigated by DSC, which demonstrated the occurrence of recrystallization, but did not allow identification of the polymorphs. XRPD of the pastilles revealed only the monoclinic form I of PCT in the product. However, DRS showed that the monoclinic and orthorhombic forms of PCT can be distinguished from each other and the other components. Mainly, the thermodynamically stable form of PCT was observed in the pastilles, but its distribution depended strongly on the structure formed during the pastille formation and on process parameters such as the cooling rate and time. In this respect, the XRPD and Raman investigations supplement thermal analysis in the determination of the polymorphs present. The pastilles hardness proved to be relatively hard (125 ± 5 N). Their PCT content, 40.12 ± 0.31 mg, satisfied the requirements of the European Pharmacopoeia (Ph. Eur. 8.), and in vitro dissolution studies showed that 100 % of the PCT dissolved in from the drop-melted pastille <15 min. It may be concluded that the pastillization via melt technology is suitable for the development of PCT-containing pastilles as a solid dosage form.

This work allows the application of developed carrier system and the melt technology to have a PCT-containing pastille as new lozenge dosage form for children therapy.

References

1. Damian F, Blaton N, Kinget R, van den Mooter G. Physical stability of solid dispersions of the antiviral agent UC-781 with PEG 6000, Gelucire® 44/14 and PVP K30. Int J Pharm. 2002;244:87–98.
2. Broman E, Khoo C, Taylor RL. A comparison of alternative polymer excipient and processing methods for making solid dispersions of poorly water soluble drug. Int J Pharm. 2001;222:139–51.
3. Six K, Verreck G, Peeters J, Augustijns P, Kinget R, Van den Mooter G. Characterization of glassy itraconazole: a comparative study of its molecular mobility below Tg with that of structural analogues using MTDSC. Int J Pharm. 2001;213:163–73.
4. Redenti E, Peveri T, Zanol M, Ventura P, Gnappi G, Montenero A. A study on the differentiation between amorphous piroxicam: beta-cyclodextrin complex and a mixture of the two amorphous components. Int J Pharm. 1996;129:289–94.
5. Bashiri-Shahroodi A. Dropping method as a new possibility in preparation of solid dispersions. Doctoral dissertation Szeged; 2007.
6. Wendt K, Petersen S, Ulrich J. Application of in situ coating on a two-compound system. Chem Eng Technol. 2014;37:1408–12.
7. Ulrich J, Abouzeid A, Hartwig A, Petersen S, Wendt K. Geht es nicht einfacher? In situ coating—Beschichtung direkt aus der Schmelze CIT plus 2015;3:44–45.
8. Abouzeid A, Petersen S, Ulrich J. Utilizing melt crystallization fundamentals in the development of a new tableting technology. Front Chem Sci Eng. 2014;8:346–52.
9. Sholaei AH. Buccal mucosa as a route for systemic drug delivery. J Pharm Pharmaceut Sci. 1998;1:15–30.
10. Fousteris E, Tarantili PA, Karavas E, Bikiaris D. Poly(vinyl pyrrolidone)-poloxamer-188 solid dispersions prepared by hot melt extrusion. J Therm Anal Cal. 2013;113:1037–47.
11. Newa M, Bhandari KH, Kim JA, Yoo BK, Choi HG, Yong CS, Woo JS, Lyoo WS. Preparation and evaluation of fast dissolving ibuprofen-polyethylene glycol 6000 solid dispersions. Drug Deliv. 2008;15:355–64.
12. Newa M, Bhandari KH, Li DX, Kim JO, Yoo DS, Kim JA, Yoo BK, Woo JS, Choi HG, Yong CS. Preparation and evaluation of immediate release ibuprofen solid dispersions using polyethylene-glycol 4000. Biol Pharm Bull. 2008;5:939–45.
13. Leonardi D, Barrera MG, Lamas MC, Salomón CJ. Development of prednisone: polyethylene glycol 6000 fast-release tablets from solid dispersions: solid-state characterization, dissolution behavior, and formulation parameters. AAPS PharmSciTech. 2007;8:221–8.
14. Garr JSM, Rubinstein MH. Direct compression characteristics of xylitol. Int J Pharm. 1990;64:223–6.
15. Mártha C, Jójárt-Laczkovich O, Szabó-Révész P, Ulrich J. Investigation of the crystallinity of sugar alcohols co-ground with polymeric excipients. J Therm Anal Cal. 2014;115:2479–86.
16. Hamishehkar H, Emami J, Najafabadi AR, Gilani K, Minaiyan M, Mahdavi H, Nokhodchi A. Effect of carrier morphology and surface characteristics on the development of respirable PLGA microcapsules for sustained-release pulmonary delivery of insulin. Int J Pharm. 2010;389:74–85.
17. Sugar alcohol eutectic and process for producing the same EP 1842436 A1. Accessed 24 Nov 2015.
18. Gombás Á, Szabó-Révész P, Regdon G Jr, Erős I. Study of thermal behavior of sugar alcohols. J Therm Anal Cal. 2003;73:615–21.
19. Diarce G, Gandarias I, Campos-Celador Á, García-Romero A, Griesser UJ. Eutectic mixtures of sugar alcohols for thermal energy storage in the 50–90 °C temperature range. Sol Energy Mater Sol C. 2015;134:215–26.
20. Chiou WL, Riegelman S. Pharmaceutical applications of solid dispersion systems. J Pharm Sci. 1971;60:1281–302.
21. http://i-systems.dechema.de/detherm/dbOverview.php?ID=170431. Accessed 19 Nov 2015.
22. Rycerz L. Practical remarks concerning phase diagrams determination on the basis of differential scanning calorimetry measurements. J Therm Anal Cal. 2013;113:231–8.
23. Behera S, Ghanty S, Ahmad F, Santra S, Banarjee S. UV-visible spectrophotometric method development and validation of assay of paracetamol tablet formulation. J Anal Bioanal Tech. 2012;6:1000151.
24. Talja RA, Roos YH. Phase and state transition effect on dielectric, mechanical and thermal properties of polyols. Thermochim Acta. 2001;380:109–21.
25. Akiladevi D, Shanmugapandiyan P, Jebashingh D, Basak S. Preparation and evaluation of paracetamol by solid dispersion technique. Int J Pharm Sci. 2011;1:188–91.
26. Perlovich GL, Volkova TV, Bauer-Brandl A. Relative stability of the monoclinic and orthorhombic phase revisited by sublimation and solution calorimetry. J Therm Anal Cal. 2007;89:767–74.

III.

Formulation of paracetamol-containing pastilles with in situ coating technology

CrossMark

Gábor Katona [a,b], Balázs Szalontai [c], Mária Budai-Szűcs [a], Erzsébet Csányi [a], Piroska Szabó-Révész [a,*], Orsolya Jójárt-Laczkovich [a]

[a] Department of Pharmaceutical Technology, University of Szeged, Eötvös u. 6, H-6720 Szeged, Hungary
[b] Richter Gedeon Plc., Budapest, Gyömrői út 19-21, H-1103 Budapest, Hungary
[c] Institute of Biophysics, Biological Research Centre of the Hungarian Academy of Sciences, Temesvári krt. 62, H-6701 Szeged, Hungary

ARTICLE INFO

ABSTRACT

The focus of this research was to apply the in situ coating technology for producing paracetamol- (PCT-) containing pastilles for paediatric use from a eutectic of two sugar alcohols (sorbitol, xylitol) in one step. This type of melt-technology is more cost-efficient and simpler than other conventional tableting technologies, whereby the formation of the pastilles and their coating occur upon the same fabrication step. We managed to produce pastilles having a softer core and a harder, resistant shell in one cooling step. Adding polyethylene glycol (PEG) 2000 or 6000 to the PCT-containing eutectic, the dissolution rate of PCT could be considerably increased, especially when using PEG 2000, reaching equal dissolution characteristics both under mouth- and gastric-specific conditions. Distributions of the components within the pastilles have been determined by X-ray scattering and Raman spectroscopy. Physico-chemical parameters of the xylitol-sorbitol eutectic and their changes upon adding PCT and PEGs have been determined, and it has been revealed that xylitol and sorbitol form a new entity with a distinguished crystal structure. The significant changes in viscosity were explained and the interaction in the eutectic mixture was investigated using Fourier transform infrared spectroscopy (FT-IR). The uniformity of the physical parameters of the pastilles (including size, weight and drug content) also demonstrates the feasibility of using the cost-efficient and simple one-step eutectic-cooling technology for manufacturing pastilles.

© 2016 Elsevier B.V. All rights reserved.

1. Introduction

In situ coating is a novel approach in melt technology developed by Ulrich et al. (Wendt et al., 2014; Ulrich et al., 2015; Abouzeid et al., 2014), in which the formation of the pastille and its coating occur in the same step. Upon using a eutectic mixture of two compounds (e.g. sugars or sugar alcohols), phase separation can take place and either of the components may form a coating. As phase separation is a thermal process, recrystallization of the amorphized components can be investigated (Patterson et al., 2005; Mah et al., 2015; Löbmann et al., 2013). Drop-melting method is a suitable technique for pastille formation, where solidification takes place at the surface of the pastilles, corresponding to the recrystallization of the components. Viscosity is a critical parameter of this technology: it influences drop size, whereas a relatively high viscosity decreases molecular mobility, thereby hindering the recrystallization process and surface solidification (i.e. formation of the "coating" or "shell"). In case of high viscosity, seed crystals or ultrasonic agitation can be used to initiate nucleation (Wendt et al., 2014).

Sugar alcohols such as xylitol, mannitol and sorbitol are often used as sweeteners in orally disintegrating drug formulations (Ciper and Bodmeier, 2005; Slavkova and Breitkreutz, 2015) or in chewing gums because of their low glycaemic index and anticariogenicity (Burt, 2006; Aslani and Jalilian, 2013; Kartal et al., 2007). They can also be used as plasticizers in films (Talja et al., 2007; Zhang and Han, 2006; Krogars et al., 2002; Sharma et al., 2016) and may substitute for glycerol in preparing soft gelatine capsules (Moreton and Armstrong, 1998). Sugars and sugar alcohols form eutectic mixtures with each other in certain ratios, resulting in a system with a lower melting temperature than that of either of the components (*Sugar alcohol eutectic and process for producing the same EP 1842436 A*1, 2015). Literature examples of eutectic-forming mixtures include xylitol–isomalt (Wendt et al., 2014) and xylitol–sorbitol (Diarce et al., 2015).

In the USA, a buccal pharmaceutical preparation, Meltaways® (Tylenol) containing 80 mg of paracetamol (PCT) is available as a chewable tablet in paediatric therapy with the aim of easy administration and fast release. Although it is most often used for a localized painkiller effect in the mouth, it can also be used for systemic therapy provided that the drug is in contact with the oral cavity for an extended period or is swallowed. By means of buccal absorption, several disadvantages

* Corresponding author.
  E-mail address: revesz@pharm.u-szeged.hu (P. Szabó-Révész).

of oral administration can be avoided, including the hepatic first-pass metabolism or enzymatic degradation within the gastrointestinal tract, which prevent the oral administration of certain classes of drugs, particularly of proteins and peptides (Sholaei, 1998). Additionally, by buccal administration a lower amount of drug is needed to achieve the desired therapeutic effect.

In our previous studies we applied melt technology for the formulation of pastilles containing PCT (15.63%) as a model active agent, plus xylitol (61.25%), mannitol (15.31%) and polyethylene glycol 6000 (PEG 6000) (7.81%) as carriers (Katona et al., 2016). It was found that the components of the pastilles underwent recrystallization at different rates within the first 5 days after production, and phase separation, resulting in the appearance of a "shell" on the surface of the pastilles was detected. As an extension of our previous research, the goal of our current study was to investigate the recrystallization of the components within the pastille, focusing on the upcoming polymorphs and the distribution of PCT within the product.

The focus of our current research was to apply an in situ coating technology to produce PCT-containing pastilles, using PEG 2000, PEG 6000 and two sugar alcohols (sorbitol and xylitol) of similar melting temperatures, as well-known taste-masking agents for paediatric therapy. Cooling of a eutectic mixture can produce either an "overcooled" liquid core or a recrystallized outer shell. We aimed to discover how sorbitol as a "good glass former" material influences the glass transition value (T_g) of the eutectic. All physical parameters of possible relevance in terms of medical application of such pastilles were characterized. Further aims of our study were to investigate the wetting effect of PEG 2000 and 6000 affecting the extent of dissolution of PCT compared to the simple eutectic, as well as their softening and viscosity-enhancing effects affecting the formation of the pastille shape. Solidification was studied both by X-ray powder diffraction (XRPD) and by dispersive Raman spectroscopy (DRS), whereas the molecular interactions between the components within the pastilles were investigated by Furier transform infrared spectroscopy (FT-IR).

2. Materials and methods

2.1. Materials

D-Xylitol ((2R,3R,4S)-pentane-1,2,3,4,5-pentol), polyethylene glycol 2000 (PEG 2000) and polyethylene glycol 6000 (PEG 6000) were purchased from Sigma-Aldrich Chemie GmbH (Mannheim, Germany). D-Sorbitol ((2S,3R,4R,5R)-hexane-1,2,3,4,5,6-hexol) was purchased from Molar Chemicals Ltd. (Halásztelek, Hungary). The monoclinic form of PCT (N-(4-hydroxyphenyl)acetamide) was chosen as a model active agent for the experimental work; and it was obtained from Sanofi Aventis (Frankfurt am Main, Germany).

2.2. Investigations of the xylitol–sorbitol eutectic composition

2.2.1. Differential scanning calorimetry (DSC)

DSC measurements were carried out to characterize the eutectic mixture of xylitol and sorbitol, and to investigate the role of PEG. DSC data were recorded with a Mettler-Toledo 821^e DSC instrument (Mettler-Toledo GmbH, Greifensee, Switzerland). 100 mg of xylitol–sorbitol solid dispersions with xylitol contents of 10, 30, 40, 50, 60, 70, and 90 wt.% were prepared in a trituration mortar. Samples of 5 ± 0.2 mg were crimped in 3-hole aluminium pans and were examined in the temperature interval of 25–110 °C at a heating rate of 2 °C min^{-1} under a constant argon flow of 150 ml min^{-1}. Next the samples were cooled to -40 °C and then reheated to 110 °C at a heating rate of 2 °C min^{-1} under a constant argon flow of 150 ml min^{-1} and a nitrogen flow of 50 ml min^{-1} to study glass transition (T_g). Data were analyzed by a STAR^e software. Each measurement was normalised to sample size.

2.2.2. Viscosity measurements

Rheological measurements were carried out at 110 °C using a Physica MCR101 rheometer (Anton Paar GmbH, Graz, Austria). A parallel-plate measuring device was used with a diameter of 25 mm and 0.20 mm gap height. Shear rate was increased from 0.1 to 100 s^{-1} in a controlled rate mode. Shearing time was 300 s.

2.2.3. Contact angle measurements

The melted compositions were cast on a slide, where they solidified with a flat surface on which contact angle measurements were carried out. The contact angle (θ) was determined by means of the sessile drop technique, using an OCA 20 Optical Contact Angle Measuring System (Dataphysics, Filderstadt, Germany) and the method of Wu. The liquid mediums used for our contact angle measurements included bidistilled water (interfacial tension of polar component (γ^p) = 50.2 mN/m, interfacial tension of disperse component (γ^d) = 22.6 mN/m) and diiodomethane ($\gamma^p = 1.8$ mN/m, $\gamma^d = 49$ mN/m). Polarity percentage was calculated from the interfacial tension of the polar component (γ^p) and the surface free energy (γ) values as follows:

$$\text{Polarity}(\%) = \left(\frac{\gamma^p}{\gamma}\right) * 100 \tag{1}$$

2.3. Pastillization process

Eutectic mixtures of xylitol and sorbitol with PEGs as carrier additives were prepared and melted in a heated pipette at 110 °C. PCT was dispersed in the melted carrier. The melted solid dispersion was dropped onto a 25 °C thermostated cooling plate, where it solidified to form flat-bottomed pastilles (Fig. 1) (Bülau and Ulrich, 1997). Four mixtures were studied, including (1) xylitol/sorbitol 50–50 wt.% (*referred to as eutectic*) without PCT, (2) xylitol-sorbitol with PCT (14.29%) (*referred to as EuPCT*), (3) xylitol–sorbitol–PCT with PEG 2000 (7.81%) (*referred to as EuPCT 2000*) and (4) xylitol-sorbitol-PCT with PEG 6000 (7.81%) (*referred to as EuPCT 6000*).

2.4. Investigation of pastilles of different compositions

2.4.1. X-ray powder diffraction

XRPD analysis was performed using a Bruker D8 Advance diffractometer (Bruker AXS GmbH, Karlsruhe, Germany) with Cu K λI radiation ($\lambda = 1.5406$ Å) and a VÅNTEC-1 detector. Samples were scanned at 40 kV and 40 mA. The angular range was 3° to 40° 2θ, at a step time of 0.1 s and a step size of 0.007°. The sample was placed on a quartz holder, and measured at ambient temperature and ambient relative humidity. All manipulations, including Kα 2-stripping, background removal and smoothing of the area under the peaks of the diffractograms were performed using the DIFFRACTPLUS EVA software.

2.4.2. Raman spectroscopy

To investigate the difference between the shell and the core structures of the pastilles, Raman spectra were acquired by a Thermo Fisher DXR Dispersive Raman instrument (Thermo Fisher Scientific. Inc., Waltham, MA, USA) equipped with a CCD camera and a diode laser operating at a wavelength of 780 nm. Raman measurements were carried out with a laser power of 12 mW at a slit size of 25 μm on a spot size of 2 μm. Spectra of the individual PEGs, sorbitol and xylitol were collected with an exposure time of 6 s, for a total of 48 scans in the spectral range of 1700–200 cm^{-1} with cosmic ray and fluorescence corrections.

2.4.3. Furier transform infrared spectroscopy (FT-IR)

Kalium bromide pastilles were prepared by hydraulic press containing either the eutectic or a physical mixture of the components, and their spectra were compared to each other. FT-IR spectra were recorded by an Avatar 330 FT-IR spectrometer (Thermo Nicolet, USA), equipped
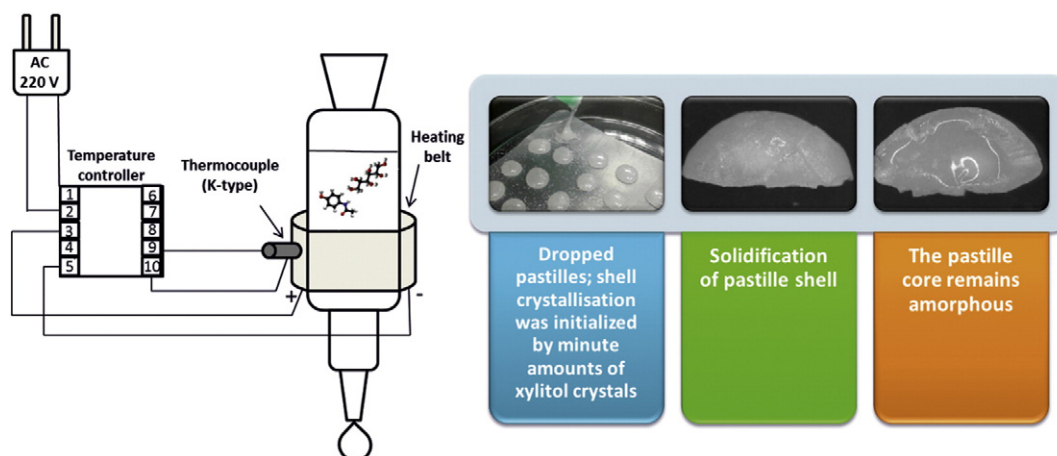
Fig. 1. Pastillation process and solidification of the pastilles.

with a DTGS (deuterated triglycyl sulfate) detector, in the range of 4000–400 cm^{-1}. The spectral resolution was 4 cm^{-1}, and 64 scans were collected to provide a good signal-to-noise ratio. All spectral manipulations were performed using a GRAMS/AI Ver. 7 (Thermo Galactic, USA) software.

2.4.4. Geometrical parameters and hardness

The diameter and the height of 20 pastilles were measured with a screw micrometer (Starrett Co., Athol, MA, USA) and their masses were measured using an analytical scale (Mettler Toledo AX205 Delta Range analytical scale, Mettler Toledo GmbH, Greifensee, Switzerland).

Hardness of the pastilles was analyzed by a Heberlein hardness tester (Heberlein & Co. AG, Switzerland). Five randomly selected pastilles were investigated to calculate the average and the standard deviation.

2.4.5. Drug content analysis

A powdered pastille plus 15 ml of methanol was shaken in a 100 ml volumetric flask until the powder got dissolved. Then 85 ml of water was added to adjust the volume to 100 ml. Next a 1 ml aliquot was transferred to a 100 ml volumetric flask and was mixed with methanol/water 15:85 to 100 ml. The dissolved amount of PCT was analyzed spectrophotometrically at 244 nm (PerkinElmer, Lambda 20 spectrophotometer, Dreieich, Germany) (Behera et al., 2012).

2.4.6. In vitro dissolution studies

The dissolution profile of PCT from pastilles of different compositions was determined according to the USP-2 paddle method (Pharmatest, Heinburg, Germany). The rotating velocity of the paddle within the dissolution vessel was 75 rpm. The dissolution studies were carried out in 100.0 ml of phosphate buffer solution at pH 6.8 ± 0.1 characteristic of the oral cavity and at normal body temperature of 37 ± 0.5 °C, as well as in 900.0 ml of 0.1 N HCl at a gastric pH of 1.2 ± 0.1 at 37 ± 0.5 °C (Mashru et al., 2005; Gahel et al., 2009). At predetermined time intervals, 5 ml samples were taken and filtered immediately (using a Minisart SRP 25, Sartorius, Göttingen, Germany; pore size: 0.2 μm,), and the amount of dissolved drug was determined spectrophotometrically at 244 nm (PerkinElmer, Lambda 20 spectrophotometer, Dreieich, Germany).

3. Results and discussion

3.1. Studies of the eutectic xylitol–sorbitol composition

3.1.1. DSC studies

100 mg solid xylitol–sorbitol dispersions of different ratios were prepared. DSC curves of pure sorbitol, pure xylitol and of the investigated dispersions are presented in Fig. 2. As it is apparent, sorbitol is

characterized by two endothermic peaks, showing that it consists of two polymorphic forms. The peak at 85.4 °C indicates the melting point of the Δ form, whereas the peak at 98.2 °C indicates the melting point of the γ form. The Δ form of sorbitol was used by constructing the phase diagram. Pure xylitol has a characteristic melting point at 93.4 °C.

The DSC curves of the dispersions indicate that sorbitol and xylitol form a binary eutectic system, as supported by literature data (Diarce et al., 2015). A binary phase diagram was constructed based of the DSC curves to find the eutectic concentration of xylitol and sorbitol (Fig. 3).

The point of intersection of the two curves on the binary phase diagram indicates the eutectic concentration at 50 wt.% sorbitol and 50 wt.% xylitol. The melting point of the eutectic composition proved to be 76.9 °C. The phase diagram suggests that phase separation between sorbitol and xylitol is theoretically possible.

Eutectic melting enthalpy ΔH (J/g) values for the different xylitol–sorbitol dispersions, as determined by the integration of the eutectic peak area, were plotted versus the mass ratio of xylitol in order to construct the Tamman's triangle showing the eutectic ratio of sugar alcohols at the maximal melting enthalpy value (Fig. 4) (Rycerz, 2013).

The enthalpy of the eutectic composition is maximal (ΔH = 101.1 J/g) and converges to zero for compositions corresponding to the pure components. These data confirm that xylitol and sorbitol form a eutectic mixture in a 50–50 wt.% ratio.
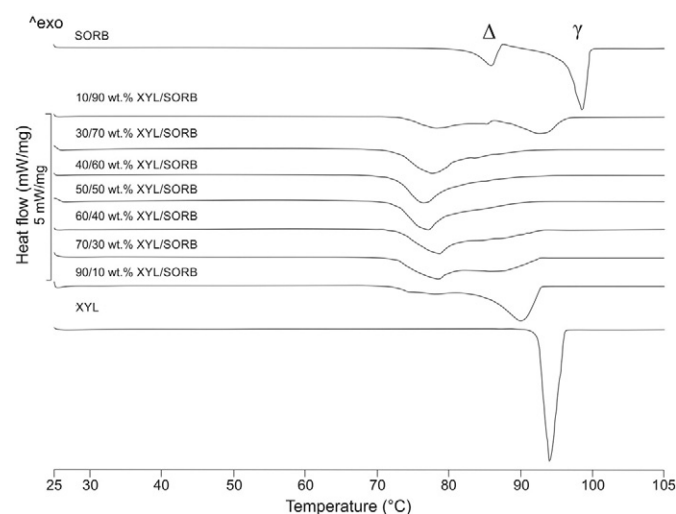

Fig. 2. DSC curves of pure sorbitol (SORB), pure xylitol (XYL) and solid dispersions of various ratios of xylitol–sorbitol (XYL/SORB).
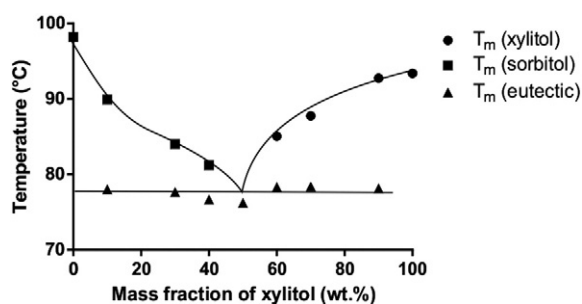
Fig. 3. Binary phase diagram of the xylitol–sorbitol system by plotting the melting points of xylitol–sorbitol compositions versus their different weight ratios.
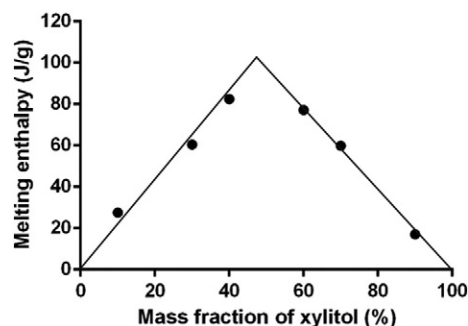

Fig. 4. Construction of the Tamman's triangle by plotting the xylitol–sorbitol eutectic melting enthalpies ΔH at 76.9 °C versus their different weight ratios.

After identifying the eutectic composition, PEG 2000 (7.81%) and 6000 (7.81%) were added to the eutectic dispersions. Melting points (T_m) and T_g of the different eutectic xylitol–sorbitol + PEG compositions were studied by DSC. The first heating curve shows the melting points of each component and every composition, whereas the second heating allows the detection of glass transitions (Table 1.). It has been revealed that during heating both PEGs melt separately from the compositions. We suppose that the lower T_m and T_g values of the eutectic + PEG 6000 mixture results from the interaction of PEG 6000 with one of the eutectic components (Table 1).

3.1.2. Viscosity measurements

Viscosity of the melted dispersions is a critical parameter for drop formation. High viscosity decreases molecular mobility, and therefore hinders recrystallization. For our viscosity measurements, all the dispersions were melted on a heated magnetic stirrer, then the melt was thermostated on the plate of the viscosity measuring device. Measurements were carried out at a constant temperature of 110 °C. All measurements were performed in triplicate and the average values are shown in Table 2.

Viscosity values of all samples were similar. Viscosity of the sample containing PEG 2000 was slightly higher than that of the one containing PEG 6000. This phenomenon was unexpected because the viscosity of pure PEGs is known to increase with their molecular weight. To clarify

Table 1
Melting points (T_m) and glass transitions (T_g) of the xylitol–sorbitol–PEG compositions and the pure components studied.

	First heating			Second heating	
	T_m (°C)	T_{mPEG} (°C)	T_g (°C)	T_m (°C)	T_g (°C)
Sorbitol	98.2	–	–	–	−1.6
Xylitol	93.4	–	–	–	−19.5
Eutectic	76.9	–	–	–	−10.9
Eutectic + PEG 2000	77.6	51.8	–	51.8	−11.0
Eutectic + PEG 6000	72.4	60.0	–	60.1	−14.3

Table 2
Viscosity data of the compositions to be pastilled (n = 3).

Composition	Viscosity (mPas)
Eutectic	368 ± 3
Eutectic + PEG 2000 (7.81%)	370 ± 20
Eutectic + PEG 6000 (7.81%)	359 ± 13

this behaviour of the samples, viscosity measurements were expanded using other compositions containing PEGs in different ratios (5%, 10%, 15%, 20%, 60%, 100%). Fig. 5 shows the viscosity of the different compositions.

Fig. 5 shows that the viscosity of the eutectic without PEG 6000 and that of pure PEG 6000 is almost the same, suggesting that no significant viscosity changes for the eutectic plus PEG 6000 composition can been expected. However, our results showed that the viscosity curve has a minimum at 10% PEG 6000 concentration. On the contrary, PEG 2000 is characterized by a significantly lower viscosity than the eutectic without PEG 2000, thus increasing the concentration of PEG 2000 in the composition is associated with a drastic decrease of the viscosity of the sample (Fig. 5). This viscosity-changing effect of PEGs strongly depends on their molecular weight. Therefore, using a low (<20%) PEG concentration, samples containing either PEG 2000 or 6000 are characterized by similar viscosity values.

3.1.3. Contact angle measurements

Wettability of the pastilles has a significant influence on the dissolution rate and the drug release characteristics of oral drug delivery. Wettability is characterized by the contact angle of the liquid (water). A smaller contact angle indicates a better wettability of the pastille. To formulate a pastille with appropriate dissolving characteristics, a well-wetting surface is fundamental. The polarity percentage can be calculated from the interfacial tension of the polar component (γ^p) and the surface free energy (γ) as follows: $(\gamma^p/\gamma) * 100$ (Table 3).

The results show that PEGs increase the surface free energies and polarities of the compositions containing no PCT. Data for the PCT-containing samples show that PCT has no effect on the γ value, indicating that PCT dissolves in the melt of the eutectic and recrystallizes during the solidification. For those compositions containing both PCT and PEG, the PEG component (especially PEG 2000) decreases γ and increases polarity, which promotes the wetting of the pastille, and thus its dissolution.
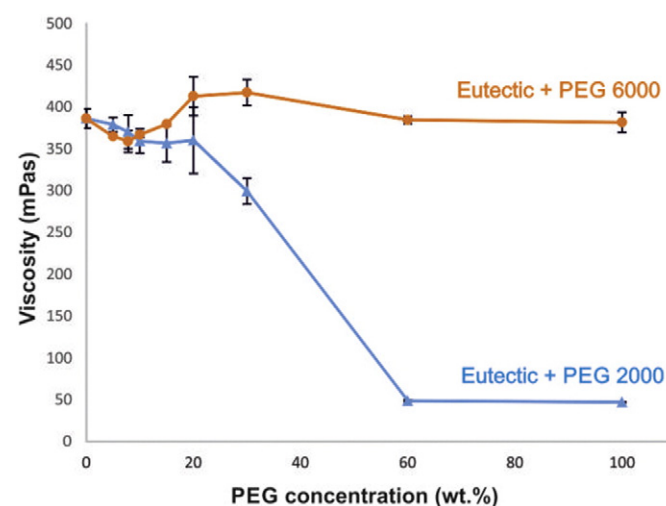

Fig. 5. Viscosity of eutectic xylitol–sorbitol + PEG compositions containing different concentrations of PEGs.

Table 3
Contact angles, surface free energies and polarities of the different eutectic compositions studied.

Composition	θ_{water} (°)	$\theta_{diiodomethane}$ (°)	γ^d (mN/m)	γ^p (mN/m)	γ (mN/m)	Polarity (%)
Eutectic	28.1 ± 3.6	20.5 ± 2.9	42.96	31.74	74.70	42.49
Eutectic + PEG 2000	17.0 ± 1.47	29.7 ± 1.62	39.98	36.60	76.58	47.79
Eutectic + PEG 6000	21.6 ± 3.63	19.5 ± 2.72	43.22	34.03	77.25	44.05
EuPCT	26.7 ± 4.71	22.7 ± 1.84	42.33	32.49	74.82	43.24
EuPCT 2000	34.0 ± 1.82	47.9 ± 2.91	32.41	33.17	65.58	50.58
EuPCT 6000	30.1 ± 3.40	35.9 ± 1.45	37.62	32.77	70.39	46.55

3.2. Pastillization process

Pastillization took place on the surface of a thermostated cooling plate at 25 °C for 24 h. During this process the relatively high viscosity of the melt decreased molecular mobility and crystallization was hindered in the core. PEG 2000 and 6000, applied as softeners to form appropriate pastilles, did not prevent the recrystallization of the components. Crystallization was initiated by pure xylitol crystals as seeds (Talja and Roos, 2001).

3.3. Studies of the pastilles of different compositions

3.3.1. X-ray powder diffraction

XRPD measurements were carried out to analyze the shell and the core structures of the pastilles. The diffractograms of the pure components (Fig. 6A) were compared to that of the pastilles of different compositions (Fig. 6B).

The EuPCT shell contains PCT and xylitol, thus the characteristic peaks of sorbitol at 10.055° and 10.595° 2θ could not be detected. The diffractogram of the EuPCT core shows amorphous signs, but also contains PCT crystals. These results suggest a homogenous distribution of PCT within the pastille. The EuPCT 2000 shell and EuPCT 6000 shell contain not only PCT and xylitol, but also the characteristic peaks of sorbitol are detected. The EuPCT 2000 core contains PCT crystals, plus some amorphous signs are detected. The diffractogram of the EuPCT 6000 core shows that the core structure is partly amorphous and contains sorbitol and PCT crystals. Since some characteristic peaks of the components overlap, we needed to use Raman spectroscopy to locate the components.

3.3.2. Analysis of Raman spectra of the pastilles

Fingerprint regions (900–1700 cm⁻¹) of Raman spectra of the pastille components and spectra collected at different locations/compositions of the pastilles were used for the analysis. To make these comparable, all spectra were normalised to unit integral (i.e. each data point of the spectrum was divided by the average intensity of the spectrum and then multiplied with the number of the data points in the spectrum). This approach assumes that the probabilities of the Raman scattering, and the scattering/collecting conditions of the Raman spectrum are the same for each component. Considering that none of the components were absorbing around the Raman excitation wavelength (780 nm), this seems to be a rather fair approximation.

Fig. 7A shows the Raman spectra of the pastille components. Raman spectra of the pastilles recorded at different locations and in the presence/absence of different PEG molecules are shown in Fig. 7B. These spectra were fitted with the linear combination of the component spectra, and the residuals remaining after fitting are shown in Fig. 7C. Note that in agreement with the composition of the pastilles, either PEG 2000 or PEG 6000 may be used in the fits.

Certain regions of the residual spectra show large deviations from zero both in the positive and the negative directions, indicating that the combination of the components form a new quality within the pastilles. This corresponds to molecular interactions which affect the vibrational coordinates of the components, and might either be chemical interactions, or just strong associations affecting the molecules.

In Fig. 7C two vertical lines indicate the region of largest turbulence in the residual spectra. In this region mainly xylitol, but also sorbitol and PEG have complex bands (see Fig. 7A). We suppose an interaction for
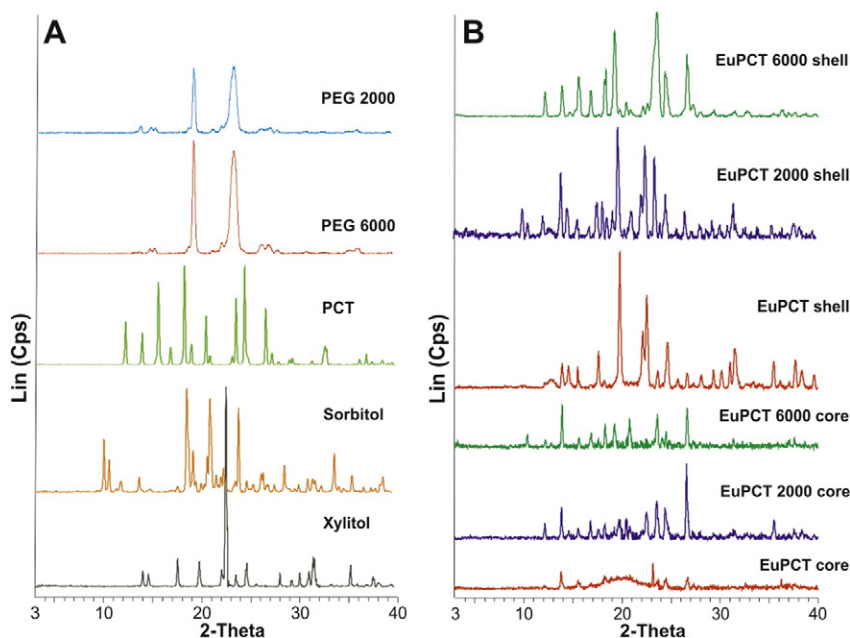

Fig. 6. (A) Diffractograms of the pure components, compared to (B) the shell and the core structures of pastilles containing EuPCT plus different PEGs.

xylitol and sorbitol, as these are very similar molecules. In addition, our former studies (Katona et al., 2016) on similar pastilles containing no sorbitol revealed no such anomaly in the residuals (see the insert in Fig. 7C).

In spite of the local perturbations in the residuals, it is worth doing calculations based on the weights in the fits and on the amounts of the components at the different locations/compositions of the pastilles. These results are shown in Fig. 8.

As shown in Fig. 8 the sums are close to 1 (or exceed 1 if we take the averages of the repeated measurements at the different shell locations), except for the cores, where they are considerably below one. This difference results from the lower weights of sorbitol and xylitol spectra in the core measurements. This can be explained if we suppose that a new entity is formed from these compounds of different Raman spectra, that we could not consider in the fits, and there is obviously more time to form this entity in the core than in the shell which cools faster. Indeed, the Raman spectrum of the xylitol–sorbitol eutectic (not shown) exhibited very different peak ratios in the 800–1200 cm^{-1} region as compared to its constituents. This fact further supports the complex formation of sorbitol and xylitol as suggested by the localized errors in the differences of the measured and the component-reconstituted Raman spectra of the pastilles (see the text above and Fig. 7C).

3.3.3. FT-IR analysis of the eutectic and the physical mixture

FT-IR measurements were carried out to investigate the interaction between xylitol and sorbitol. Both a physical mixture and the eutectic of the sugar alcohols were examined and their spectra were compared to each other (Fig. 9).

Within the range of 900–600 cm^{-1}, the spectrum of the physical mixture contains vibrations of C structure's deformation. These bands decrease remarkably in the spectrum of the eutectic, indicating that the product is in the amorphous state. On the other hand, it also denotes the presence of chemical bondings within the product (Jójárt-Laczkovich and Szabó-Révész, 2011). In case of sugar alcohols, the non-hydrogen bonded OH groups absorb strongly in the 3700–3584 cm^{-1} range, where we could not observe a strong absorption. Intermolecular hydrogen bondings occur as concentration increases, accompanied by an absorption shift to lower frequencies (3550–3200 cm^{-1}, typically at 3300 cm^{-1}), at the expense of the free OH band, which could be observed. These data confirm the presence of H-bondings in the eutectic, which caused the anomaly when fitting the residuals at the Raman evaluation.

3.3.4. Geometrical parameters and hardness

The mass of 20 pastilles of different compositions were measured using an analytical scale and their diameter and height were measured
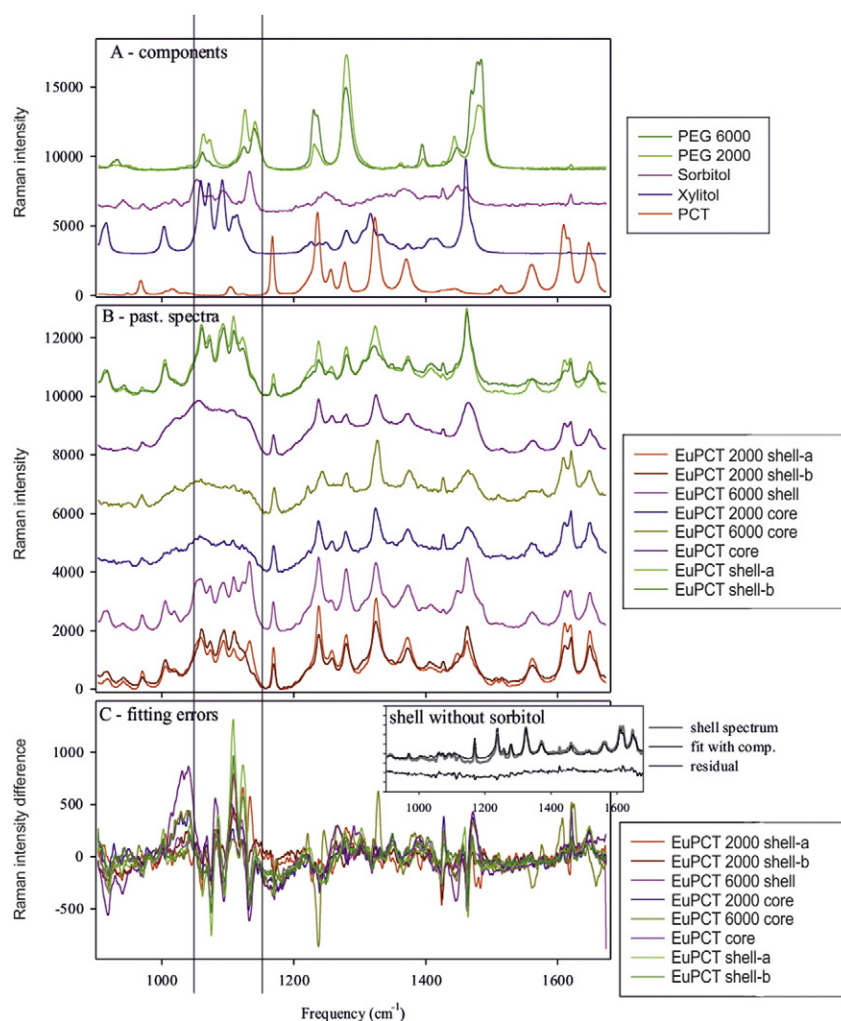

Fig. 7. Raman spectroscopy of paracetamol-containing pastilles. (A) Spectra of the individual components. (B) Raman spectra of the pastilles (**EuPCT** – eutectic mixture + PCT) at different locations (**shell** and **core**) and in the presence of different PEG molecules (**2000** – PEG 2000, **6000** – PEG 6000). The spectra are vertically displaced for a better visibility. Overlaid spectra represent repetitions on the same type of pastille surface at different locations. (C) The errors of the Raman spectra of the pastilles when fitted with the linear combination of the component spectra. Insert seen in part C: Raman spectrum of a similar paracetamol-containing pastille that contains no sorbitol. Note the smooth residual spectrum.
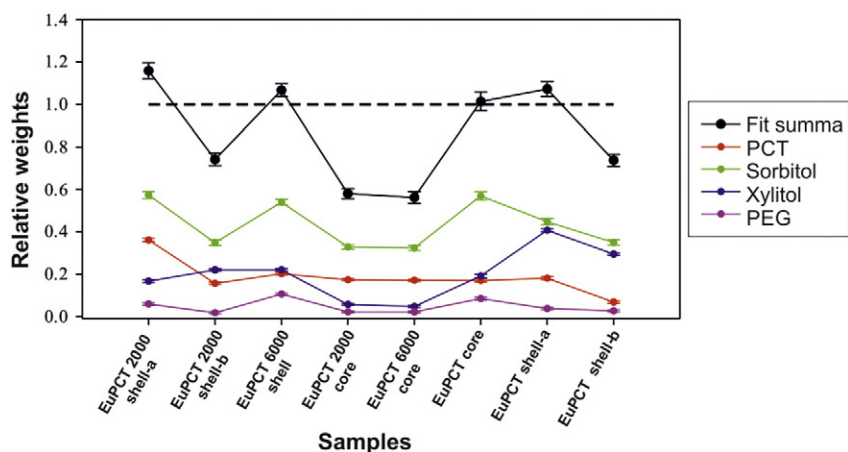
Fig. 8. Weights of the components in the fits of pastille spectra recorded at different locations/compositions calculated from normalised spectra. Note that the sum of the weights for each fit should equal to 1 as shown by the dashed line.
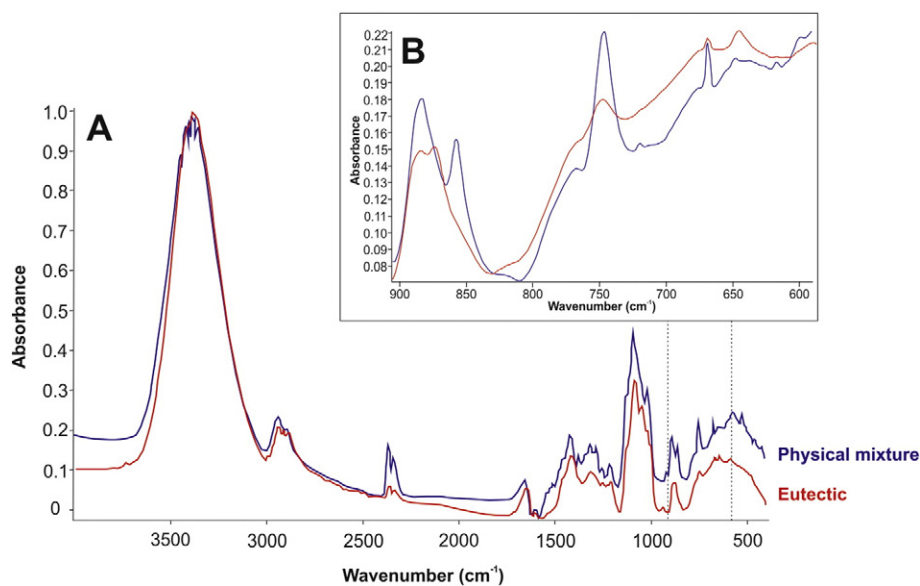

Fig. 9. (A) FT-IR spectra of the physical mixture and the eutectic, and (B) the enlarged spectra within the wavenumber range of 900–600 cm^{-1} after fitting the curves on each other.

using a screw micrometer. In average, mass of the pastilles was 279 ± 2 mg, the diameter was 11.2 ± 0.4 mm and the height was 3.5 ± 0.2 mm. Breaking hardness was measured on 5 pastilles. The average breaking hardness of the pastilles made of the eutectic plus PCT combination was 29 ± 5 N, while that of the pastilles made of the eutectic + PEG 2000 + PCT was 27 ± 6 N and average breaking hardness value for the pastilles made of the eutectic + PEG 6000 + PCT was 27 ± 4 N.

3.3.5. Drug content analysis

The drug contents of the pastilles of different compositions were determined spectrophotometrically. Three different batches of each composition were investigated. Average PCT contents of the pastilles were found to be 39.9 ± 0.3 mg (eutectic), 40 ± 0.2 mg (eutectic + PEG 2000) and 40.1 ± 0.2 mg (eutectic + PEG 6000).

3.3.6. In vitro dissolution studies

After recrystallization of the components within the pastilles (5 days), in vitro dissolution studies were carried out. In three parallel measurements, PCT dissolutions of the pastilles of different compositions were compared at the oral cavity pH (pH 6.8 ± 0.1) and in the gastric juice (pH 1.2 ± 0.1) (Figs. 10 and 11).

In all three cases, PCT was found to be practically fully dissolved in the medium of the oral cavity (pH 6.8 ± 0.1) within 20 min.

In the acidic medium (pH 1.2 ± 0.1) PCT also practically fully dissolved from PEG-containing pastilles within 20 min, while pastilles
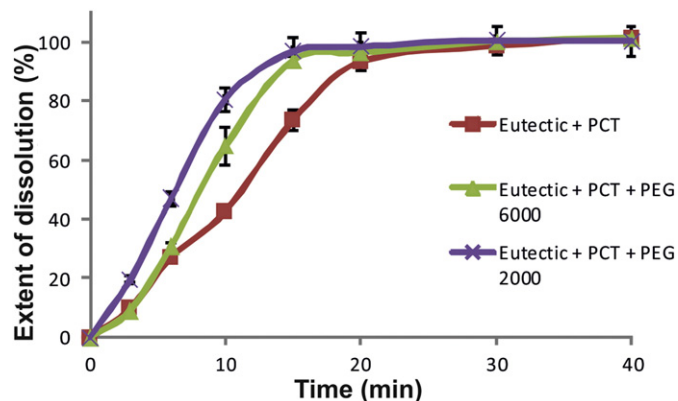

Fig. 10. Extents of dissolution of drop-melted pastilles at the oral cavity pH of 6.8 ± 0.1 and at a temperature of 37 ± 0.5 °C (average value ± SD, n = 3).
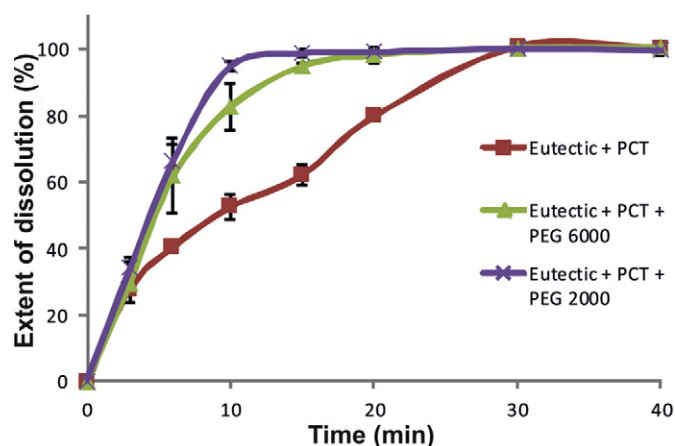
Fig. 11. Extents of dissolution of drop-melted pastilles at the gastric pH of 1.2 ± 0.1 and at a temperature of 37 ± 0.5 °C (average value ± SD, n = 3).

without PEG dissolved after 30 min only. These differences in the extents of dissolution can be explained by the differences in the surface free energies of the pastilles. A lower surface free energy of the PEG-containing pastilles resulted in a higher polarity and a faster dissolution compared to the pastilles without PEG. Thus, it can be concluded that using PEGs improves wettability and therefore the dissolution time of the pastilles. When the pastille is swallowed, full liberation of PCT lasts 5 min longer than in the mouth, which justifies the formulation of a pastille dosage form, compared Fig. 10 to Fig. 11.

4. Conclusions

The focus of our current research was to produce PCT-containing pastilles using an in situ coating technology with additives (PEG 2000 and 6000). The eutectic composition of sorbitol and xylitol was first determined by constructing the binary phase diagram and the Tamman triangle from the DSC data. Both methods confirmed that sorbitol and xylitol form a 50–50 wt.% eutectic mixture. Contact angle measurements showed that wettability can be improved by using PEGs in the formulations, keeping in mind that the viscosity-changing effect of PEGs strongly depends on their molecular weight. Analytical studies of the pastilles of different compositions revealed that solidification occurred in the pastilles and the shell consisted of xylitol, sorbitol and PCT. Raman measurements showed a homogenous distribution of the components within the pastilles. Our X-ray scattering, Raman and FT-IR measurements made it evident that sorbitol and xylitol form a new entity, which is characterized by a distinguished crystal structure and specific intermolecular interactions. Our in vitro dissolution studies showed that the extent of PCT dissolution was faster from the pastilles containing PEGs compared to the pure eutectic (30 min). The pastille containing PEG 2000 showed the fastest dissolution in the mouth, because of its lower surface free energy and higher polarity.

References

Abouzeid, A., Petersen, S., Ulrich, J., 2014. Utilizing melt crystallization fundamentals in the development of a new tableting technology. Front. Chem. Sci. Eng. 8, 346–352.

Aslani, A., Jalilian, F., 2013. Design, formulation and evaluation of caffeine chewing gum. Adv. Biomed. Res. 2, 72.

Behera, S., Ghanty, S., Ahmad, F., Santra, S., Banarjee, S., 2012. UV–visible spectrophotometric method development and validation of assay of paracetamol tablet formulation. J. Anal. Bioanal. Techniques. 6, 1000151.

Bülau, H.C., Ulrich, J., 1997. In: Ulrich, J. (Ed.), Parameters Influencing the Properties of Drop-Formed Pastilles, CGOM. Shaker Verlag, Aachen, pp. 123–130.

Burt, B.A., 2006. The use of sorbitol- and xylitol-sweetened chewing gum in caries control. J. Am. Dent. Assoc. 137, 190–196.

Ciper, M., Bodmeier, R., 2005. Preparation and characterization of novel fast disintegrating capsules (Fastcaps) for administration in the oral cavity. Int. J. Pharm. 303, 62–71.

Diarce, G., Gandarias, I., Campos-Celador, Á., García-Romero, A., Griesser, U.J., 2015. Eutectic mixtures of sugar alcohols for thermal energy storage in the 50–90 °C temperature range. Sol. Energ. Mat. Sol. C. 134 (245–226).

Gahel, M.C., Parikh, P.P., Aghora, P.P., Nagari, S.A., Delvadia, R.R., Dabhi, M., 2009. Application of simple lattice designe and desirability function for the formulation development of mouth dissolving film of salbutamol sulphate. Curr. Drug. Deliv. 6, 486–494.

Jójárt-Laczkovich, O., Szabó-Révész, P., 2011. Formulation of tablets containing an 'in process' amorphized active pharmaceutical ingredient. Drug Dev. Ind. Pharm. 37, 1272–1281.

Kartal, A., Björqvist, M., Lehto, V.P., Marvola, M., Säkkinen, M., 2007. Stability and compatibility study of L-cysteine with commonly used chewing gum excipients. Eur. J. Pharm. Sci. 32, 29.

Katona, G., Sipos, P., Frohberg, P., Ulrich, J., Szabó-Révész, P., Jójárt-Laczkovich, O., 2016. Study of paracetamol-containing pastilles produced by melt technology. J. Therm. Anal. Calorim. 123, 2549–2559.

Krogars, K., Antikainen, O., Heinämäki, J., Laitinen, N., Yliruusi, J., 2002. Tablet film-coating with amylose-rich maze starch. Eur. J. Pharm. Sci. 17, 23–30.

Löbmann, K., Laitinen, R., Grohganz, H., Strachan, C., Rades, T., Gordon, K.C., 2013. A theoretical and spectroscopic study of co-amorphous naproxen and indomethacin. Int. J. Pharm. 453, 80–87.

Mah, P.T., Laaksonen, T., Rades, T., Peltonen, L., Strachan, C.J., 2015. Differential scanning calorimetry predicts the critical quality attributes of amorphous glibenclamide. Eur. J. Pharm. Sci. 80, 74–81.

Mashru, R.C., Sutariya, V.B., Sankalia, M.G., Parikh, P.P., 2005. Development and evaluation of fast-dissolving film of salbutamol sulphate. Drug. Deliv. Ind. Pharm. 31, 25–34.

Moreton, R.C., Armstrong, N.A., 1998. The effect of film composition on the diffusion of ethanol through soft gelatine films. Int. J. Pharm. 161, 123–131.

Patterson, J.E., James, M.B., Forster, A.H., Lancaster, R.W., Butler, J.M., Rades, T., 2005. The influence of thermal and mechanical preparative techniques on the amorphous state of four poorly soluble compounds. J. Pharm. Sci. 94, 1998–2012.

Rycerz, L., 2013. Practical remarks concerning phase diagrams determination on the basis of differential scanning calorimetry measurements. J. Therm. Anal. Calorim. 113, 231–238.

Sharma, P., Kamboj, S., Singh, G., Rana, V., 2016. Development of aprepitant loaded orally disintegrating films for enhanced pharmacokinetic performance. Eur. J. Pharm. Sci. 84, 55–69.

Sholaei, A.H., 1998. Buccal mucosa as a route for systemic drug delivery. J. Pharm. Pharm. Sci. 1, 15–30.

Slavkova, M., Breitkreutz, J., 2015. Orodispersible drug formulations for children and elderly. Eur. J. Pharm. Sci. 75, 2–9.

Sugar alcohol eutectic and process for producing the same EP 1842436 A1 Accessed .

Talja, R.A., Roos, Y.H., 2001. Phase and state transition effect on dielectric, mechanical and thermal properties of polyols. Thermochim. Acta 380, 109–121.

Talja, R.A., Helén, H., Roos, Y.H., Jouppila, K., 2007. Effect of various polyols and polyol contents on physical and mechanical properties of potato starch-based films. Carbohydr. Polym. 67, 288–295.

Ulrich, J., Abouzeid, A., Hartwig, A., Petersen, S., Wendt, K., 2015. Geht es nicht einfacher? In situ Coating – Beschichtung direkt aus der Schmelze. CIT plus 3, 44–45.

Wendt, K., Petersen, S., Ulrich, J., 2014. Application of in situ coating on a two-compound system. Chem. Eng. Technol. 37, 1408–1412.

Zhang, Y., Han, J.H., 2006. Mechanical and thermal characteristics of pea starch films plasticized with monosaccharides and polyols. J. Food Sci. 71, 109–118.

IV.

Investigation of recrystallization of amorphous trehalose through hot-humidity stage X-ray powder diffraction

Orsolya Jójárt-Laczkovich [a,*], Gábor Katona [a,b], Zoltán Aigner [a], Piroska Szabó-Révész [a]

[a] *Department of Pharmaceutical Technology, University of Szeged, Szeged, Hungary*
[b] *Richter Gedeon Plc., Gyömrői 19-21, H-1103 Budapest, Hungary*

A B S T R A C T

The aim of this work was an investigation of the physical changes of the amorphous model material spray-dried trehalose through the use of various analytical techniques and to identify a suitable, rapid method able to quantify the changes. The crystallinity changes and recrystallization process of amorphous samples were investigated by hot-humidity stage X-ray powder diffractometry (HH-XRPD) with fresh samples, conventional X-ray powder diffractometry (XRPD) used stored samples and by differential scanning calorimetry (DSC). The data from the three methods were compared and the various forms of trehalose were analysed. HH-XRPD demonstrated that the recrystallization began at 40 and 60 °C up to 45% RH and at 70 °C up to 30% RH into dihydrate form. At 70 °C up to 60% RH the anhydrous form of trehalose appeared too. Conventional XRPD results showed, that in the 28 days stored samples the dihydrate form was detected at 40 °C, 50% RH. Storage at 60 °C, 40% RH resulted in the appearance of the anhydrous form and at 60 °C, 50% RH both polymorphic forms were detected. By carrying out the DSC measurements at different temperatures the fraction of recrystallized trehalose dihydrate was detected. The recrystallization investigated by HH-XRPD and DSC followed Avrami kinetics, the calculated rate constants of isothermal crystallization (*K*) were same. Both HH-XRPD and conventional XRPD was suitable for the detection of the physical changes of the amorphous model material. DSC measurements showed similar results as HH-XRPD. Primarily HH-XRPD could be suggested for prediction, because the method is fast and every changes could be studied on one sample.

1. Introduction

Trehalose is a natural sugar, but it is also synthesized and produced on a large scale industrially. It is widely applied in the cosmetic, agricultural, food and drug industries. In drug formulations, it is utilized as an active pharmaceutical ingredient or as a technological auxiliary agent. Trehalose could be also an active agent as chemical chaperone which is used to treat Creutzfeldt-Jakob disease, cystic fibrosis and amyloid disorders that prevent protein aggregation (Aguib et al., 2009). In oral medication, it displays antidepressant properties in the mouse model of depression, possibly through reducing the p62/Beclin-1 ratio and increasing autophagy in the frontal cortex (Kara et al., 2013).

The most important applications of trehalose as a pharmaceutical excipient are to preserve enzymes, to stabilize vaccines at room temperature for storage, and to protect mammalian cells from damage during lyophilization. Trehalose concentrates the water near the protein, and it can be transformed to its native structure after lyophilization and regain its function (Timasheff, 2002). The protein-stabilizing ability of

trehalose is utilized in many areas of industry, e.g. as a moisturizer or to stabilize liposomes (Tanaka et al., 1992). As an auxiliary component, it is often applied as a carrier of dry powder inhalation (DPI) systems. For this purpose, α-lactose monohydrate is normally used, but lactose may react with the amino group, so proteins and peptides cannot be formulated with it. In this case, lactose must be substituted with trehalose, raffinose or sucrose. These non-reducing sugars have the common advantage of protecting proteins or peptides against different stress conditions during spray-drying. They substitute the hydrogen-bonds in water, and form viscous mixtures with proteins, resulting in products with high glass temperatures of the product (Maas et al., 2011).

Trehalose is often produced as an excipient by spray-drying (Ógáin et al., 2011; Islam and Gladki, 2008; Gradon and Sosnowski, 2014; Pomázi et al., 2011; Maurya et al., 2005a; Maurya et al., 2005b; Moran and Buckton, 2007a; Amaro et al., 2015), freeze-drying (Murugappan et al., 2013; Nakamura et al., 2008; Crowe et al., 2003; Jovanovoc et al., 2006; Claus et al., 2011) and spray-freeze-drying (Tonnis et al., 2014; Yu et al., 2006) in pharmaceutical technology. Trehalose tends to undergo amorphization, and the amorphous form is readily prepared by using a solvent method such as spray- or freeze-drying. The recrystallization kinetics can be followed which is important because of the appearance of polymorph forms (Sussich and Cesáro, 2008). Trehalose has 4

* Corresponding author at: Department of Pharmaceutical Technology, University of Szeged, H-6720 Szeged, Eötvös u. 6, Hungary.
E-mail address: laczkovo@pharm.u-szeged.hu (O. Jójárt-Laczkovich).

Table 1
Melting points of trehalose polymorphs (Sussich and Cesáro, 2008).

Polymorph	Melting point (°C)
Trehalose-α (anhydrous)	120
Trehalose-β (anhydrous)	215
Trehalose-γ (anhydrous)	118–122
Trehalose-h (dihydrate)	100–110

Table 3
Different storage conditions of amorphous samples.

Temperature (°C)	Relative humidity (%)	Storage time (day)
25 ± 2	32 ± 5	1
40 ± 2	30 ± 5	28
	40 ± 5	28
	50 ± 5	28
60 ± 2	30 ± 5	28
	40 ± 5	28
	50 ± 5	28

polymorphic forms (Table 1). This is especially important in the case of DPI because of the preparation methods and the storage conditions of the product. In this work one of the most efficient amorphization technology, spray-drying was selected for preparing amorphous trehalose. This method results in a monodisperse product with suitable particle size and excellent flowability.

Various analytical methods are available to investigate amorphization (Jójárt-Laczkovich and Szabó-Révész, 2010; Jójárt-Laczkovich and Szabó-Révész, 2011; Danciu et al., 2014; Jug and Bećirević-Laćan, 2004), recrystallization, polymorphic conversions, and the dehydration and rehydration mechanisms of different materials (Szakonyi and Zelkó, 2012). Common techniques are differential scanning calorimetry (DSC) and X-ray powder diffraction (XRPD) measurements. Besides these possibilities, dynamic vapour sorption (Jones et al., 2006), Karl Fischer moisture titration, isothermal thermogravimetric analysis (Taylor and York, 1998) and simultaneous techniques (DSC-XRPD and TG-DTA) have also been described in the case of trehalose (Furuki et al., 2005; Mah et al., 2015). A modern investigation method is hot-humidity stage X-ray powder diffraction (HH-XRPD), whereby temperature and RH are variable. Through HH-XRPD analysis, complex pharmaceutical solid-state reactions, including crystal structure transformations, can be in situ characterized and followed. This method rapidly provides information about polymorph conversions and recrystallization kinetics, and short-term stability testing can be carried out during preformulation studies. Examples of the polymorphic transformation of some active and auxiliary agents (naloxone, naltrexone and aspartame) are to be found in the literature (Guguta et al., 2009; Guguta et al., 2008).

The focus of this work was an investigation of the recrystallization process of the amorphous model material spray-dried trehalose and to find a suitable method to predict the recrystallization of amorphous sample during a preformulation study. In a comparison study three, different methods (HH-XRPD, XRPD, DSC) were used to analyse the crystallinity changes.

2. Materials and methods

2.1. Materials

D-(+)-trehalose dihydrate h-form was purchased from Karl Roth GmbH + Co. KG. (Karlruhe, Germany). This was regarded as 100% crystalline material. The water content was $9.5 \pm 0.5\%$ and the sulphate content was <0.5%. Its specific rotation was $178 \pm 2°$.

Anhydrous D-(+)-trehalose β-form was produced by dehydration of trehalose dihydrate at 85 °C during 4 h under vacuum (Nagase et al., 2002) and checked the within 24 h both with DSC and XRPD.

Table 2
Operation parameters for the preparation of spray-dried trehalose.

Operating parameters	Settings
Inlet temperature (°C)	130–140
Outlet temperature (°C)	75–92
Feed rate (ml/min)	2
Pressure (bar)	4,8
Atomizer flow rate (normolitre/h)	600
Aspirator (%)	80

2.2. Preparation of spray-dried trehalose

Trehalose dihydrate was spray-dried from 10% solutions in water (5 g of trehalose and 45 g of water), using a Büchi 191 Mini Spray Dryer (Büchi, Switzerland). The parameters used are given in Table 2 (Moran and Buckton, 2007b). The spray-dried products were stored in a desiccator over cobalt(II) chloride-contaminated silicon dioxide (25 ± 2 °C, $32 \pm 5\%$ RH) until use and were X-ray amorphous.

2.3. Preparation of physical mixtures

Physical mixtures of spray-dried (amorphous) and the two different crystalline form of trehalose were prepared to achieve 0, 5, 10, 30, 50, 70, 90, 95 and 100% crystalline content by mass. The components were weighed to a total amount of 0.50 g and were mixed homogenous in a trituration mortar.

2.4. HH-XRPD

HH-XRPD analysis was performed on the spray-dried amorphous samples within 24 h by using a Bruker D8 Advance X-ray Diffractometer (Bruker AXS GmbH, Karlsruhe, Germany) with Cu K λI radiation ($\lambda = 1.5406$ Å) installed with an MRI Basic hot-humidity stage and a VÅNTEC-1 detector. The samples were scanned at 40 kV and 40 mA. The angular range was from 3° to 40° 2θ, at a step time of 0.1 s and a step size of 0.007°. An ANS-Sycoshot humidity control device was coupled to the XRPD, which injected humidity into a controlled dry gas flow. The carrier gas was compressed air with a 0.5 l/min flow. The sample was taken in a Ni-coated sample holder. The RH was set at 10, 20, 30, 40, 45, 50, 60 and 70% at 40 °C, 60 °C and 70 °C controlled temperatures, and the samples were kept in each condition for 1 h before measurement. All manipulations, Kα 2-stripping, background removal and signal to noise smoothing of the area under the peaks of diffractograms were performed with DIFFRACTPLUS EVA software.

2.5. XRPD

XRPD analysis was performed with a Bruker D8 Advance diffractometer (Bruker AXS GmbH, Karlsruhe, Germany) with Cu K λI radiation ($\lambda = 1.5406$ Å) and a VÅNTEC-1 detector. Both the physical mixtures and the stored amorphous samples were scanned at 40 kV and 40 mA. The angular range was 3° to 40° 2θ, at a step time of 0.1 s and a step size of 0.007°. The sample was placed on a quartz holder, measured at ambient temperature and RH. All manipulations, Kα 2-stripping, background removal and smoothing of the area under the peaks of diffractograms were performed with DIFFRACTPLUS EVA software. The determination of the polymorph form was based on the Cambridge Crystallographic Data Centre (CCDC ID: AI631510) X-ray powder diffractograms.

2.6. Storage conditions

One part of the spray-dried product was stored in a desiccator over cobalt(II) chloride-contaminated silicon dioxide (25 ± 2 °C, $32 \pm 5\%$
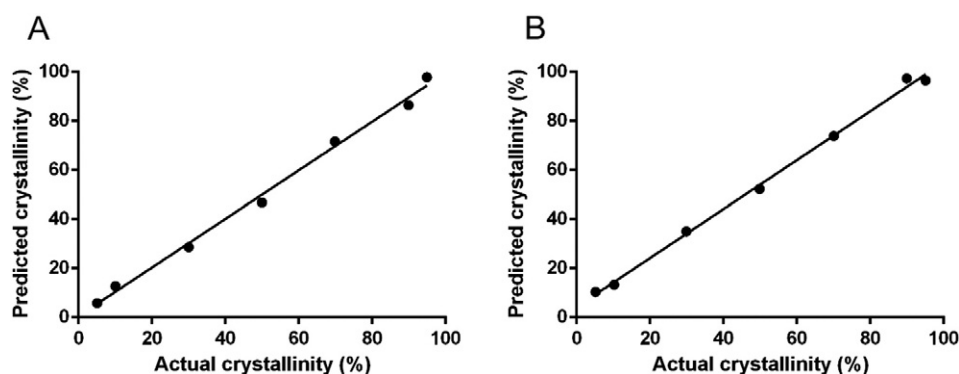
Fig. 1. Relation between predicted and actual crystallinity of physical mixtures of crystalline trehalose dihydrate - amorphous form (A), anhydrous trehalose - amorphous form (B) determined by conventional X-ray powder diffraction.

RH) until HH-XRPD measurements. The reminder was divided into 6 parts and stored for 28 days at 40 °C and 60 °C, in 3-3 hygrostats, where the RH was set to 30%, 40% and 50% RH. In each dessicator and hygrostates, there was a digital humidity meter during the storage for controlling the relative humidity. These samples were investigated with XRPD (Table 3).

2.7. Calculation of the recrystallization kinetics

The recrystallization kinetics was modelled by using the Avrami equation (Eq. (1)):

$$1 - \alpha = \exp(-Kt^n) \tag{1}$$

where α is the fraction of recrystallized trehalose at time t, K is the rate constant and n is the Avrami index, a parameter characteristic of the nucleation and growth mechanism of crystals.

The fraction of recrystallized trehalose (α) was calculated from the area under the characteristic peaks using the following equation (Eq. (2)):

$$\alpha = \frac{A_{crystalline}}{A_{crystalline} + A_{amorphous}} * 100 \tag{2}$$

where α is the crystalline fraction, A is the area of characteristic crystalline peaks and amorphous sign. Three characteristic peaks each were selected from the diffractograms of trehalose dihydrate (at 8.531°, 12.552° and 14.224° 2θ) and anhydrous trehalose (at 6.572°, 20.351° and 24.792° 2θ). The XRPD instrument was calibrated every day with corundum during the 28 days measurement to minimalize the day to day intensity changes in XRPD emission.

Table 4
The degree of crystallinity calculated from the HH-XRPD data (A: amorphous, h-form: dihydrate, β-form: anhydrous).

Time [min, RH%]	Form of trehalose			Degree of crystallinity (%)		
	40 °C	60 °C	70 °C	40 °C	60 °C	70 °C
0, 0	A	A	A	0	0	0
60, 10	A	A	A	0	0	0
120, 20	A	A	A	0	0	0
180, 30	A	A	h-form	0	0	11.7
240, 40	A	A	h-form	0	0	31.1
300, 45	h-form	h-form	h-form	14.8	27.2	65.2
360, 50	h-form	h-form	h-form	35.8	62.4	100
420, 60	h-form	h-form	β/h-form	70.2	78.8	100
480, 70	h-form	h-form	β/h-form	100	100	100

The Avrami parameters were obtained from the experimental data by using the double logarithmic form of Eq. (1):

$$\ln[-\ln(1-\alpha)] = \ln K + n \ln t \tag{3}$$

The activation energy of the recrystallization was calculated by using the Arrhenius equation (Eq. (4)):

$$k = k_0 \exp\left(-\frac{E_a}{RT}\right) \tag{4}$$

In the model, k is the rate constant at temperature T, k_0 is the frequency factor, R is the gas constant and E_a is the activation energy. The logarithmic form of Eq. (4) allows determination of the activation
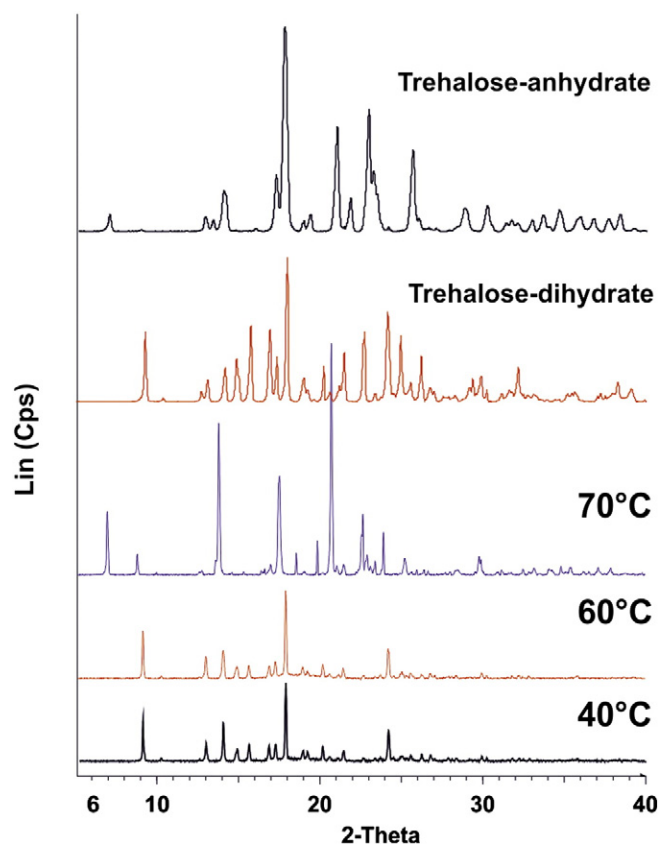

Fig. 2. The recrystallized trehalose polymorphs at 40, 60 and 70 °C controlled temperatures.
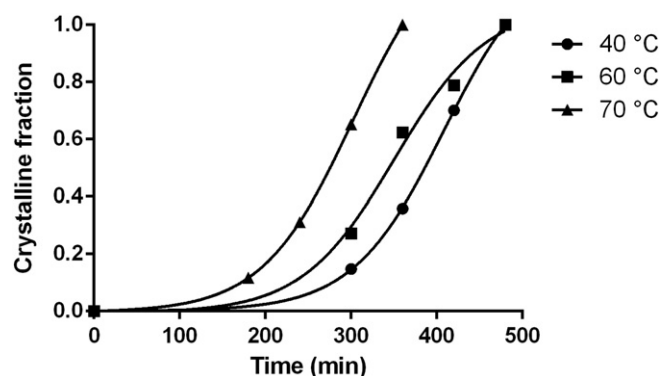
Fig. 3. Crystallization kinetics by fitting the Avrami equation to the HH-XRPD data.

energy (Eq. (5)) (Mazzobre et al., 2001):

$$\ln k = \ln k_0 - \frac{E_a}{RT} \tag{5}$$

2.8. DSC

DSC measurements were carried out with a Mettler-Toledo 821^e DSC instrument (Mettler-Toledo GmbH, Switzerland). Samples loaded at different RH (10, 20, 30, 40, 45, 50 and 70%) in the XRPD humidity chamber for 1 h were crimped in aluminium pans with three holes and were examined in the temperature interval 25–250 °C at a heating rate of 10 °C min^{-1} under a constant argon flow of 150 ml min^{-1}. Every measurement was normalized to sample size. The fraction of recrystal-lized trehalose dihydrate was calculated from the integral of sharp en-dotherm at 108 °C.

3. Results and discussion

3.1. Determination of calibration curves with XRPD

The peak intensities of the individual components are proportional to the quantities of components in the mixture. Three characteristic peaks each were selected from the diffractograms of trehalose dihydrate (at 8.531°, 12.552° and 14.224° 2θ) and anhydrous trehalose (at 6.572°, 20.351° and 24.792° 2θ). Multiple linear regression (MLR) was used to determine the calibration curve. The dependent variable was the crys-tallinity and the independent variables were the relative intensity values at chosen 2θ values. After determination of the degree of crystal-linity from w/w ratio of the physical mixtures, a calibration curve was fitted. Linear regression of the data produced an $r^2 = 0.995$ and a slope of 0.990 for trehalose dihydrate (Fig. 1A). For anhydrous trehalose, $r^2 = 0.997$ and the slope was 0.997 (Fig. 1B).
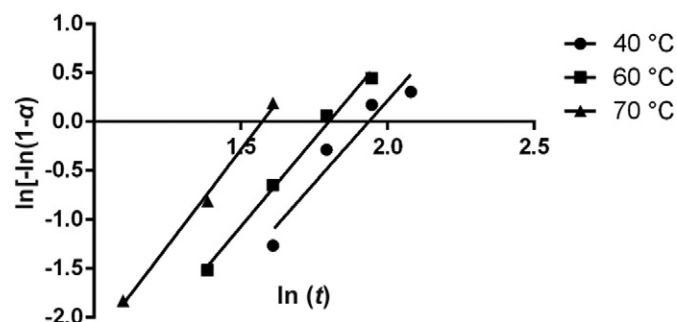

Fig. 4. Determination of the Avrami parameters n and K from HH-XRPD data.
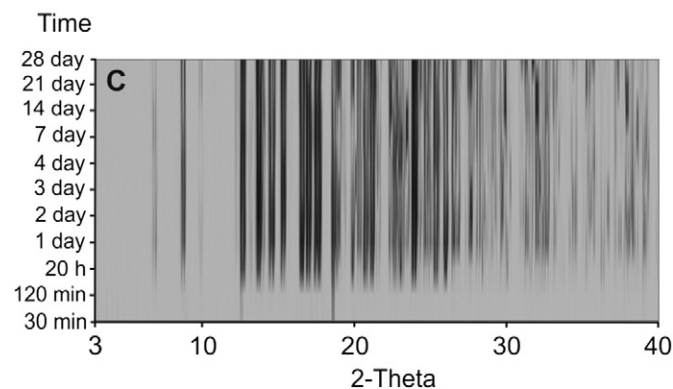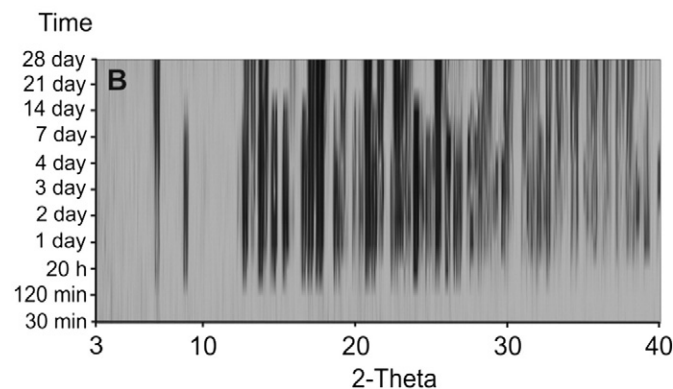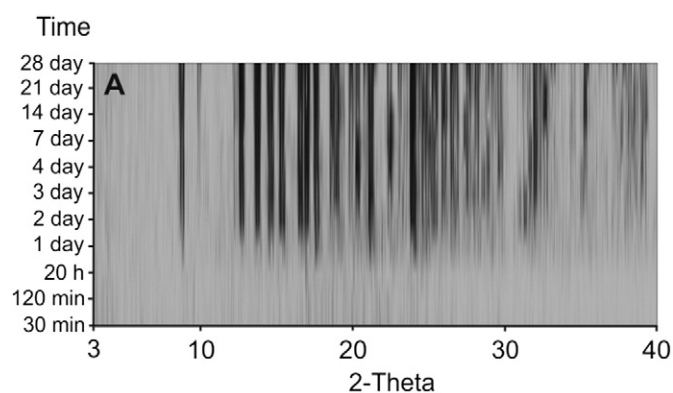

Fig. 5. Top-view pictures of XRPD investigations of samples stored for 28 days at 40 °C, 50% RH (A), 60 °C, 40% RH (B) and 60 °C, 50% RH (C).

Because of the well-correlating r^2 values the degree of crystallinity can be quantified.

3.2. Calculation of crystallization kinetics

3.2.1. Hot-humidity stage XRPD analysis

For the development and qualification of solid compositions it is im-portant to investigate and determine changes of the crystalline phases or the effect of crystallization inhibitor, when materials are exposed to changing humidity and temperature. Increasing the humidity in small intervals (10%) at the exact temperature, good estimation could be gained during few hours at the exact temperature about the samples be-haviour, which could be reflected on the results of conventional stability test. There is no need for additional hygrostats and extra samples, the measurement takes place directly in the chamber conducted to the in-strument. These investigations are not only important to establish pro-cedures for storage, production and shipment, but also emulate the indigestion of the respective drug and its first interactions with the
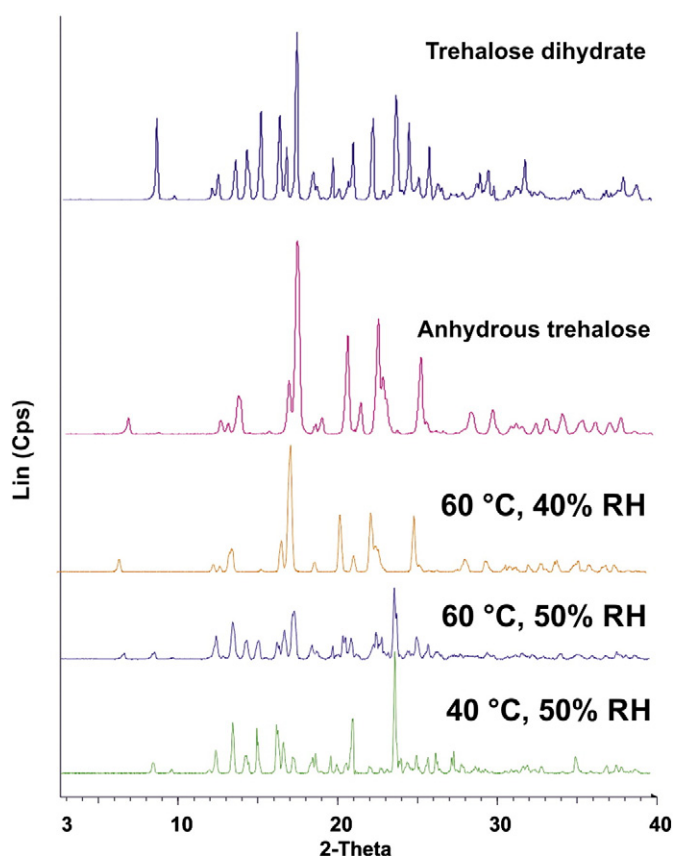
Fig. 6. Diffractograms of samples stored for 28 days under different conditions, compared with trehalose forms in CCDC.

Table 6
ΔH of melting and the crystalline fraction (α) at different temperatures with increasing the RH.

RH (%)	ΔH (J g^{-1})			α (%)		
	40 °C	60 °C	70 °C	40 °C	60 °C	70 °C
30	–	–	17.1	0	0	11
40	–	–	27.3	0	0	17.6
45	44.5	33.0	128.1	28.7	21.3	82.7
50	63.8	66.0	137.6	41.2	42.6	88.8
60	130.4	123.5	141.4	84.2	79.7	91.3
70	153.5	153.0	153.8	99.1	98.8	99.3

Eq. (1) were in good agreement ($r^2 > 0.992$) with the experimental points (Fig. 3).

The sigmoidal curves showed that increased temperature accelerates the recrystallization and reduces the crystallization half-time. To acquire information about the velocity of the process and the dimensions of crystal growth, the parameters K and n were determined by using the linearized Avrami equation (Eq. (3)) (Fig. 4) and the activation energy was calculated via the logarithmic form of the Arrhenius model (Eq. (5)) (Table 7).

3.2.2. Analysis of samples stored in hygrostats (XRPD)

To the comparison study amorphous samples were stored for 28 days at 40 °C and 60 °C in 3 hygrostats each, where the RH had been set to 30%, 40% and 50%. The fractions of recrystallized trehalose were measured at different times during the 28 days of storage. The conventional XRPD analysis showed, that the samples stored at 40 °C, 30% and 40% RH, and at 60 °C, 30% RH remained amorphous. The samples stored at 40 °C, 50% RH recrystallized in the dihydrate form. The storage conditions at 60 °C, 40% RH, resulted in recrystallization of the anhydrous form, and in the sample stored at 60 °C, 50% RH, both polymorphs appeared, the h-form (dihydrate) and the β-form (anhydrous) (Fig. 5).

Fig. 5B shows that the stripe at 8.531° 2θ disappears after storage for 14 days, and there is a polymorph conversion of trehalose dihydrate into the anhydrous form, confirmed by the characteristic thick stripe at 6.572° 2θ. Fig. 5A and C do not indicate any polymorph conversion. The diffractograms measured after 28 days storage are shown in Fig. 6.

The degree of crystallinity of the recrystallized polymorphs was calculated by evaluating the diffractograms in Fig. 6 according to the MLR model. The results showed that amorphous fractions remained in the samples, but decreased at higher temperature and RH (Table 5).

By means of the 28-days stability tests, the different recrystallized polymorph forms can be detected and quantified. The results showed that, at 40 °C and 50% RH the dihydrate was detected, but the bulk of the investigated sample remained amorphous. Storage at 60 °C and 40% RH resulted in the appearance of the anhydrous form and only a minor proportion of the sample remained amorphous. At 60 °C and 50% RH, both polymorphic forms were detected and almost the whole sample recrystallized. This conventional method is often used as a long-term stability test in the development of a drug delivery system.

patient. In this context HH-XRPD was used to predict the tendency to re-crystallization, which is presented in Table 4.

The samples measured at 40 and 60 °C were amorphous up to 45% RH, when recrystallization began in the trehalose dihydrate polymorph. The samples measured at 70 °C were amorphous up to 30% RH, than they recrystallized to dihydrate form and up to 60% RH the anhydrous form appeared too. The determination of the polymorph forms was based on the Cambridge Crystallographic Data Centre (CCDC ID: AI631510) X-ray powder diffractograms (Fig. 2).

The diffractograms measured at 40, 60 and 70 °C showed an increasing tendency to recrystallization. The relative intensities and integrals of the peaks increased with the temperature, and the temperature therefore influences the tendency of trehalose to recrystallize.

To investigate the temperature dependence of recrystallization, the recrystallized fractions were plotted against time for each temperature. As the calibration showed, before XRPD the method could be used for quantitative measurements. The curves obtained by fitting the Avrami

Table 5
The degree of crystallinity calculated from the XRPD data after 28 days.

Condition [°C, RH%]	Form of trehalose			Quantity (%)		
	Amorphous	Dihydrate (h-form)	Anhydrous (β-form)	Amorphous	Dihydrate (h-form)	Anhydrous (β-form)
40, 30	+	–	–	100	0	0
40, 40	+	–	–	100	0	0
40, 50	+	+	–	63.1	36. 9	0
60, 30	+	–	–	100	0	0
60, 40	+	–	+	25.5	0	74.5
60, 50	+	+	+	0.4	58.2	41.5

Table 7
Avrami parameters and activation energy of recrystallization investigated with HH-XRPD and DSC.

Method	t (°C)	n	K	E_a (kJ mol^{-1})
HH-XRPD	40	3.373	5.79E-04	47.215
	60	3.566	1.70E-03	
	70	3.934	2.84E-03	
DSC	40	3.378	1.69E-03	41.645
	60	2.989	5.98E-03	
	70	3.156	6.29E-03	

Fig. 8. Determination of Avrami parameters n and K from DSC data.

3.2.3. DSC investigation

The amount of recrystallized trehalose dihydrate was calculated from the integral of the endothermic peaks at 108 °C, which is the melting point of trehalose dehydrate β-form. Table 6 shows the enthalpy changes (ΔH) of melting and the calculated crystalline fraction (α) at different temperature increasing the RH.

The amount of crystalline fractions showed, that the recrystallization of the amorphous sample is more significant with increasing RH and at 70% RH total recrystallization of the samples occurred at all 3 temperatures. Comparison of these results with those in Table 4 shows that DSC and HH-XRPD measurements correlate well. With this method, only the fraction of recrystallized trehalose dihydrate can be determined. Since the anhydrous form has high melting point, the dihydrate form is conversed into the anhydrous form resulting in false measurement data. However, the method can be used for fast stability testing during the preformulation.

The crystalline fractions calculated from the DSC data (Table 6) were plotted against time for each temperature with $r^2 > 0.983$ (Fig. 7).

The sigmoidal curves showed that increased temperature accelerates the recrystallization, and reduces the crystallization half-time. To acquire information about the velocity of the process and the dimensions of crystal growth, the Avrami parameters should be determined. The parameters K and n were determined by using the linearized Avrami equation (Eq. (3)). A plot of ln [-ln (1-α)] against ln (t) yields a straight line with slope n and intercept ln K (Fig. 8). The activation energy was calculated via the logarithmic form of the Arrhenius model (Eq. (5)). Table 6 shows the parameters of the recrystallization process.

The values of rate constant K show that increasing temperature accelerates the recrystallization process. There are differences between the measurement results of the two methods, but the results correlate well. Comparison of the HH-XRPD data with the DSC measurements demonstrates that increasing temperature accelerates the recrystallization and reduces the crystallization half-time. The parameters K and n were determined by using the linearized Avrami equation (Eq. (3)) (Fig. 8).
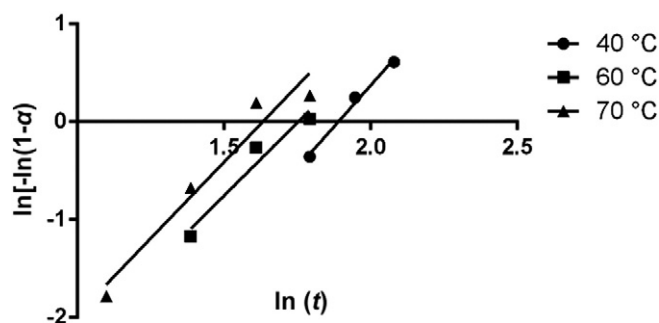
4. Conclusions

In the comparison study the three analytical methods (HH-XRPD, XRPD, DSC) were used to investigate the recrystallization of amorphous trehalose. The focus of this work was to suggest such method, which is sensitive and rapid to predict the recrystallization process in the preformulation study.

HH-XRPD was used to investigate the effects of temperature and rapid RH changes. Different RH conditions resulted in different crystalline forms of trehalose, which means that recrystallization can start during the process of the investigation. In this way, the control of crystallinity is necessary. The measurement demonstrated that the recrystallization began at 40 and 60 °C up to 45% RH and at 70 °C up to 30% RH into dihydrate form. At 70 °C up to 60% RH, the anhydrous form of trehalose appeared too. It could be concluded that the temperature and RH dependence of recrystallization are determining factors. This can be expressed in a numerical relationship by the Avrami and Arrhenius equations. HH-XRPD is a good choice for gaining a good estimation over a few hours about the samples behaviour, which could be reflected on the results of a conventional stability test.

The conventional storage at different temperatures and RH gave information about the recrystallized polymorphs. Over the course of 28 days, both RH and temperature changes can cause the recrystallization of amorphous trehalose. The dihydrate form was detected at 40 °C, 50% RH. Storage at 60 °C, 40% RH resulted in the appearance of the anhydrous form and at 60 °C, 50% RH both polymorphic forms were detected. In this light, the suitable choice of the storage conditions can protect the amorphous trehalose samples from crystallization.

By carrying out the DSC measurements at different temperatures, the fraction of recrystallized trehalose dihydrate can be determined. The degree of crystallinity of trehalose dihydrate determined by DSC correlated well with the HH-XRPD measurements.

It could be concluded that HH-XRPD is faster than other conventional techniques and a good prediction for the recrystallization of amorphous compounds during preformulation, moreover the physical changes could be studied on one sample.

Fig. 7. Crystallization kinetics by fitting the Avrami equation to the DSC data.

References

Aguib, Y., Heiseke, A., Gilch, S., Riemer, C., Baier, M., Schatzl, H.M., Ertmer, A., 2009. Autophagy induction by trehalose counteracts cellular prion infection. Autophagy 5, 361–369.

Amaro, M.I., Tajber, L., Corrigan, O.I., Healy, A.M., 2015. Co-spray dried carbohydrate microparticles: crystallization delay/inhibition and improved aerosolization characteristics, through the incorporation of hydroxypropyl-β-cyclodextrin with amorphous raffinose or trehalose. Pharm. Res. 32, 180–195.

Claus, S., Schoenbrodt, T., Weiler, C., Friess, W., 2011. Novel dry powder inhalation system based on dispersion of lyophilisates. Eur. J. Pharm. Sci. 43, 32–40.

Crowe, J.H., Tablin, F., Wolkers, W.F., Gousset, K., Tsvetkova, N.M., Ricker, J., 2003. Stabilization of membranes in human platelets freeze-dried with trehalose. Chem. Phys. Lipids 122, 41–52.

Danciu, C., Soica, C., Oltean, M., Avram, S., Borcan, F., Csányi, E., Ambrus, R., Zupkó, I., Muntean, D., Dehelean, C.A., Craina, M., Popovici, R.A., 2014. Genistein in 1:1 inclusion complexes with ramified cyclodextrins: theoretical, physicochemical and biological evaluation. Int. J. Mol. Sci. 15, 1962–1982.
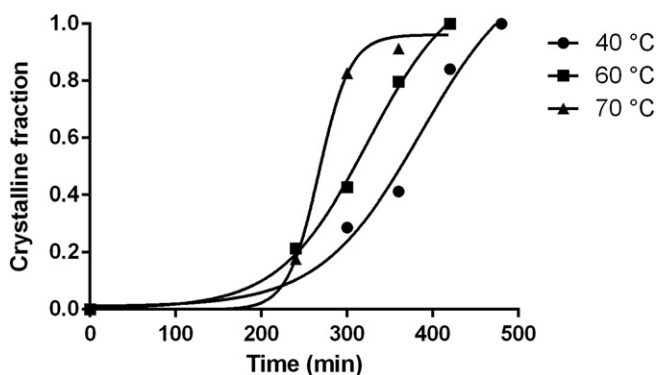
Furuki, T., Kishi, A., Sakurai, M., 2005. De- and rehydration behavior of α,α-trehalose dihydrate under humidity-controlled atmospheres. Carbohydr. Res. 340, 429–438.

Gradon, L., Sosnowski, T.R., 2014. Formation of particles for dry powder inhalers. Adv. Powder Technol. 25, 43–55.

Guguta, C., Meekes, H., de Gelder, R., 2008. The hydration/dehydration behavior if aspartame revisited. J. Pharm. Biomed. Anal. 46, 617–624.

Guguta, C., van Eck, E.R.H., de Gelder, R., 2009. Structural insight into the dehydration and hydration behavior of naltrexon and naloxon hydrochloride. Dehydration-induced expansion versus contraction. Cryst. Growth Des. 9, 3384–3395.

Islam, N., Gladki, E., 2008. Dry powder inhalers (DPIs)—a review of device reliability and innovation. Int. J. Pharm. 360, 1–11.

Jójárt-Laczkovich, O., Szabó-Révész, P., 2010. Amorphization of a crystalline active pharmaceutical ingredient and thermoanalytical measurements on this glassy form. J. Therm. Anal. Cal. 102, 243–247.

Jójárt-Laczkovich, O., Szabó-Révész, P., 2011. Formulation of tablets containing an 'inprocess' amorphized active pharmaceutical ingredient. Drug Dev. Ind. Pharm. 37, 1272–1281.

Jones, M.D., Hooton, J.C., Dawson, M.L., Ferrie, A.R., Price, R., 2006. Dehydration of trehalose dihydrate at low relative humidity and ambient temperature. Int. J. Pharm. 313, 87–98.

Jovanovoc, N., Bouchard, A., Hofland, G.W., Witkamp, G.J., Crommelin, D.J.A., Jiskoot, W., 2006. Distinct effects of sucrose and trehalose on protein stability during supercritical fluid drying and freeze-drying. Eur. J. Pharm. Sci. 27, 336–345.

Jug, M., Bećirević-Laćan, M., 2004. Influence of hydroxypropyl-β-cyclodextrin complexation on piroxicam release from buccoadhesive tablets. Eur. J. Pharm. Sci. 21, 251–260.

Kara, N.Z., Toker, L., Agam, G., Anderson, G.W., Belmaker, R.H., Einat, H., 2013. Trehalose induced antidepressant-like effects and autophagy enhancement in mice. Psychopharmacology 229, 367–375.

Maas, S.G., Schaldach, G., Littringer, E.M., Mescher, A., Griesser, U.J., Braun, D.E., Walzel, P.E., Urbanetz, N.A., 2011. The impact of spray drying outlet temperature on the particle morphology of mannitol. Powder Technol. 213, 27–35.

Mah, P.T., Laaksonen, T., Rades, T., Peltonen, L., Strachan, C.J., 2015. Differential scanning calorimetry predicts the critical quality attributes of amorphous glibenclamide. Eur. J. Pharm. Sci. 80, 74–81.

Maurya, M., Murphyb, K., Kumarb, S., Shib, L., Leea, G., 2005a. Effects of process variables on the powder yield of spray-dried trehalose on a laboratory spray-dryer. Eur. J. Pharm. Biopharm. 59, 565–573.

Maurya, M., Murphyb, K., Kumarb, S., Mauerera, A., Lee, G., 2005b. Spray-drying of proteins: effects of sorbitol and trehalose on aggregation and FT-IR amide I spectrum of an immunoglobulin G. Eur. J. Pharm. Biopharm. 59, 251–261.

Mazzobre, M.F., Soto, G., Aguilera, J.M., Buera, M.P., 2001. Crystallization kinetics of lactose in systems co-lyophilized with trehalose. Analysis by differential scanning calorimetry. Food Res. Int. 34, 903–911.

Moran, A., Buckton, G., 2007a. Adjusting and understanding the properties and crystallisation behaviour of amorphous trehalose as a function of spray drying feed concentration. Int. J. Pharm. 343, 12–17.

Moran, A., Buckton, G., 2007b. Adjusting and understanding the properties and crystallisation behaviour of amorphous trehalose as a function of spray drying feed concentration. Int. J. Pharm. 343, 12–17.

Murugappan, S., Patil, H.P., Kanojia, G., ter Veer, W., Meijerhof, T., Frijlink, H.W., Huckriede, A., Hinrichs, W.L.J., 2013. Physical and immunogenic stability of spray freeze-dried influenza vaccine powder for pulmonary delivery: comparison of inulin, dextran, or a mixture of dextran and trehalose as protectants. Eur. J. Pharm. Biopharm. 85, 716–725.

Nagase, H., Endo, T., Ueda, H., Nakagakib, M., 2002. An anhydrous polymorphic form of trehalose. Carbohydr. Res. 337, 167–173.

Nakamura, T., Sekiyama, E., Takaoka, M., Bentley, A.J., Yokoi, N., Fullwood, N.J., Kinoshita, S., 2008. The use of trehalose-treated freeze-dried amniotic membrane for ocular surface reconstruction. Biomaterials 29, 3729–3737.

Ógáin, O.N., Li, J., Tajber, L., Corrigan, O.I., Healy, A.M., 2011. Particle engineering of materials for oral inhalation by dry powder inhalers. I-particles of sugar excipients (trehalose and raffinose) for protein delivery. Int. J. Pharma. 405, 23–35.

Pomázi, A., Ambrus, R., Sipos, P., Szabó-Révész, P., 2011. Analysis of co-spray-dried meloxicam–mannitol systems containing crystalline microcomposites. J. Pharm. Biomed. Anal. 56, 183–190.

Sussich, F., Cesáro, A., 2008. Trehalose amorphization and recrystallization. Carbohydr. Res. 343, 2667–2674.

Szakonyi, G., Zelkó, R., 2012. The effect of water on the solid state characteristics of pharmaceutical excipients: molecular mechanisms, measurement techniques, and quality aspects of final dosage form. Int. J. Pharma. Investig. 2, 18–25.

Tanaka, K., Takeda, T., Fujii, K., Miyajima, K., 1992. Cryoprotective mechanism of saccharides on freeze-drying of liposome. Chem. Pharm. Bull. 40, 1–5.

Taylor, L.S., York, P., 1998. Effect of particle size and temperature on the dehydration kinetics of trehalose dihydrate. Int. J. Pharm. 167, 215–221.

Timasheff, S.N., 2002. Protein hydration, thermodynamic binding, and preferential hydration. Biochemistry 41, 13473–13482.

Tonnis, W.F., Amorij, J.P., Vreeman, M.A., Frijlink, H.W., Kersten, G.F., Hinrichs, W.L.J., 2014. Improved storage stability and immunogenicity of hepatitis B vaccine after spray-freeze drying in presence of sugars. Eur. J. Pharm. Sci. 55, 36–45.

Yu, Z., Johnston, K.P., Williams, R.O., 2006. Spray freezing into liquid versus spray-freeze drying: influence of atomization on protein aggregation and biological activity. Eur. J. Pharm. Sci. 27, 9–18.

NYILATKOZAT SAJÁT MUNKÁRÓL

Név: Dr. Katona Gábor

A doktori értekezés címe: Formulation of microcomposites and pastilles using spray-drying and melt technology

Én, *Dr. Katona Gábor* teljes felelősségem tudatában kijelentem, hogy a Szegedi Tudományegyetem Gyógyszertudományok Doktori Iskolában elkészített doktori (Ph.D.) disszertációm saját kutatási eredményeimre alapulnak. Kutatómunkám, eredményeim publikálása, valamint disszertációm megírása során a Magyar Tudományos Akadémia Tudományetikai Kódexében lefektetett alapelvek és ajánlások szerint jártam el.

Szeged, 2017. 04. 12.